Spring 2009

Helical force flow: a new engineering mechanics model for biological materials

Jeffery S. Thomas
Missouri University of Science and Technology, jthomas@mst.edu

Department: Mechanical and Aerospace Engineering

HELICAL FORCE FLOW: A NEW ENGINEERING MECHANICS MODEL FOR BIOLOGICAL MATERIALS

by

JEFFERY SCOTT THOMAS

A DISSERTATION

Presented to the Faculty of the Graduate School of the

MISSOURI UNIVERSITY OF SCIENCE AND TECHNOLOGY

In Partial Fulfillment of the Requirements for the Degree

DOCTOR OF PHILOSOPHY

in

ENGINEERING MECHANICS

2009

Approved by

L. R. Dharani, Advisor
V. Birman
D. R. Carroll
K. Chandrashekhara
G. P. MacSithigh

ABSTRACT

The author has long speculated that the prevalence of helical structures in botany and zoology hints to an optimized pathway for force and/or energy transfer. His goal has been to realize an alternative approach to the standard stress analysis used in engineering in order to more efficiently and accurately deal with biological materials. Improved tools for these natural materials should in turn aid the design and analysis of engineered materials.

Following the role of a *navigator* in L. C. Levesque's book *Breakthrough Creativity*, the author typically searches for ideas in a variety of places, including physics, materials science, biomimetics, dimensional analysis, etc., and attempts to link seemingly disconnected pieces of information into a consistent cognitive framework. In this document he presents his ideas for *unit maps,* which allow systematic searches to be made for innovative concepts in science and engineering, and *unit mechanics,* which helps to classify concepts that span multiple levels of structural hierarchy and spatial dimension. As an example, he explores the concept of *force per time* or *force flow*, where photons follow helical paths through a material's structure. He also presents the concept of *close-packed helices* in crystal lattices.

On the experimental side, the author gives attention to flexible, spatially-scalable probe tests, such as hardness, instrumented indentation, and a simple, qualitative form of integrated photoelasticity. He puts forth his ideas on *property mapping* of botanical materials and, in particular, preliminary results for shortleaf pine.

PREFACE

Having taught courses in engineering mechanics and engineering design for thirteen years to 4400 students and supervised the instruction of 6700 students with the help of 130 assistants, I still struggle with what seems the most basic of concepts—*what is force?* As a laboratory manager with over 1700 consultations to characterize the mechanical response of various materials and products, I have had plenty of opportunity to answer my curiosities. But alas, I have not. What follows is a summary of my search for a better understanding of force and how it operates within materials and structures.

ACKNOWLEDGMENTS

I would like to thank Doctors Lokeswarappa Dharani, Victor Birman, Douglas Carroll, K. Chandrashekhara and Gearoid MacSithigh for their guidance and patience. I would also like to thank my wife, Sarah, and son, Micah, for their love and motivation, Tom Bryson for his suggestions, and the many students who have asked questions that I did not know how to answer.

TABLE OF CONTENTS

LIST OF ILLUSTRATIONS

LIST OF TABLES

1. INTRODUCTION

"Engineering is the science and art of efficient dealing with materials and forces..." – J. A. L. Waddell, F. W. Skinner, and H. E. Wessman (1933)

This first section offers a history lesson on *force* and how it relates to engineering mechanics and then highlights several biological materials and structures that are optimized for their mechanical function. The author concludes by pointing out shortcomings he sees in the modeling and characterization of biological materials and his goals for addressing them.

1.1. PROBLEM IDENTIFICATION

What is force? It seems such a simple question, but the author has long struggled to reconcile the gulf between the macro view of force used by engineers and what physicists say is the true, very-small nature of force. The following is a summary of his search for a better understanding of force and how it operates within materials and structures.

1.1.1. History of Force. Engineering students are told in their sophomore year that force is a vector quantity, with magnitude and direction. They are trained how to model, add, subtract and replace these quantities with equivalent ones on a variety of structures. Shortly thereafter they are told that torque can be represented by a pair of forces, and they go on to do the same kind of operations with torques.

It is not long before force, torque, centroids, moments of inertia, stress, strain, energy, and power become almost trivial and the focus shifts to the design of better, faster, safer, more efficient devices and processes. But what, fundamentally, is force?

1.1.1.1 From antiquity to Newton. Looking at ancient structures that have survived earthquakes, weather and human attack, it is obvious that the cultures responsible for these structures had a good understanding of force and materials and how the two interact. What we now call *statics* was first developed by the Greeks, with

Archimedes (287-212 BC) describing the equilibrium of levers and how to locate centers of gravity. The engineering skills gained by the Greeks and Romans were set aside during the Middles Ages, but interest grew again during the Renaissance. Leonardo da Vinci (1452-1519) described mechanics as "the paradise of mathematical science because here we come to the fruits of mathematics" (Timoshenko, 1983). Simon Stevin (1548-1620) was considered to have a "complete doctrine of equilibrium" (Cajori, 1899). In 1586 he published De Beghinselen der Weeghcons in which he described the *triangle of forces* and used an early form of vector mathematics to evaluate the static loads on machine elements (Otto and Wood, 2001). Galileo Galilei (1564-1642) is credited with initiating the field of *dynamics*. He also understood centrifugal force and formulated the *parallelogram of forces* (Cajori, 1899). During this same period Descartes developed a theory of vortices, which was widely accepted during the early years of Isaac Newton (1643-1727) and is described as follows.

> All space is filled with a fluid, or ether, the parts of which act on each other and cause circular motion. Thus the fluid was formed into a multitude of vortices of different size, velocity, and density. There is an immense vortex around the sun… Each planet is in the center of another vortex… Still smaller vortices produce cohesion between parts of a body. (Cajori, 1899)

In 1638 Galileo published *Discoursi e Dimonstazioni matematiche*, which described stress analysis in beams (Otto and Wood, 2001). Edme Mariotte (1620-1684), Antoine Parent (1666-1716), and C.A. Coulomb (1736-1806) further developed the distribution of forces in the cross section of beams (Timoshenko, 1983). In 1687 Newton published Philosophiæ Naturalis Principia Mathematica, where he provided an explicit definition of force—"as the time-derivative of momentum" (Wikipedia, 2008a). The text is arguably "the most influential book in the history of science" (Wikipedia, 2008c) because it laid the groundwork for classical mechanics and the basis for modern engineering.

1.1.1.2 The link between force and matter. With the formation of engineering schools during the eighteenth century, and thereby increased exposure to the best mathematicians and scientists of the day, the understanding and use of mechanics

grew (Timoshenko, 1983). In 1753 Leonhard Euler (1707-1783) published *Recherches sur la veritable courbe que decrivent les corps jete dans l'air ou dans un autre fluid quelconque*, which applied Newtonian mechanics to engineering analysis (Otto and Wood, 2001). In his second volume of Natural Philosophy, Thomas Young (1773-1829) not only presented solutions to practical problems of his day but estimated the size of molecules (Timoshenko, 1983). The following excerpts by Stephen Timoshenko (1878-1972) provide a fairly detailed background to this connection between force and matter.

> The idea had existed since Newton's time, that the elastic properties of bodies can be explained in terms of some attractive and repulsive force between their ultimate particles. This notion was expatiated by [Roger Joseph] Boscovich [1711-1787] who assumed that between every two ultimate particles and along the line connecting them forces act which are attractive for some distances and repulsive for others. Furthermore, there are distances of equilibrium for which these forces vanish.
>
> Using this theory, with the added requirement that the molecular forces diminish rapidly with increase of the distances between the molecules, [Pierre-Simon] Laplace [1749-1827] was able to develop his theory of capillarity.
>
> The application of Boscovich's theory in analyzing the deformations of elastic bodies was initiated by [Siméon Denis] Poisson [1781-1840] in his investigation of bending of plates. He considers the plate as a system of particles distributed in the middle plane of the plate. A further advance was made in the molecular theory of an elastic body by [Claude-Louis] Navier [1785-1836]. He assumes that there are two systems of forces…acting on the particles of an elastic solid. The forces…balance each other… They are assumed to be proportional to changes…of the distances between the particles and to act along the lines connecting them.
>
> The next important advance made with the theory of elasticity is due principally to the work of [Augustin-Louis] Cauchy [1789-1857]. Instead of discussing molecular forces between the individual particles, he introduced the notions of strain and stress and in this way immensely simplified the derivation of the fundamental equation.
>
> Cauchy…applies the notion of pressure on a plane (a concept which was familiar to him from hydrodynamics) and assumes that this pressure is no longer normal to the plane upon which it acts in an elastic body. … The total stress on an infinitesimal element of a plane taken within a deformed elastic body is defined as the resultant of all the actions of the molecules situated on one side of the plane upon the molecules on the other, the directions of which (actions) intersect the element under

> consideration. By dividing the total force by the area of the element, the magnitude of stress is obtained.
>
> The principal results obtained by Poisson [1781-1840]… Starting his work with a consideration of a system of particles between which molecular forces act, he obtains the three equations of equilibrium and the three conditions at the boundary. These are similar to those given previously by Navier and Cauchy. He proves that these equations are not only necessary but that they are also sufficient to ensure the equilibrium of any portion of the body. He succeeds in integrating the equations of motion and shows that if a disturbance is produced in a small portion of a body, it results in two kinds of waves. In the faster moving wave, the motion of each particle is normal to the wave front and is accompanied by volume changes (or dilation); in the other wave the motion of each particle is tangential to the wave front and there is only distortion without volume change during the motion. (Timoshenko, 1983)

Gabriel Lamé (1795-1870) and Benoît Paul Émile Clapeyron (1799-1864) later showed that for a point in an elastic body "for each plane passing through the point, the ends of all such vectors will be on the surface of an ellipsoid," called the Lamé stress ellipsoid. Lamé later published the first book on theory of elasticity—"Leçons sur la Théorie Mathématique de l'Élasticité des Corps Solides" (Timoshenko, 1983).

> In the closing chapters, Lamé discusses the principles upon which the foundational equations of the theory of elasticity are based. He no longer favors the use of Navier's derivation of the equations (involving molecular forces) and prefers Cauchy's method (in which only the statics of a rigid body is used). Then he takes up Cauchy's assumption that the components of stress are linear functions of the components of strain. With isotropic materials, this assumption leads us to require two elastic constants which can be found from simple tension and simple torsion tests. In this way, all the necessary equations are obtained without making any hypotheses regarding molecular structure and molecular forces. (Timoshenko, 1983)

1.1.1.3 Faraday's views on force. Michael Faraday (1791-1867) studied the lines of magnetic force and said, "Such lines may possibly be lines of flow of ether, lines of action at a distance or lines of vibrations" (Berkson, 1974). He concluded that, "What is needed is a new mechanics—a mechanics of the force field."

> …Faraday ascribed continuous motion in space and time to the lines of force; and he believed from very early in his career that force is conserved. … Faraday believed that force conserved its identity through continuous changes in space and time. This is the hallmark of a physical substance, and it was precisely this which Einstein…denied. (Berkson, 1974)

Berkson (1974) points out that Faraday didn't mean *energy* or *power* when he described *conservation of force*, unlike others of his day (e.g. On the Conservation of Force by Hermann von Helmholtz). Instead, Faraday commented, "What I mean by the word *force*, is the cause of a physical action; the source or sources of all possible changes amongst the particles or materials of the universe" (Faraday, 1857). Gooding (1980) noted that, "Faraday's forces are not mere properties of more fundamental entities: they are the active basis of physical activity. … The concepts of (inertial) mass, space and time are not fundamental in his system."

> Faraday's discovery of electromagnetic induction in August 1831 followed nearly a decade of unsuccessful attempts to produce electrical effects directly from magnetism. Historians have stressed the importance of Oersted's discovery of 1820 and Faraday's belief in the unity of correlation of force… Faraday's explanation of his next major discovery—the law of the definite chemical action of electricity—also relies directly on the quantitative determinacy of 'force' during conversion. … Of course, voltaic electricity is evolved by the *decomposition* of matter, not the *conversion* of atoms of matter directly into force. (Gooding, 1980)

Faraday promoted that "electricity and magnetism propagate as a series of interconversions of mutually perpendicular forces. In 1846 he proposed that light is transmitted as a vibration in the lines of force…" His wave theories led to his view of a force field, where "A single atom, mass, charge, or magnetic pole cannot be perceived without the field, in which its properties are manifested as transfers of force" (Gooding, 1980).

1.1.1.4 Modern views. As witnessed by the following excerpts, Faraday may have been the last firm believer in the fundamental nature of force.

> But whereas he [Faraday] continued to treat forces both as causes and as entities essential to conversion, his contemporaries came to deny the reality of force in either role. Mechanical force is not conserved, does not possess energy (except in the colloquial sense, of 'activity'), and is not observable as such. It is merely a theoretical intermediary between energy states. (Gooding, 1980)

> With the Cartesians *work* as a derived notion; with the Leibnizians *force* was a derived notion. … The Cartesian view, followed by Newton and the modern writers of elementary text-books, makes force, mass, momentum, the original notions; the Leibnizian view, followed usually by [Christiaan] Huygens [1629-1695] and by the school of [Jean-Victor] Poncelet [1788-1867], makes work, mass, *vis viva* (energy), the original notions. (Cajori, 1899)

James Maxwell (1831-1879) answered Faraday's appeal for a new type of mechanics with his classical electromagnetic theory, which is considered the "second great unification in physics" (Nahin, 1992), with Newton's work being the first. William Thomson (Lord Kelvin, 1824-1907) and Albert Einstein (1879-1955) are said to have "both regarded forces as a redundant feature to be eventually eliminated" (Berkson, 1974).

> …with Faraday we have a field of substantial forces which obey non-Newtonian laws; with the ether theory [of Kelvin] we have a substantial, non-force ether obeying Newton's laws; and with Einstein we have a non-force, not fully substantial field obeying new non-Newtonian field laws. (Berkson, 1974)

Within the twentieth century Standard Model of elementary particle physics, massless force carrying particles are called bosons, which include the gluons (strong nuclear force), photons (electromagnetic force), W+, W-, and Z (weak nuclear force), and graviton (gravitational force). Force is said to occur due to the exchange of these particles (Pink, 2007).

Bosons do not obey the Pauli Exclusion Principle, which states that "no two of the same type [particle] can exist in the same state at the same place and time" (Stanford Linear Accelerator Center [SLAC], 2008a). Instead, bosons, "in a certain sense, favor states with many particles in the same state" (SLAC, 2008b).

The following is an interesting description of the fundamental nature of force from Wikipedia.com.

> In modern particle physics, forces and the acceleration of particles are explained as the exchange of momentum-carrying gauge bosons. With the development of quantum field theory and general relativity, it was realized that "force" is a redundant concept arising from conservation of momentum (4-momentum in relativity and momentum of virtual particles in quantum electrodynamics). The conservation of momentum, from Noether's theorem, can be directly derived from the symmetry of space and so is usually considered more fundamental than the concept of a force. Thus the currently known fundamental forces are considered more accurately to be "fundamental interactions". (Weinberg, 1994)
>
> When particle A emits (creates) or absorbs (annihilates) particle B, a force accelerates particle A in response to the momentum of particle B, thereby conserving momentum as a whole. This description applies for all forces arising from fundamental interactions. While sophisticated mathematical descriptions are needed to predict, in full detail, the nature of such interactions, there is a conceptually simple way to describe such interactions through the use of Feynman diagrams. … The utility of Feynman diagrams is that other types of physical phenomena that are part of the general picture of fundamental interactions but are conceptually separate from forces can also be described using the same rules. …
>
> It is a common misconception to ascribe the stiffness and rigidity of solid matter to the repulsion of like charges under the influence of the electromagnetic force. However, these characteristics actually result from the Pauli Exclusion Principle. Since electrons are fermions, they cannot occupy the same quantum mechanical state as other electrons. When the electrons in a material are densely packed together, there are not enough lower energy quantum mechanical states for them all, so some of them must be in higher energy states. This means that it takes energy to pack them together. While this effect is manifested macroscopically as a structural *force*, it is technically only the result of the existence of a finite set of electron states. (Wikipedia, 2008a)

This provides a somewhat satisfying tie between the explicit, fundamental models of physics and the non-fundamental models of engineering, where “force is usually defined only implicitly, in terms of the equations that work with it” (Wikipedia, 2008a).

1.1.1.5 Is there still value in force? Of course, the concept of force is still used and will continue to be used in engineering and other areas. Berkson even goes so far as to suggest that Faraday’s ideas on force may still have value.

> …Faraday sees the world as a field of forces whereas Einstein sees the field as curved space in which the concept of force is eliminated. … Does a force field allow for field behavior which cannot be formulated in the language of curved space? … It might be in the end that the field laws may be equally well described in terms of a force field or a curved space theory. … Just the existence of a different viewpoint may be very valuable for the development of new theory, as Maxwell pointed out in his paper 'On Physical Lines of Force'. (Berkson, 1974)

According to Berkson (1974), the logical starting point for this field would be with volume forces (force/distance^3). Perhaps in the same way Cauchy linked *pressure* and *stress*, which has served as the starting point for engineering analysis for the last two centuries, one may find a useful link between the *force density* of fluid mechanics and Faraday's vision of force?

1.1.2. Natural Materials. Today in many engineering programs the study of biology is seen as being just as relevant as chemistry, physics, and calculus. However, the field of engineering mechanics has struggled to satisfactorily describe the mechanical behavior of biological materials.

As seen in the last section, the concepts of stress and strain were developed and implemented in the same era that railway engineering was taking shape. Here large cast- and malleable-iron members were being used to create larger and more rigid structures (Timoshenko, 1983), and the size of these components was much larger than the substructure of the materials.

While the field of engineering mechanics has developed much since the days of Cauchy, the fundamental usefulness of stress and strain to the engineer remains the ability to resize components on paper, before a prototype or the actual product is built, in order to optimize the design for safety, cost, etc. Today, many engineered components are made from composite materials and at sizes which approach the size of the material substructure, where "the classical continuum representation of a material depends on the structure size to be much smaller than the specimen size" (Butchner and Lakes, 2003).

The author's feeling is that the current era of functionally-graded, multi-phase, hierarchical and/or biological materials and advances like nano-range construction necessitates a second look at the fundamentals of mechanics. Can a new paradigm be

found to augment, or perhaps replace, the concepts of stress and strain and help the engineer to better deal with these issues?

1.1.2.1 The hierarchy of natural materials. Materials scientists and engineers can control many of the characteristics of engineered materials, but the same cannot be said of natural materials. Here, there is very little direct control over the external shape (morphology), internal structure (anatomy), chemical makeup, etc. In light of the following, classical mechanics schemes become more and more inadequate.

> The seven hierarchical levels in the [Euplectella] sponge skeleton represent major fundamental construction strategies, such as laminated structures, fiber-reinforced composites, bundled beams, and diagonally reinforced square-grid cells, to name a few. (Aizenberg et al., 2005)

> The hierarchical order of a material may be defined at the number of levels of scale with recognized structure. … Hierarchical structures in biological materials span many orders of magnitude; from the macromolecular level (tropocollagen units, 10^{-9} m in diameter) up to whole organisms such as trees (giant redwood, 10 m trunk diameter at base). … Integrated sub-structuring is the common theme of biological materials, far more subtle and extensive than in any man-made material or structure. … When problems arise on another scale they cannot be solved with previous parameters. (Elices, 2000)

Table 1.1 provides a quick comparison of the hierarchical levels of metals, biological systems in general, bone, muscle, and wood.

1.1.2.2 Common building blocks. What are the design principles of natural materials? According to Campbell, Mitchell and Reece (1997), "Life has a simple yet elegant molecular logic: Small molecules common to all organisms are ordered into macromolecules, which vary from species to species and even from individual to individual." A nice introduction to this logic is provided in the following.

> *polypeptides* – A peptide is defined in biochemistry as a molecular structure composed of two or more aminoacids covalently linked. A chain of peptides (10-100 elements) is called a polypeptide, and one or more polypeptides may link to form a protein. Proteins, even though assuming different roles, such as enzymes, receptors and hormones, are mainly employed for architectural purposes in the living cell. This is the function of a large group of water-insoluble proteins, the scleroproteins, which can

Table 1.1. Comparison of Hierarchical Levels

<table>
<tr><th>Length (m)</th><th colspan="2">Metals</th><th colspan="2">Biology</th><th>Bone</th><th colspan="2">Muscle</th><th>Wood</th></tr>
<tr><td>10^{-10}</td><td></td><td rowspan="3">atomic, crystallo-graphic, monomeric</td><td colspan="2" rowspan="3">molecular</td><td></td><td colspan="2"></td><td></td></tr>
<tr><td>10^{-9}</td><td></td><td>collagen molecule</td><td colspan="2" rowspan="2">tropo-collagen, micro-fibril</td><td></td></tr>
<tr><td>10^{-8}</td><td rowspan="6">micro-structure</td><td></td><td></td><td>proto-fibrils</td></tr>
<tr><td>10^{-7}</td><td></td><td></td><td rowspan="2">organelle</td><td>hydroxyapatite, collagen fibril</td><td rowspan="2">fibril</td><td>sub-fibril</td><td rowspan="2">micro-fibrils, cellulose fibers, laminated cell walls</td></tr>
<tr><td>10^{-6}</td><td></td><td rowspan="3">cellular</td><td>collagen fiber</td><td></td></tr>
<tr><td>10^{-5}</td><td></td><td></td><td>lamellae</td><td rowspan="2">fibroblasts</td><td></td><td>cell diameter</td></tr>
<tr><td>10^{-4}</td><td></td><td></td><td>Haversian osteon</td><td>fascicle</td><td></td></tr>
<tr><td>10^{-3}</td><td rowspan="4">macro-structure</td><td></td><td></td><td></td><td></td><td></td><td>cell length</td></tr>
<tr><td>10^{-2}</td><td colspan="2">organ</td><td rowspan="2">organ</td><td colspan="2" rowspan="2">organ</td><td rowspan="2">growth rings</td></tr>
<tr><td>10^{-1}</td><td colspan="2">organ system</td></tr>
<tr><td>10^{0}</td><td></td><td colspan="2">organism</td><td>organ system</td><td colspan="2">organ system</td><td rowspan="2">trunk</td></tr>
<tr><td>10^{1}</td><td></td><td></td><td></td><td></td><td></td><td></td></tr>
</table>

be found in skin, ligaments, tendons, bone, cartilage, hair, nails, among others. Belonging to the scleroproteins are some of the most important proteins in biochemistry: collagens, elastins, myosin and actin, to name a few.

- *collagen* – The collagen fibril is a complex structure composed of many collagen rods linked together. A single collagen rod is composed of three polypeptidic chains wrapped around one another in a triple helix. It is, the main component of a number of tissues, such as cartilage, tendons, and ligaments.
- *elastin* – Elastin is constituted by many polypeptide chains crosslinked together. The disarranged distribution of cross-links is responsible for its rubber-like properties: the molecules uncoil when stretched and regain spontaneously the original shape as soon as the stretching force is relaxed. In coexistence with collagen, elastin determines the elasticity and compliance of the structure: the higher the percentage of elastin, the higher the elasticity.

- *myosin* – Myosin is a very long fibrous protein composed of two light and two heavy polypeptidic chains. The heavy chains form a helicoidal rod with two heads at the extremities, to which the two light chains are linked. It is the longest polypeptidic chain known to exist, and is responsible, together with actin, for the contraction of the muscles.
- *actin* – Actin is shorter than myosin, and typically exists as a monomer G-Actin and in the polymerized form as F-Actin.

polysaccharides – Polysaccharides are relatively complex polymers composed of many monosaccharides (sugars) joined together, which makes them very large, often branched, water insoluble molecules. Two of the most important structural polysaccharides are cellulose and chitin.

- *cellulose* – Cellulose is a polysaccharide made of more than 3,000 glucose units covalently bonded together. It is the most important structural component of plant cell walls, and it makes up 90% of cottons and 50% of woods, ranking as the most abundant organic compound in the world. Even though glucose is an extremely important substance in our body (it is the sugar used in cellular respiration), cellulose cannot be digested by humans for lack of the appropriate enzymes. Animals like cows, sheep and horses are, on the contrary, able to hydrolyze cellulose.
- *chitin* – Chitin is an unbranched polysaccharide analogous in chemical structure to cellulose, composed of units of a nitrogen containing glucose derivative. It is the main constituent of the exoskeleton of arthropods (like crabs, lobsters and insects), which covers the body and is periodically replaced by a new shell. Chitin is rigid except when it is cast off very thin, to allow for movement of adjacent body segments. It is also found in the cell walls of some fungi.

minerals – Minerals are natural crystalline compounds formed through geological processes. They range in composition from pure elements to simple salts to very complex silicates with thousands of known forms (organic compounds are usually excluded). One of the most important minerals in biological structures is hydroxyapatite (contained in bones and teeth). (Conza, 2005)

1.1.2.3 Wood anatomy. Tree substructures cross approximately ten orders of magnitude in metric size and eight hierarchical levels:

- trunk (10^1 m diameter)
- bulk tissue (wood)
- laminated annual growth layers
- individual cells (average 4 mm length and 40 μm diameter in loblolly pine)

- laminated cell walls
- cellulose fibers
- microfibrils
- protofibrils (10^{-8} m diameter)

The mesostructure in trees is composed of annual rings of earlywood (spring) and latewood (summer), differentiated by cell diameter and wall thickness. The modulus of elasticity for individual latewood fibers has been shown to be 30% to 700% higher than for earlywood fibers (Biblis, 1969; Groom, Mott, and Shaler, 2002a,b,c). However, attempts to show mesostructure trends through the height of the tree, typically using small groupings of cells in tension or flexure, have been inconclusive or even contradictive (Cramer et al., 2003; Kretschmann et al., 2002).

1.1.2.4 Hierarchy in the human body. Bone, which has been described as "fibrous, laminar, particulate, and porous structure at different size scales," (Lakes, 1993) has the following structural hierarchy.

organ: whole-bone
tissue: cortical, trabecular
microstructure: osteons, trabeculae

- Haversian osteon, 200 mm
- lamellae, 10 mm
- collagen fiber, 1 mm
- hydroxyapatite, collagen fibril, 100 nm
- collagen molecule, 1 nm

Muscle has the following substructure components (Bartel, Davy and Keaveny, 2006).

- fiber (or muscle cell), 10-100 micron diameter
- myofibrils (or myofibers), 1-2 micron diameter
- thin myofilaments, 6 nm diameter
- thick myofilaments, 16 nm diameter

The hierarchy for tendon and ligament is provided in Table 1.2.

Table 1.2. Comparison of Tendon and Ligament Substructure (Kastelic, Galeski, and Baer, 1978)

Tendon	Ligament
fascicle, 100-500 μm	fascicle, 250 μm diameter or larger
fibroblasts, 50-300 μm	sub-fascicular unit, 100-250 μm
	fibers, 1-20 μm diameter
fibril, 50-500 nm diameter	fibril, 150-250 nm diameter
sub-fibril, 10-20 nm diameter	sub-fibril, 10-20 nm diameter
micro-fibril, 3.5 nm diameter	micro-fibril, 3.5 nm diameter
tropo-collagen, 1.5 nm diameter	tropo-collagen, 1.5 nm diameter

1.1.2.5 Biological response to force. Natural materials often have the remarkable ability to adapt to their load environment. *Mechanobiology* studies the interaction between mechanical signals and biological processes in cells and tissues (Bartel, Davy and Keaveny, 2006). Lang (2007) describes the *mechanome*, which "has been developed to describe the general role of force, mechanics, and machinery in biology. Like the genome, the mechanome promises to improve our understanding of biological machinery and ultimately open the way to new strategies and targets for fighting disease. … Higher level mechanical systems include musculoskeletal, respiratory, cardiovascular, lymphatic, and integumental systems."

Lang also defines *mechanotransduction* as "the process whereby cells actively respond to mechanical signals through changes in morphology, signaling, and biochemical response." As an example he offers that "mesenchymal stem cells grown on a matrix with elasticity resembling that of tissues such as 1 kPa brain, 10 kPa muscle, and 100 kPa bone differentiate into cells resembling neurons, muscles, and osteoblasts, respectively." He offers the following in regard to experimental techniques.

> A broad range of complementary force-probe methods can meet these force requirements. These include the atomic force microscope (AFM), micropipette manipulation, magnetic traps, microfabricated canti-levers, and optical traps. ... Many additional advances, such as light-based methods of laser scissors, photobleach recovery, triggering, un-caging, and

time-resolved measurements, can be integrated to produce powerful new tools.

1.1.2.6 Wood's adaptive nature. Thigmomorphogensis, the mechanically adaptive behavior of trees as new cells are formed under load, is commonly documented. Mattheck (1991) concluded that trees self-optimize by equalizing mechanical stress levels on the tree surface, through changes in external geometry. He also noted that annual growth rings align with principal stress trajectories, resulting in minimized shear and maximized tension and compression loading along the rings. Much research effort has focused on sub-cellular characteristics, primarily examining arrangement of cellulose fibers within the cell wall.

One study showed that mechanical flexure of the juvenile trunks of two Populus hybrids resulted in increased radial growth, especially in the direction of the loading, decreased height to diameter growth ratio, and increased flexural rigidity (Pruyn, Ewers, and Telewski, 2000). One hybrid showed increased elastic modulus whereas the other did not. Similar trends have been seen in other plants, e.g. elm (Ulmus Americana) (Telewski, and Pruyn, 1998), kale (Brassica napus) (Cipollini, 1999), and tobacco (Hepworth and Vincent, 1999).

Natural tree loads tend from wind, ice, direct contact with other objects, and gravity. The mechanism to equalize surface stress can be overruled by other tropisms, such as heliotropism as the tree reaches (leans) for more light (Jeronimidis, 2000). Unbalanced loads on the trunk and limbs lead to *reaction wood* (*compression wood* in softwood species and *tension wood* in hardwood species), characterized by increased density, eccentric growth, and altered strength and dimensional stability (Forest Products Laboratory [FPL], 1999). Compression wood has also been connected to increased stem respiration, inhibition of terminal shoot growth (Little and Lavigne, 2002), and altered shoot hydraulic properties (Spicer and Gartner, 2002).

Juvenile wood, typically defined as material 5 to 20 rings from the pith in softwoods, is known to have significantly different strength and stiffness characteristics from mature wood (FPL, 1999). Shortleaf pine generally sheds lower limbs as it grows, unless neighboring trees are absent and direct sunlight reaches the lower limbs. It should be noted that juvenile trunk tissue is locally influenced by wind, ice and gravity loading

carried by the limbs into the trunk, whereas these loads only secondarily influence trunk tissue developed later in the absence of limbs. The author speculates that the switch from local stress fluctuations in juvenile wood to a uniform state of flexure and compression in the mature trunk leads to the observed property changes.

1.1.2.7 Adaptation of bone. While there is no consensus on the exact cause and effect, the following is an interesting description of bone's adaptive ability.

> The small-scale architecture of our bones constantly changes. The distal region of the femur is fully replaced every 5 to 6 months. Bone is remodeled in response to the mechanical stress it experiences. For example, both the osteons of compact bone and the trabeculae of spongy bone are constantly replaced by new osteons and trabeculae that are more precisely parallel to newly experienced compressive stresses. Furthermore, bone grows thicker in response to the forces of exercise and the force of gravity. At birth, all bones are relatively smooth and featureless. However, as the child uses its muscles more and more, the bones develop projections and other markings. (Marieb and Mallatt, 1997)

1.1.2.8 Modeling natural materials. Buechner and Lakes (2003) point out that "a classically elastic or viscoelastic continuum view of bone does not correspond to reality since classical continua allow no size effects." Niklas (1992) describes a similar situation in botany.

> Even at a particular developmental instant, most plant materials exhibit properties that conform to those of neither ideal solids nor ideal fluids. ...we will see that our ability to treat viscoelastic plant materials is limited to phenomenological descriptions of their behavior. This inadequacy stems from the fact that most plant materials show nonlinear viscoelasticity, for which no adequate mechanistic theory has as yet been developed. (Niklas, 1992)

As one last example, Shadwick (1998) points out some interesting design features and challenges of arteries.

> Like most biological materials...blood vessels exhibit nonlinear elasticity. ...nonlinear elasticity gives arteries the particular capability needed for a cylindrical vessel. ...a blowout pressure...about 10 times the normal mean

> blood pressure of a healthy adult... ...deflating arteries lose 15-20 percent of their potential strain energy. ... The lost strain energy helps to attenuate pressure pulses that propagate along arteries.
>
> In other experiments, Roy investigated the thermoelastic properties of arterial tissues. He showed that an artery wall releases heat during extension, and that applying heat to a piece of artery that has been stretched by a suspended weight reduces the amount of stretch. In other words, heating makes artery walls stiffer, so that an applied stress produces less strain. These properties appeared contrary to the known behavior of crystalline elastic solids, but Roy recognized that an artery wall had an elastic mechanism that was thermodynamically like that of caoutchouc, natural latex rubber, although the physics of this type of elastic material was not understood in Roy's day. Modern research on synthetic rubber-like polymers, as well as on animal rubbers like elastin, has revealed that the elasticity of such polymer networks arises from changes in the entropy of the molecular chains. An imposed strain increases order in the molecular network, thereby decreasing its entropy. The elastic force arises from the tendency of the network to return to conformational states of higher entropy, or disorder, according to the laws of thermodynamics. (Shadwick, 1998)

1.1.3. Mechanical Characterization. Material properties are often divided into physical, chemical, mechanical, thermal, electric, magnetic, acoustic, and optical classes (Davis, Troxell, and Wiskocil, 1964). Structural designers focus on a subset of these, with the mechanical class of properties receiving the most attention. These properties include responses of the material to various load inputs, such as strength, stiffness, ductility, and durability. The following gives an overview of mechanical characterization techniques for engineered composites.

1.1.3.1 Response models. Mechanical characterization is based upon a combination of material models and mechanics models. Materials are usually classified as having an elastic, plastic, viscoelastic, or combination deformation response to various load types. Mechanics models then try to tie the macroscopic response with the microscopic structure of the material – crystal structures for homogeneous materials and constituent properties and geometries for inhomogeneous materials. These mechanics models include mechanics of materials, elasticity, plasticity, viscoelasticity, aeroelasticity, energy methods, continuum mechanics, micromechanics, fracture mechanics, fatigue analysis, modal analysis, and plate and shell theory.

The concepts of stress and strain are introduced to provide scalability between geometries for laboratory specimens and real-world applications. The generalized Hooke's law for relating stress and strain is given by $\sigma_{ij} = E_{ijkl}\,\varepsilon_{kl}$ where the 81 components of the fourth-order tensor E_{ijkl} are known as the *elastic constants* (Agarwal, Broutman, and Chandrashekhara, 2006; Boresi, Schmidt, and Sidebottom, 1993; Haddad, 2000). For materials described by anisotropic, linear-elastic behavior, it can be shown that this tensor can be reduced to 21 distinct components. For orthotropic materials this number is reduced to nine components. For isotropic materials this number is further reduced to two components, commonly known as Young's modulus and Poisson's ratio.

Mechanical testing facilities are typically tasked with determining the numerical values for these elastic constants and for ultimate strength and strain values. To complicate the matter, the components are influenced by conditions not easily accounted for by purely-mechanical models. The primary influences are test velocity and environmental conditions, which include many different variables, but most of the variables can be traced to time and energy variations on the system. Traditional testing methods fix most of these influences while studying the relationship between load and deformation (or stress and strain). Comparisons can then be made by incrementally changing certain variables if desired.

1.1.3.2 General characterization techniques. Table 1.3 was prepared to provide an overview of the numerous characterization techniques employed in determining mechanical properties (Kobayashi, 1987). As stated above, the basic goal is to measure deformation for various load inputs at given rate and environmental conditions.

1.1.3.3 Characterization of engineered composites. Composite materials are defined differently depending on context, but Figure 1.1 shows a classification scheme from a structural point of view.

As an example of the experimental approach to engineered materials with hierarchy, the following focus will be on fiber-reinforced composites. Unlike isotropic materials, where the mechanical properties scale predictably from laboratory-sized specimens to structural sizes using Hooke's law, composite materials typically require a stepped characterization approach from constituents, to lamina, to laminates, to products.

Table 1.3. Mechanical Characterization Categories

Load Methods	Rate Regimes	Deformation Measurement
tension	quasi-static	*point-per-point*
compression	dynamic	strain gages
bearing	cyclic	extensometers
shear	high strain rate	LVDT
hardness	creep	*full-field*
bend	stress rupture	photoelasticity
torsion	stress relaxation	moiré
pressure	fatigue	interferometry
multiaxial		shadow optical
combined		brittle coating
Environmental	**Nondestructive**	**Miscellaneous**
elevated/low temperature	penetrant	formability
moisture	magnetic	wear
chemicals	Eddy-current	modal analysis
corrosion	radiographic	residual stresses
	ultrasonic	fracture mechanics
	acoustic emission	stress concentration
	thermography	

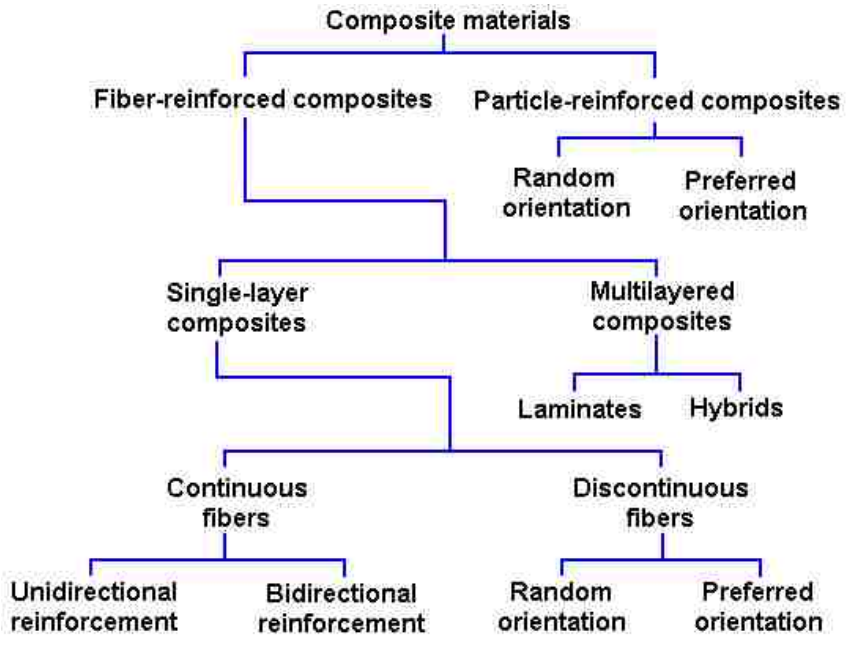

Figure 1.1. Classification Scheme for Structural Composites (Agarwal, Broutman, and Chandrashekhara, 2006)

In fiber-reinforced laminated composites, characterization of the constituent materials is performed for use in micromechanics models (Kobayashi, 1987; Carlsson and Pipes, 1987). These models are used to predict the behavior of the lamina. The most common test at this level is uniaxial tension. Accurate compression properties are difficult to obtain due to premature failure by crushing or buckling of the fibers, and flexure properties are also troublesome due to the combined tension-compression stress state.

Validation of the micromechanics models is then performed on the unidirectional lamina. Lamina characterization is also performed to fine tune the models for laminate behavior. Here a variety of traditional, quasi-static techniques are employed. Tension is used to determine the major and minor Poisson's ratios and the longitudinal and transverse Young's moduli, tensile strengths and ultimate tensile strains. Compression is still difficult to employ at this point due to fiber buckling, but a variety of fixtures have been designed to approximate the compressive properties of longitudinal and transverse compressive moduli, compressive strengths, and ultimate compressive strains. Full characterization requires that in-plane shear properties parallel to the fibers also be determined. These properties include shear modulus, in-plane shear strength, and ultimate shear strain. Test methods include the +/- 45^{o} coupon, 10^{o} off-axis, rail shear, and torsion tests.

At the lamina level of analysis several other quantities, that are not necessarily mechanical in nature, may become of interest to the design engineer. These quantities include density, fiber volume ratio, longitudinal and transverse coefficients of thermal and moisture expansion, glass transition temperature, and fiber pullout properties.

Characterization of the laminate and validation of the lamination models are performed next. The laminate properties are used to predict product behavior. However, multiaxial laminate performance is hard to predict from lamina properties alone, so empirical results are added to the mechanics models at this point using the following tests: off-axis coupon or ring, cross-beam sandwich specimen, bulge plate, rectangular plate in biaxial tension, and thin-walled tubular specimen. Fracture and stress concentration characterization is also performed at this level. Fracture mechanisms and

modes, initiation, and propagation are studied from the fracture mechanics side, and holes, fillets, and cracks are studied from the stress concentration side.

In addition to the traditional static techniques, some lamina and laminate properties can be determined with dynamic, non-destructive techniques (Raju and Gibson, 1993). Such techniques include, but are not limited to, acoustic emission and scattering, ultrasonic testing, and vibration testing. Similar approaches have also been used to locate and study flaws in laminates and finished products.

As the last step in the iterative evaluation process, characterization of the product is performed. Methods are continually being developed or enhanced to test for integrity and reliability of full-scale structures.

While the above technique appears somewhat straight forward, one should note that wood—one of the most basic of building materials—has twice as many hierarchical levels and spans a far great spatial range. Designing a test regime that spans all of these levels, carrying it out, and then making use of the data seems monumental. This will be addressed in more detail in Section 3.

1.2. NEED

A gulf currently stands between the practical, everyday definition of force in the engineering world and that of modern physics. The traditional definition of force based on Newtonian mechanics has served the engineering community well for three centuries, but advances in material design, medicine, and green construction (to name just a few) almost necessitate a reworking of Newton's ideals and the engineering mechanics models that have expanded over time from the basic concepts of stress and strain. Along with this, new spatially-scalable approaches to mechanical characterization will most likely be needed.

1.3. OBJECTIVES

The author's objectives over the term of this project have changed many times. As with most scientific (and creative) expeditions, where the map is created and refined

during the trip, the author has spent a lot of time going in what seem like circles. Perhaps he went in so many circles that he eventually became fixated with the helices of Section 4.

One goal that has remained consistent is the desire to better understand nature. Hopefully this document will provide evidence of that by showing what the author believes is a unique view of force. It is the author's desire that this view may someday afford engineers the opportunity to by-pass the conventional concepts of stress and strain and more directly link force and deformation. Millon (1991) points out that, "Prevailing frameworks must continue to be challenged, and imaginative alternatives encouraged."

Suppose force is a stream of items—perhaps particles smaller than an atom. This stream under certain circumstances could be represented by a force vector, and under other circumstances it could be represented by a moment vector. It might even be represented by a combination of normal and shear stresses or a *flow* of principal stresses. Also suppose that this stream travels through a material's atomic structure along a helical path, perhaps with the atomic cloud serving as a floating freeway. Why a helix? For starters, nature is full of them. Secondly, a helix is packed with mathematical variables that can be utilized by the materials scientist or engineer. By chance this concept might even be expanded to describe a variety of wave phenomena. Far fetched? Probably. Cranky? Sure. But interesting? The author thinks so.

While the author does not claim to be a physicist, he does like to borrow ideas from physics, biology, and a variety of other disciplines. His ultimate goal is to provide a new engineering tool for investigating the flow of force through materials and structures while enjoying the thrills of creative exploration.

1.4. TECHNICAL APPROACH

The approach followed by the author and presented in this document may seem a bit unorthodox but, then again, so is the objective. The author started out as a naturalist, observing widely the structures of plants, trees, and humans. The challenge quickly became one of cataloging and categorizing these observations because they crossed so many traditional boundaries.

> The field of biological materials and system is extensive, representing an interdisciplinary topic encompassing mechanics, materials science, and the breadth of engineering disciplines in conjunction with biology and medicine. (Brown, Peterson, and Grande-Allen, 2006)

The author eventually adopted the Library of Congress cataloging system to store his photographs, data, references, etc. This way he did not have to create his own system and continually revise it.

Without the luxury of a medical program on campus, the author limited his experimental investigations to botanical specimens. This way the specimens could be more easily and cheaply obtained, tested and disposed of. To span spatial dimensions the author focused on probe-based tests—hardness, instrumented indentation, and a simple, qualitative form of integrated photoelasticity.

The author used the principle of biomimetics, dimensional analysis, a variety of creativity techniques, and active teaching and experimentation to develop his thoughts.

The next section of this document looks at natural structures—helical structures in particular—and design principles that might be gleaned from them. Section 3 looks at the author's experimental efforts with oak and pine trees and discusses plans to map the mechanical properties throughout a tree. Section 4 introduces tools designed to help scientists and engineers search for and organize novel concepts. It also attempts to tie together all four sections of this document by developing the idea of force following a helical path through materials.

2. STRUCTURAL BIOMIMETICS

"What has fins like a whale, skin like a lizard, and eyes like a moth? The future of engineering." – Mueller (2008)

Much can be learned by observing the natural environment. The following section looks at biological materials and structures and makes comparisons to engineered materials. Helical structures both within and without biology are particularly highlighted.

2.1. LEARNING FROM NATURE

Biomimetics is "the study of the formation, structure, or function of biologically produced substances and materials (as enzymes or silk) and biological mechanisms and processes (as protein synthesis or photosynthesis) especially for the purpose of synthesizing similar products by artificial mechanisms which mimic natural ones" (Webster.com). Benyus (2002) offers some examples in Table 2.1.

Table 2.1. Application of Nature to Engineering (Benyus, 2002)

Natural System	Engineered System
lily pads and bamboo stems	architectural struts and beams
termite tower's steady 86 degrees F	central heating and air-conditioning
bat's multifrequency transmission	stealthy radar
dolphin's skin, butterfly's proboscis	smart materials
rotary motor in bacteria flagellum	wheel, motors

She continues by saying, "If the biomimics had their way, these lessons would be the backbone of every materials engineer's education:

1. life-friendly manufacturing processes

a. powered by sunlight
b. recycle everything
c. curb excess from within

2. ordered hierarchy of structures
3. self-assembly
4. templating of crystals with proteins"

A recent example of the biomimetic progress in adhesive science is described as, "A new type of dry glue designed to mimic gecko feet is 10 times stickier than the gravity-defying lizards, and three times stickier than other gecko-inspired glues…" (Steenhuysen, 2008).

Fisher (2001) emphasizes a fundamental difference between natural and engineered materials. Natural materials are constructed from smart molecules (proteins, carbohydrates, lipids, or DNA) and simple and robust processing, whereas engineered materials are constructed from simple elements (metal alloys, ceramics, or polymers) and sophisticated processing. Gao (2001) provides the example, "Sea shells are made of nano composites consisting of alternating layers of minerals and proteins. Such composites exhibit mechanical strengths which are orders of magnitude higher than the constituent phases alone."

2.2. BIOLOGICAL STRUCTURES

The author has spent several years studying the structure of plants, animals, and humans. He has dissected and photographed artichoke, bamboo, banana, beat, bean, bok choy, broccoli, carrot, celery, chayote squash, corn, endive, escarole, grapefruit, grape, kalarabi, leek, onion, orange, parsnip, radish, rhubarb, spinach, swish chard, and turnip plants. He has done the same with trees, bamboo, vines, etc. Many of these photographs are used in his class notes and available to the public on his academic web site. Figure 2.1 provides a small sampling of these photographs.

As hinted to in Figure 2.1, trees are great examples of efficient cantilever beams, and the cell orientation around stress concentrations such as limbs can be related to fiber-reinforced composites. Broccoli has a thick fibrous shell penetrated by smaller fiber bundles that continue into the florets. Celery can be related to reinforced concrete, but

here the fibers only appear on the tension side, due to wind loading, of each stalk. An interested reader should compare these fiber locations to that of rhubarb. A reinforcing ring of fibrous material is located where a celery stalk begins to leaf off and stress concentrations might cause the stalk to rip. Fibers from a celery leaf cross over fibers running down the stalk and join further inside the stalk, again relating to design guides for fiber-reinforced composites. Kalarabi offers an interesting example for anchoring of fibrous composites. Red leek has rows of unconnected fibers in regions where the stress field appears more uniform, but the fibers begin to intersect near stress concentrations and the material edges.

An interesting observation made by the author is that maple seeds—the natural *helicopters* enjoyed by children—and some insect wings, as seen in Figure 2.2, both follow a helical path as they are dropped.

The adaptation of trees to contact forces, structural defects, and mechanical overloads studied by Mattheck (1991) and described in his text *Design in Nature: Learning from Trees* was readily identified. Figure 2.3 shows some examples collected by the author. The *overload* images are for trees that were damaged due to excessive loads but survived. The deformed geometry caused reaction wood to form over time in response to the modified stress patterns in the trunk or limb. The *contact* examples show modified growth due to the trunk or limb making contact with metal fencing, an adjacent limb, and a vine. The *defect* examples show how the tree responded to a crack running parallel to the trunk or limb.

Perhaps in a few years, mechanically stimulated plants will have their properties tailored to end-use products, e.g. baseball bats that are stiffer yet less susceptible to cracking, musical instruments with unique acoustic signatures, and vegetables with unique textures. Plantations specializing in mechanical stimulation would sprout up, and the author's dream of growing civil structures would not be far off. For more information, one should look into the work of Axel Erlandson (1884-1964) and Richard Reames (arborsmith.com) and the Fab Tree Hab concept by Team H.E.D. [Human Ecology Design] at Massachusetts Institute of Technology (archinode.com/bienal.html).

Figure 2.1. Example Biological Structures

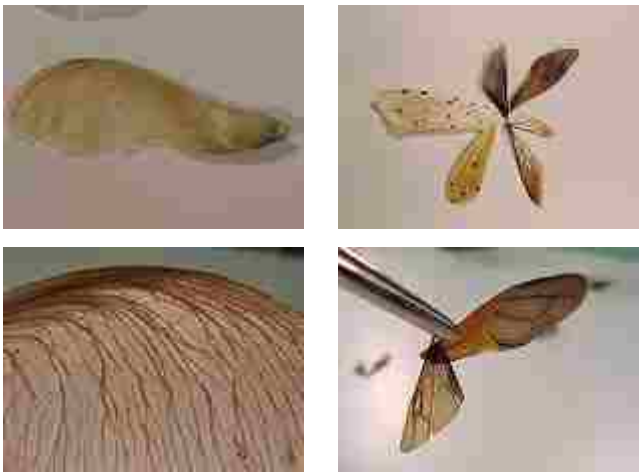

Figure 2.2. Comparison of Seeds and Wings

Obviously engineers and scientists can learn a lot from nature. The following discussion will point out what appears to be a common theme in nature—the helical structure.

2.3. ZOOLOGICAL HELICES

Most people think of DNA when they hear the word *helix* and rightly so. DNA is a right-handed double-helical macromolecule. The polypeptides and polysaccharides found in bone, muscle, cell walls of plants mentioned previously are also modeled as helical macromolecules. Conza (2005) points out that, "A single collagen rod is composed of three polypeptidic chains wrapped around one another in a triple helix." Going up a hierarchy level, collagen fibers are arranged in alternating helices in lamellae bone. The type I collagen found in the annulus fibrous of the intervertebral disc is arranged in alternating ±30-35° fiber orientations (Bartel, Davy, and Keaveny, 2006).

> [Cardiac] muscle cell orientation in the adult left ventricular myocardium, or muscle wall, is not uniform. Throughout the wall, the cells' angles are distributed from approximately -60° to +60°. The angle gradient is closely related to the left ventricle's ability to contract. (Biophotonics International, 2005)

Figure 2.3. Tree Adaptation

The egg capsules of dogfish are largely constructed from laminae of parallel orientated collagenous fibrils arranged longitudinally, near-diagonally, and near-transversely. (Hepworth et al., 1994)

Bowyer (2008) compares the "double helical braiding of collagen fibers in skin (or body wall)" of earth worms to octopus tentacles. He says, "Worms (and tentacles in general) work by balancing pressures against fibres and muscles in tension. Differential swelling produces bending and twisting motion."

The inner skeleton of the Venus Flower-Basket—a deep-sea sponge—is described as an "…intricately reinforced internal skeleton composed of glasslike silica. The skeleton gives shape to the animal and has a structure that is optimally reinforced for strength" (Discover, 2005).

> On a small part of the ocean floor close to the Philippine Islands lives a sponge called the *Venus flower basket*. This creature is curved like the sheath of a Turkish dagger, but circular around its long axis. The sponge owes its name to the structure of the inner skeleton of its mantle. This consists of a tissue of fine silica needles, perforated like the wickerwork of a wooden chair back. This tissue is interwoven both in a right-angled network and diagonally. The Venus flower basket is considered a masterpiece of biomineralisation: tiny elementary building blocks of silica (silicon dioxide) three nanometres in diameter first connect the cells of the sponge together in superfine layers. These are then rolled up to form the silica needles, the basic element of the wickerwork structure, which can withstand high pressure variations. (European Commission, 2004)

2.4. BOTANICAL HELICES

The following examples point to a similar helical architecture in plants.

> In most plants cells the cellulose fibres are laid down at a large angle to the longitudinal axis. Hence when the cell wall is softened and the cell expands it only extends. In cells of roots that have been severely impeded the fibres are laid down at a low angle to the longitudinal axis and so expand the cells outward. (Ennos, 2005)

A link between the structure of plant cells and engineered pressure vessels can be found in that, "Plants are high-pressure hydraulic micro-machines with pressures typically in the 0.5-2.0 MPa range" (Tomos, 1997).

Helices (and spirals) can again be found on multiple levels of hierarchy, for example not only in the cell wall but also in various macro-level components of the plant, described as follows.

> Curved and twisted structures are ubiquitous in nature, yet there are relatively few biomechanical studies involving large curvature and torsion. (Silk, 1997)

> Shoots are reinforced by an outer ring of rigid material and are rigid in both flexure and torsion. Shoots reinforced by isolating axially oriented fibres are rigid in flexure but compliant in torsion, while reinforcement by helically wound fibres gives a shoot that is compliant in both flexure and torsion. (Ennos, 2005)

> The beautiful arrangement of leaves in some plants, called phyllotaxis, obeys a number of subtle mathematical relationships. For instance, the florets in the head of a sunflower form two oppositely directed spirals: 55 of them clockwise and 34 counterclockwise. Surprisingly, these numbers are consecutive Fibonacci numbers. The ratios of alternate Fibonacci numbers are given by the convergents to phi E -2, where phi is the golden ratio, and are said to measure the fraction of a turn between successive leaves on the stalk of a plant: 1/2 for elm and linden, 1/3 for beech and hazel, 2/5 for oak and apple, 3/8 for poplar and rose, 5/13 for willow and almond, etc. A similar phenomenon occurs for daises, pineapples, pinecones, cauliflowers, and so on.
>
> Lilies, irises, and the trillium have three petals; columbines, buttercups, larkspur, and wild rose have five petals; delphiniums, bloodroot, and cosmos have eight petals; corn marigolds have 13 petals; asters have 21 petals; and daises have 34, 55, or 89 petals—all Fibonacci numbers. (Weisstein, 2008)

Figure 2.4 provides some examples of macro-level helices found in the twining nature of vines. Represented are vines that either wrapped around other vines or trees.

2.5. OTHER HELICES

In 1862 Alexandre-Emile Béguyer de Chancourtois “made the first true periodic table, a spiral on a cylinder, to display the periodic reoccurrence of properties with an unbroken sequence of elements” (AlexanderDesign, 2008). The Alexander Arrangement of the Elements is a modern, patented version of a helical periodic chart designed by Roy

Figure 2.4. The Twining Nature of Vines

Alexander (Scientific Consulting Services International, Port Angeles, WA, 2008). In 1865 James Maxwell "established light as a form of electromagnetic radiation – radio waves and X-rays are identical to light except for differing wavelengths and energies" (Weinstock, 2006). For mathematical convenience, wave phenomena are often represented as complex helical waves (complex phasors).

The following examples point out how soot particles naturally form as spirals and ice arranges into complex helical patterns under high pressure.

> For mature soot, the TEM images we and other researchers have obtained show that, internally, the particles consist of many thin layers of flat carbon structures arranged in a spiral pattern, vaguely similar to a rolled-up scroll. The particles seem to start at one or several nucleation sites, with growth curling around each of them. The build-up is made from layers of thousands of disordered pieces. (Shaddix and Williams, 2007)

> …the ice spontaneously transformed itself into nested helices with multiple strands. In a 1.35-nanometer tube at a temperature of minus 9 degrees Fahrenheit and 40,000 atmospheres of pressure, the ice became a double helix that somewhat resembles DNA in structure, expect the outer sheath has eight strands and the inner layer has four. In another simulation of a 1.9-nanometer tube at the same temperature, when the pressure was suddenly raised from 10 atmospheres to 8,000, the water abruptly froze into a helical formation with triple-layer walls. In this case, the outermost wall had 18 strands and the two ice sheaths nested inside of it each had six. "They are intertwined together like a braid of chains," explains Zeng. "At the highest pressures, we were surprised to find that the helix is the most stable formation of ice.
>
> This helix of ice is a cooperative arrangement of tens of thousands of molecules together. They have to act in a cohesive way to form this

> kind of unique structure. It's not like a polymer where they are already connected by strong bonds," Zeng says. (Saunders, 2007)

On a much larger scale, the *heliospheric current sheet* of the Solar System—"the surface within the Solar System where the polarity of the Sun's magnetic field changes from north to south" (Wikipedia, 2008a)—has a helical appearance. Ginzburg (2006) defines a *helicola* as "a multiple-level spiral in which a helical spiral of a certain level is wound around a spiral path of a helical spiral of an adjacent lower level." He goes on to say, "Since the Sun moves around the center of our galaxy, the Milky Way, at average velocity of about 240 km/s, the observer located above the center of our galaxy will see the Earth's path as a helical spiral wound around the Sun's path…an observer located far away from the path of the Milky Way, the Earth's path will look like a dual-level spiral in which one helical spiral is wound around another helical spiral."

These are but a few of the helices that can be observed in nature. Later sections will discuss the possibly of using the prevalence of natural helices as inspiration for a new concept of force.

3. EXPERIMENTING WITH TREES

"Like the tree that's in the backyard | Blown and battered by the wind | Our love will last forever | If it's strong enough to bend." – B. N. Chapman and D. Schlitz

As a child the author often played in the woods and on the sawdust piles around his grandparents' sawmill. Looking at trees and timber properties from a professional viewpoint seemed a natural step for him as an engineer. The following section describes some of his experimental investigations.

3.1. OVERVIEW

Trees have always been a great natural resource, and they offer excellent investigative potential as easily-obtained, renewable, non-toxic, inexpensive, hierarchical, functionally-graded specimens governed by few, if any, regulatory constraints on experimentation. The tree investigations carried out by the author are divided into two categories—property scaling and property mapping. In property scaling, the goal was to (someday) link wood's mesostructure properties to its bulk properties. In property mapping, the goal was to examine how the mechanical properties of wood vary with location in the tree.

A literature search showed that the first goal has been attempted, with mixed results (discussed later), using miniaturized versions of bulk tests to obtain mesostructure (annual growth ring) properties. Instrumented indentation has the potential of overcoming at least some of the shortcomings, due to the high degree of specimen processing, in these former studies. As far as the author is aware the second goal has not been attempted. The mesostructure data he has found fails to track the same growth rings up through the tree.

In a broader sense, the study was also designed to aid in the development of a scalable testing procedure that could be utilized in future botanical-mechanical studies made by the author and other researchers, such as:

1. comparison to numerical simulations of lumber, e.g. TREEFLEX (Gaffrey and Kniemeyer, 2002), where the modulus of elasticity is modeled as changing from one annual growth ring to the next.

2. minimizing stress concentrations in engineered composites based on design of botanical structures, e.g. fiber placement strategies in stalks of celery versus rhubarb, fiber branching in high-stress zones of leek stalks, and changing properties and geometries of tree-cells as they transition from root to trunk to limb.

3. improved tree plantation practices for optimizing strength and visual properties in specialized products, e.g. wood veneer, sporting equipment, musical instruments, and custom furniture.

3.1.1. Shortleaf Pine. Shortleaf pine (Pinus echinata), one of four commercially significant conifers found in the southeastern United States (Lawson, 1990), can be found in 22 States and is the only pine species native to Missouri (Settergren and McDermott, 2000). The United States Forest Service began designating national forests in 1934, and a nursery for shortleaf pine was created in Missouri the following year (Cox, 1997). The Missouri Department of Conservation assumed management of the nursery in 1947 and has since provided millions of seedlings for Missouri forests. Peek production occurred in 1966, with 14 million seedlings, and corresponds to when the trees studied by the author were planted. As of 2001, 160,900 acres of shortleaf and loblolly pine covered Missouri, with one-third under private ownership (Moser et al., 2003). The shortleaf pine trees selected for this study are representative of the most common size class (9 to 13-inch diameter at breast height) of growing stock in the state. As of 1997, 21 million hectares of shortleaf and loblolly pine covered the Eastern United States (USDA Forest Service, 2004).

3.1.2. Wood Testing and Modeling. Most macrostructure wood characterization, where growth rings are ignored and the material is modeled as a homogeneous, orthotropic continuum (Cramer et al., 2003), has been limited to uniaxial tension, compression and flexure, because these are the load types most common to lumber usage. Design factors (load duration, member geometry and orientation, temperature, etc.) are used to leapfrog from these simplified loading situations to the more realistic biaxial and triaxial stress states in structural members. Only in recent years

have combined loading and substructure characterization come under serious investigation, accompanied by modeling efforts to connect macrostructure and microstructure (individual cells) properties. However, these efforts often seem to skip the mesostructure and its accompanying variations in grain direction (diagonal, spiral, straight, wavy, irregular and interlocked). Using characterization of fiber-reinforced composites as a role model, it would be a daunting task to characterize laminates based on fiber and matrix properties without making an intermediate analysis of the lamina. In addition, lumber suffers from an intermediate level of complexity not seen in laminated composites due to saw-pattern variations. Plainsawn, quartersawn and riftsawn boards each have a different grain orientation relative to the boards' primary dimensions. These off-axis effects have been investigated (Liu and Ross, 1998; Liu, 2000; Liu, 2002).

Many of the bulk wood tests are similar to those for metals and polymers, so details will be saved for latter parts of this proposal. However, wood hardness testing differs from that of other materials, and instrumented indentation is a relatively new technique, so the remainder of this section is devoted to these two topics.

Doyle and Walker (1985) provide a nice historical overview of wood hardness testing. They point out that Janka testing is the standard technique in the United States and much of the world, while Brinell testing is preferred in Germany and Japan. Instead of relating the deformation caused by a specified indenter geometry and load to a hardness value, the Janka test records the load required to embed a 0.444" diameter indenter up to its radius as the hardness number. The test is typically performed in all three of wood's orthotropic directions and averaged in various ways.

Instrumented indentation differs from hardness testing in that load and penetration depth are continuously monitored during both loading and unloading. A host of indenter geometries, ways of relating the measured curves to bulk stress-strain curves, and routines for carrying out the load-unload cycle (single path, intermittent partial unloading, progressively larger load-unload cycles on the same location, smaller sine-wave loading superimposed on a large continuous load, etc.) have been examined (Haggag et al., 1990; Haggag and Murty 1996; MTS, 2004). Altering loading rates and dwell times, both during and between cycles, can be used to some extent to investigate viscoelastic properties. At the time of the author's investigations, ASTM International

subcommittee E28.06 had developed WK382 Practice for Instrumented Indentation Testing (ASTM International, 2004a) in order to merge these numerous options into a standardized approach. Since that time ASTM E2546-07 Standard Practice for Instrumented Indentation Testing and ISO 14577-1, -2, -3, -4 Metallic Materials—Instrumented Indentation Tests for Hardness and Material Properties have been published.

Most bio-related instrumented-indentation models begin with Timoshenko's model (Timoshenko and Goodier, 1951) for a rigid punch on a semi-infinite elastic medium, corresponding to a steel indenter and a biological specimen of lower stiffness (King, 1987; Wolf, 2000; Cowin, 2001; Dao et al., 2001; National Physical Laboratory, 2004; Rudnitsky, Kren, Tsarik, 2004). Several models incorporate a correction factor for indenter geometry and stiffness, and some interesting work relating food texture to instrumented indentation has been developed (Bourne, 2002).

Nano-indentation has been used to probe the walls of individual wood cells (Gindl and Gupta, 2002), and a cross between Janka hardness testing and instrumented indentation was used on alfalfa cubes (Tabil et al., 2002), but the author found no prior use of instrumented indentation for wood mesostructure examination.

3.2. PROPERTY SCALING

The author's research experience with wood-based products began in 1994 with a project on glass-reinforced, recycled-paper lumber. Since then he has gained consulting experience in processed lumber, virgin-plastic lumber, recycled-plastic lumber, and flax-reinforced plastic lumber.

3.2.1. Preliminary Investigation. During 2003, the author undertook an exploratory investigation on instrumented indentation of pine and oak. Samples were purchased from a local lumberyard, cut into 2" cubes, and probed using an Instron 5583 universal testing machine equipped with a 400-lb load cell (Instron 2525-818), Jacobs-type chuck, right-circular steel probes, and 1" extensometer (Instron 2630-110) as shown in Figure 3.1. For the oak specimens, the average ring density was 13 rings per inch, moisture content was below 8%, and density was 39 lb/ft^3. Test variables included probe

diameter (0.040 to 0.228 in.), crosshead speed (0.005 to 0.5 in./min), penetration depth (0.0025 to 0.0125 in.), position on specimen surface (randomly selected, and repeated probes of same location), and loading direction (L-longitudinal, R-radial, T-transverse). A single-path loading-unloading cycle was utilized for all tests.

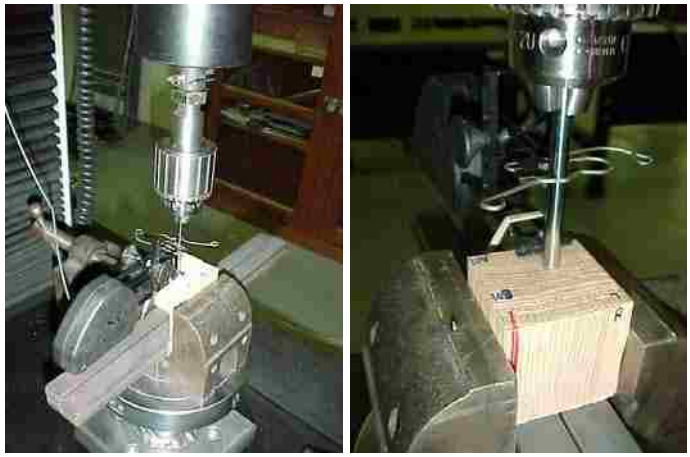

Figure 3.1. Instrumented Indentation of Oak

Figure 3.2 shows the dents left in the L, R, and T directions of a specimen by various-diameter probes. Figure 3.3 shows how probe diameter can be adjusted to cover a different quantity of cells. Smaller probes approach the diameter of a cell (or smaller), medium size probes can cover multiple cells in the early or late-wood portions of the annual ring, and larger probes can cover multiple growth rings.

Figure 3.2. Indentation Marks in Longitudinal, Radial, and Tangential Directions

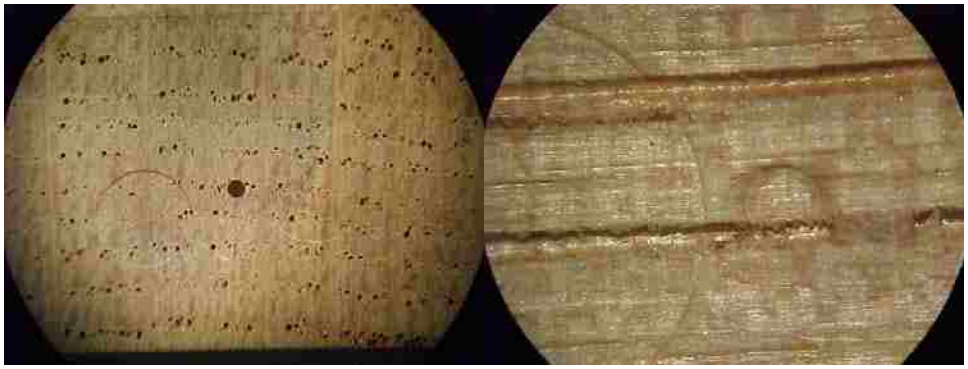

Figure 3.3. Probe Diameter versus Cell Size

The initial loading and unloading slopes were compared to published bulk reference values and experimentally obtained Janka hardness and compression moduli for the same cubes. Photos of these tests are shown in Figures 3.4 and 3.5, respectively.

Figure 3.4. Janka Hardness Testing

Figure 3.5. Compression Testing

Results were more consistent for larger probe diameters, which is expected considering variations in the mesostructure, and seemed unaffected by penetration depths greater than 0.0050 in. and crosshead speeds less than 0.2 in./min. Figures 3.6 and 3.7 show these two results, respectively. Figure 3.6 is color coded to show the slope of the withdrawal curve at progressively larger probe depths. The compressive force is shown on the vertical axis. The horizontal axis shows *strain* values because an axial

extensometer (shown in Figure 3.1) was used to monitor penetration depth. The equations in Figure 3.6 provide the slope and y-intercept of the initial withdrawal portion of each cycle, which is also color coded. Figure 3.7 is for a similar test, where a constant penetration depth was repeatedly used for increasingly rapid probe speeds. This was used to investigate the instrument's data collection capabilities.

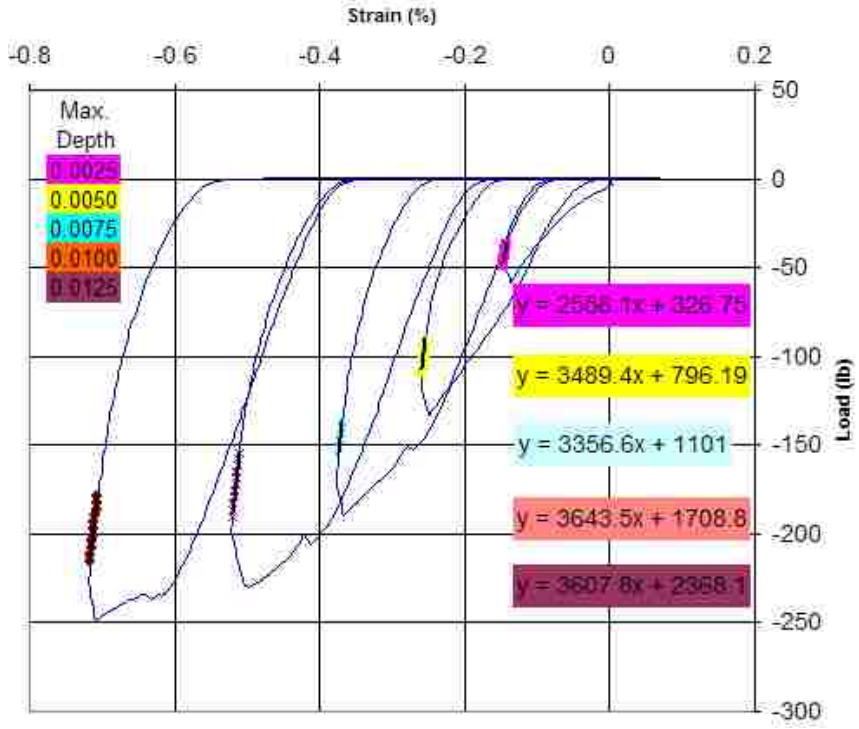

Figure 3.6. Penetration Depth Variation, with Constant Location and Speed

As seen in Figure 3.8, randomly selected positions on the specimen surface provided inconsistent results, which again is expected in light of the mesostructure variations, even though probe speed and depth were held constant. Note the variety of slopes in the color-coded equations next to the graph. Dark lines were used in the graph to highlight the initial withdrawal regions where these values were obtained.

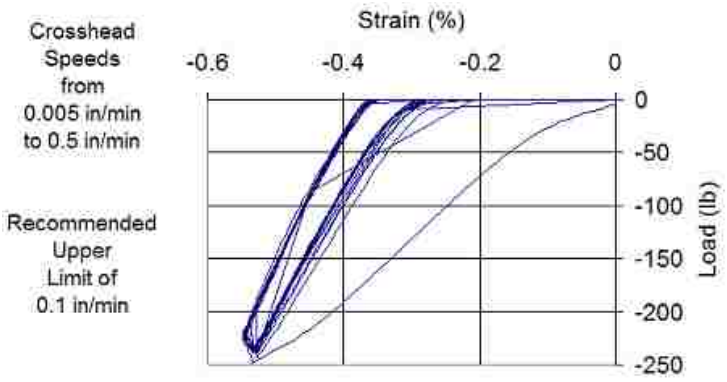

Figure 3.7. Crosshead Speed Variation, with Constant Location and Depth

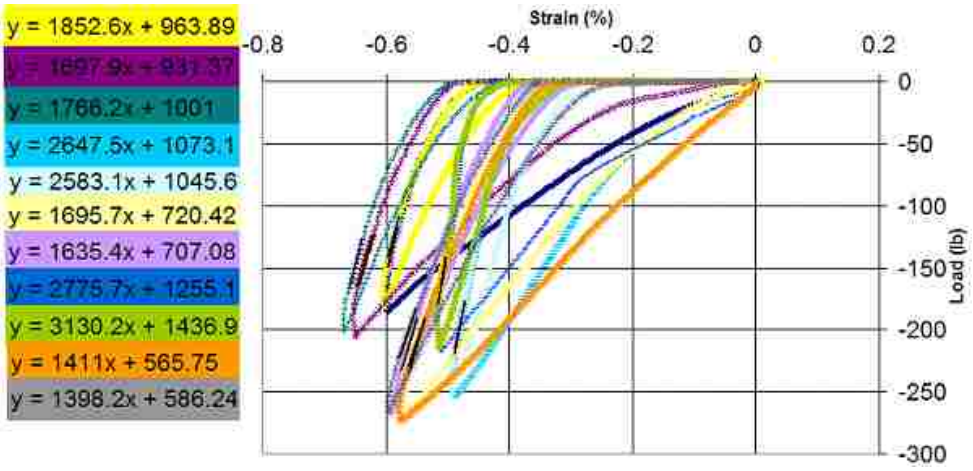

Figure 3.8. Probe Position Variation, with Constant Speed and Depth

Using established equations for right-circular probes (Timoshenko and Goodier, 1951; King, 1987; Wolf, 2000; Cowin, 2001; National Physical Laboratory, 2004), Table 3.1 shows how the initial unloading slope, or indentation modulus, related to compression modulus. Percent error in this table is defined as the absolute value of the difference between the compression and indentation moduli divided by the compression modulus.

While further study is warranted, the author speculates that the stronger correlation in the radial and tangential directions is more due to the compression technique than the indentation technique. Based on the idealized model of wood cell structure (Young, Mindess, Gray, and Bentur, 1998), substructure compressive deformation in the longitudinal orientation is more susceptible to end effects at the

Table 3.1. Modulus Comparison

	Compression modulus	Indentation modulus				
		Cowin	Timo.	King	NPL	average
E_L (psi x10^3)	1310	855	926	964	883	907
E_R (psi x10^3)	250	235	254	241	237	242
E_T (psi x10^3)	152	134	145	140	135	138
% error E_L		35%	29%	26%	33%	31%
% error E_R		6%	-2%	4%	5%	3%
% error E_T		12%	5%	8%	11%	9%

specimen-platen interface than the other two orientations, where cell deformation is dominated by collapse instead of buckling. It should be noted that the 1-inch gage length extensometer was only accurate to 0.001 in. over an average penetration depth of 0.01 in. for the results presented in Table 3.1.

Based on this preliminary effort, the author suggests the following five changes be undertaken in future studies.

1. A full regiment of bulk tests should be performed, according to applicable ASTM International standards, for comparison to instrumented indentation curves. Sectioning and imaging of substructure deformation under the indenter may prove beneficial in relating bulk and indentation properties. Examining alternate loading-unloading routines (intermittent partial unloading, multiple cycles with dwell times) may expand the number of links that can be accomplished.

2. An LVDT (+/-0.02” linear stroke, Instron 2601-061) directly mounted to the indenter, as in automated-ball-indentation testing for metals (Haggag et al., 1990; ASTM International, 2004b) and stress-strain microprobe system (Haggag and Murty, 1996), should be used in place of an extensometer.

3. Equipping the test frame with a cross-slide compound milling table and microscope head will allow greater control over specimen positioning.

4. Development of an automated means for analyzing data would greatly enhance experimental efficiency. Slopes in the preliminary study were determined using a spreadsheet, because Inston’s Merlin software did not consider unloading data in the

automated regression routines. Contact with an Instron representative to alleviate the problem proved unsuccessful, but further effort is warranted considering the time savings that can be achieved through automated routines.

5. Control of growth history, species, and grain orientation from board to board is challenging, at best, for specimens obtained at the lumberyard. A thorough examination of property variations will require hand processing of trees into specimens.

3.2.2. Probe Action in Soft Materials. To better understand the variables related to indentation of soft (low modulus, or biological) materials using instrumented indentation, the author experimented with a variety of polymers in 2004 and 2005. First, conventional photoelastic materials were used, but it was quickly discovered that these materials usually shatter before a probe can penetrate the surface. Figure 3.9 shows some of these efforts. In Figure 3.9(a) a pair of relatively stiff photoelastic materials are shown in contact. In (b) the lower material is replaced by a less stiff one. In (c) the upper material is replaced by a metal probe. This image shows an elastic penetration just prior

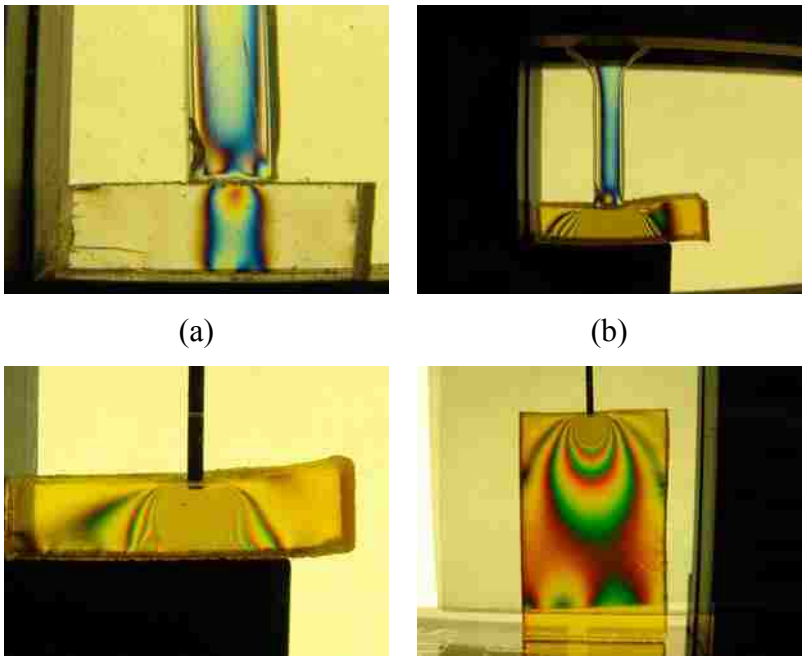

(a) (b)

(c) (d)

Figure 3.9. Photoelastic Indentation

to fracture of the lower material. In (d) the lower material is replaced with a taller one in order to visualize the contact stresses far removed from the lower support.

For a short period of time, variations in probe-tip geometries were investigated. The author was curious how easily the stress pattern under the probe tip could be manipulated. Several commercial products were looked at, including drill blanks, tubing, square stock, plug cutters, cutting and boring bits, and dowel-pin punches. Figure 3.10 shows some hand-carved indenters that were tried. The author would someday like to revisit this work, because probe tips designed to create specific stress states would allow for greater flexibility in material characterization using indentation. One tip, perhaps in combination with an initial surface-preparation step, might be used to approximate uniaxial compression, another for torsion, another for direct shear, etc.

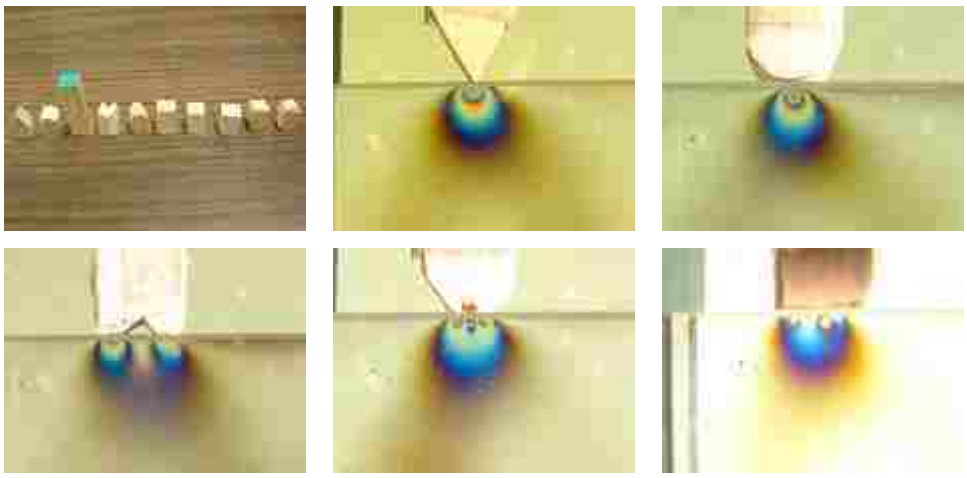

Figure 3.10. Hand-Carved Probes

With the additional goal of finding a castable matrix for isoetropic, fiber- or fabric-reinforced transversely isotropic, and orthtropic specimens, different casting and testing techniques were performed on clear, hot-melt glue sticks. A ductile, clear matrix was desired so that a modified, qualitative version of integrated-photoelasticity could be utilized near the probe tip as it plastically penetrated the specimen. Figure 3.11 gives an overview of these efforts.

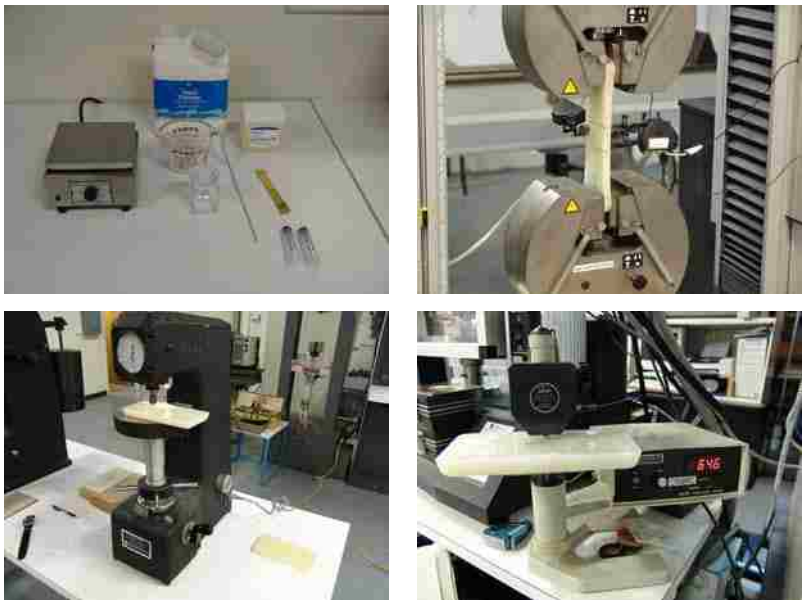

Figure 3.11. Hot-Melt Glue Tests

While a host of other products were tried and found to be unsatisfactory, Neutrogena soap showed potential. Figure 3.12 provides an overview of these tests, which were performed with circular polarizers (in the lower two images) and hand-driven punches. Figure 3.13 shows the progressive steps of a right-circular probe penetrating and withdrawing from the soap, with circular polarizers on either side of the bar.

Figure 3.12. Neutrogena Soap Tests

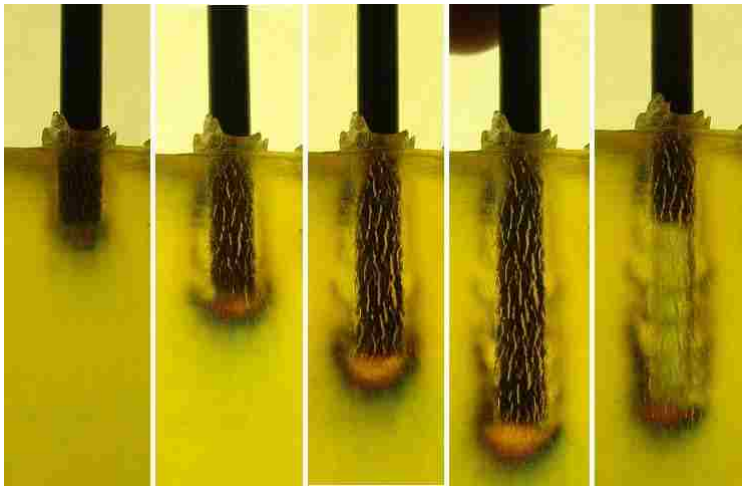

Figure 3.13. Neutrogena Penetration and Withdrawal

AromaGel from Environmental Technology Inc. showed the most promise. Casting, dehydration, rehydration, and probing techniques were tried. Unfortunately, photos of these tests were not retained, and the product line has been discontinued.

3.2.3. Future Scaling Efforts. If time, interest and funding are available the author may someday further investigate a link between the macroscopic and mesoscopic properties of wood. The boards would be obtained from a lumberyard, probed, and bulk tested according to ASTM International standards. The investigation would not address issues specific to specimen location within the original tree but, in doing so, would bypass concerns about logging, transporting, milling, planing and conditioning. The following discussion describes a plan for carrying out these investigations.

Board selection will be based upon grading-stamp information (species, mill and grade), ring density, grain alignment with the board's primary dimensions, grain curvature, and location and type of defects. Uniformity will be sought across the volume of each board and, as much as possible, from board to board.

The author will personally select the boards and decide how they should be sectioned for the following tasks. The first step will be to examine basic indentation variables, with the goal of selecting a list of *best practices* and variables for following tests. The second step will be to obtain bulk properties. The third step will draw from the knowledge gained in the first two. Here, the bulk-test specimens will be dissected

and probed, and effort will be made to model the connection between the macro and meso results.

3.2.3.1 Mesostructure characterization. The first phase of testing will repeat much of the work carried out in the preliminary work presented in Section 3.2.1, this time for pine, and expand it to include new variables. As many of the author's suggestions from the preliminary work as possible will be incorporated, i.e. LVDT mounted to the probe, frame-mounted microscope and positioning stage, and automated regression analysis. Load axes will correspond to the orthotropic wood directions, and sample preparation will be the same as for bulk characterization unless otherwise noted.

As in the preliminary work, testing variables will include probe diameter, crosshead speed, and penetration depth. Additional variables will involve position of indenter relative to the rings (tracking both along and across them), specimen thickness, proximity to specimen edges and defects, moisture content and surface conditions. An intermittent partial-unloading cycle will be utilized. Unless otherwise noted, all test variations will be performed in multiples of ten and the average response reported. A uniform laboratory temperature will be maintained through all tests. The laboratory is not currently equipped with a humidity-management system, but humidity levels will be tracked.

Probe action. Using a fixed probe position and diameter, a similar range of crosshead speeds and penetration depths to those of the preliminary work of Section 3.2.1 will be explored.

Probe geometry. Right-circular steel probes will be used in all indentation tests. The author has found that drill blanks work well as probes and come in a wide assortment of readily available diameters. From the preliminary oak samples, it was found that all indentations following the first one (at the same location, speed, depth, and diameter) followed essentially the same load-deformation curve. Ideally, permanent deformation occurs during the first loading, elastic recovery occurs during unloading, and further loading cycles repeatedly probe the elastically recovered zone. This idea can be used to *condition* samples for comparison of probe diameters. Initially, a probe diameter will be selected to cover multiple rings, and three cycles will be run with this probe. Then progressively smaller probes will be used to probe across the already probed surface,

taking note of position relative to the rings. The ratio of contact area to perimeter for the different probes and how many rings covered by each probe will be examined. Based on average growth rates for pine, a 0.1-inch-diameter probe will cover approximately one year of growth.

Specimen geometry. Variables in this portion of the investigation will include distance from the specimen edge, specimen thickness, and distance from strength altering characteristics (knots, checks, infestations, compression wood). With fixed diameter, speed, moisture content and surface conditions, the changes in data will be noted as the probe is brought closer and closer to edges and defects. As in ASTM International D1037 (ASTM International, 2004c), specimen thickness will be varied by progressively stacking thin sections of lumber on top of one another. Uniformity will be provided by keeping the same board on top and probing the same location of that board each time.

Moisture content. The relationship between indentation and moisture content will be examined by probing boards with induced moisture gradients along their length. Samples will be prepared by placing one end of a conditioned sample in a pan of water and periodically checking moisture migration. After sufficient gradient has been established, the board will be simultaneously probed with instrumented indentation and a handheld moisture meter along its length. As moisture content equilibrium may outpace data collection, the process will be repeated as many times as necessary to accumulate a sufficiently wide range of moisture content values.

Surface conditions. Course abrasive planing (24 to 80 grit) along the grain direction has been shown to crush cells, whereas knife planing provides a less damaged surface finish (Forest Products Laboratory, 1999). The effect of surface processing on indentation will be examined by probing under the following conditions: as purchased; cut with knife planer, band saw, and table saw; sanded with 60 grit, 120 grit, and 200 grit paper. For convenience in later tests, the effect of pre-marking indentation locations with pens and markers will be examined.

Durometer hardness. While not a common test procedure for wood, durometer hardness (types A, D and M) will be obtained, according to D2240 (ASTM International, 2004d), for a limited number of samples. Both previously indentation probed and adjacent positions will be tested. The author hopes this simple test can be related to

instrumented indentation and therefore be useful during travel where a full laboratory setup is generally not available and transportation of samples is troublesome.

3.2.3.2 Macrostructure characterization. Bulk characterization will follow ASTM International D143: Standard Test Methods for Small Clear Specimens of Timber (ASTM International, 2004e).

Sample preparation. As per D143 Section 5, photographs will be used to record the visible surface mesostructure. D143 Sections 6 and 21, dealing with control and measurement of moisture content and temperature, will be augmented with ASTM International D4444 method A, D4933 and E104 (ASTM International, 2004f,g,h) to speed data collection with a hand-held moisture meter and provide uniform testing conditions (68 + 6°F, 12% MC). Percent latewood and ring density will be recorded per D143 Section 7. D143 Section 22 provides for density measurement, and equipment calibration shall satisfy D143 Section 23.

Flexure. D143 Section 8 governs static bending. The secondary method, with 1x1x16 $in.^3$ sample geometry, will be followed using an Instron 4469 universal testing machine (UTM), 10-kip load cell (Instron 2525-802), and 2" LVDT (Instron 2601-064). Based on average growth rates, this method should engage one ring in tension and one ring in compression. In addition, samples turned on edge to the standard orientation will be used to engage all rings at equal load levels. One set of samples will be loaded to failure, obtaining the ultimate conditions, while another set will be stopped in the elastic region for later probe testing. The same approach of using damaged and undamaged samples will be taken with tension and compression tests.

Tension. D143 Sections 16 and 17 cover tension parallel and perpendicular to grain, respectively. The same testing machine and load cell will be used as for flexure. A 2" GL +/-0.2" extensometer (Instron 2630-114) will be used for parallel tests, and half of the samples will be equipped with strain gages to obtain tensile Poison's ratios. Typically, deformation is not recorded for perpendicular tests, but it will be obtained here in order to quantify as many trends as possible. A 1" GL +1"/-0.1" extensometer (Instron 2630-110) will be used.

Compression. D143 Sections 9 and 12 cover compression parallel and perpendicular to grain, respectively. The secondary method and an Instron 4485 UTM,

45-kip load cell (Instron 2525-172) and 2" GL +/-0.2" extensometer will be used for parallel tests. Half of the parallel samples will be equipped with strain gages to obtain compressive Poison's ratios. Perpendicular tests will utilize the Instron 4469 UTM, 10-kip cell, and a 0.1" LVDT (Instron 2601-062). In the standard perpendicular orientation, all rings experience equal load levels but can deform by unequal amounts, so samples laid on edge will also be studied, reversing the load/deformation distribution.

Shear. D143 Section 14 covers shear parallel to grain. The Instron 4469 UTM with 10-kip load cell and 0.1" LVDT will be used for these tests. Again, deflection is typically not measured, but the author considers it worthwhile since doing so requires minimal additional effort.

Shear perpendicular to grain is not described in D143, but the compression samples from D143 Section 12, where the specimen is sandwiched between a bearing plate smaller than itself and a platen larger than itself, experience shear perpendicular to grain at the edge of the bearing plate. As with different indenter sizes, the ratio of plate contact area to perimeter for different bearing-plate sizes will be examined. Due to the similarity to indentation testing, a portion of these compression samples will be sectioned perpendicular to the edge-induced shear lines in order to examine cellular deformation, using a light microscope. Hopefully this will provide some qualitative justification for relating indentation properties to particular bulk properties. Tests will be performed on both the R and T surfaces.

Hardness. Janka hardness is covered in D143 Section 13. The Instron 4469 UTM with 10-kip load cell and a Janka probe will be used in the L, R and T directions. Typically, deflection is not recorded for Janka hardness, but a 0.6" LVDT (Instron 2601-063) will be used, and hardness modulus will be determined according to D1037 Section 74.

3.2.3.3 Linking macrostructure to mesostructure. In the third phase of testing, the same samples used for bulk characterization will be sectioned and probed, under a fixed set of indentation conditions (depth, speed, diameter, MC and surface preparation) previously determined.

Flexure. Bending samples not taken to failure in the bulk tests will be sectioned every 2" along their length, and three L indentation measurements will be taken for every

ring on the sectioned surface. A weighted average, based upon mechanics of materials models for stress distribution and ring location relative to the neutral axis, will be applied to the individual indentation results and then compared to the bulk flexure properties.

Tension. Parallel-tension samples not taken to failure in the bulk tests will be sectioned every half-inch in the extensometer-covered zone. Every ring on the exposed surfaces will be L probed three times, and a non-weighted average of these results will be compared to the bulk longitudinal-tension properties. The same procedure will be used on perpendicular-tension samples, with reduced section intervals coinciding with the reduced specimen lengths.

Compression. The procedure for parallel-compression samples will be identical to that of parallel-tension. However, sectioning will be more difficult for the perpendicular-compression samples, so an incremental planing and probing operation may be employed, with a weighted average being applied to the probe results based upon contact-mechanic models for stress distribution under the bearing plate.

Shear. Samples tested in shear parallel to the grain usually result in a relatively clean fracture surface. Here, instead of using unfractured samples for probing, the failure surfaces will be prepared and probed in the perpendicular-to-grain directions. A stress-distribution weighted average will again be used to process the results.

Hardness. Contrary to prior procedures, hardness samples will be probed both before and after bulk characterization. Initial probe tests will be done on the specimen surface, using a grid of nine indentations across the forthcoming hardness-indentation zone. Following hardness indentation, the surface will be progressively planed and probed to a point below the hardness indentation depth. The same nine grid points will be probed, except for the middle point which will have disappeared during hardness testing, on each successive layer.

3.3. PROPERTY MAPPING

The author's maternal grandparents were mill owners, and many members of his extended family have spent their careers in lumber production. This family history, and the years he spent playing in the sawdust piles, sparked a curiosity in the author

concerning the growth characteristics of trees. The author donated from his own property and rough processed the trees used in the following investigation. The species of these trees was identified as shortleaf pine (Pinus echinata) through cone, needle, and bark inspection (Settergren and McDermott, 2000; Plant Information Center, 2004a,b). A thinning cycle on the pure stand performed in 1999 provided the following information.

1. The stand was initiated in the 1960s.
2. Average ring density is 4 rings per inch.
3. Trunks exhibit slight elliptical elongation in the East-West direction, corresponding to the prevailing wind direction (and therefore increased bending stress in that direction).
4. Trees are approximately 9" in diameter at 5' above the ground, are 55' tall with 40' of limb-free trunk, and have a 10' crown width.
5. Phyllotaxis, the helical arrangement of plant parts, appears to be present in limb location and orientation.

3.3.1. Preliminary Investigation. The author's efforts related to *property* mapping have focused on tracking mesostructure changes along annual growth layers from ground to crown. Based on Mattheck's constant stress model (1991), the author hypothesized that the properties of each growth cylinder remain uniform in regions far removed from stress concentrations, i.e. the tree base and load-bearing limbs. A good starting point for the definition of far removed would be Saint-Venant's principal (Timoshenko and Goodier, 1951).

In 2007 the author and his wife cut and processed a number of trees. Figure 3.14 shows the initial steps in the process.

Tree 1 was over 45-feet tall and approximately 47-years old. It was ripped down the middle, laid open, marked every 1-foot along its length, and planed smooth at these markings. Starting at the base of the tree, growth rings were traced and photographed at every 1-foot interval. Figure 3.15 shows intermediate steps of this process. Figure 3.16 highlights the rings at three-feet and thirty-nine-feet up from the base of the tree.

Figure 3.14. Tree Felling

Figure 3.15. Tree 1 Processing

Figure 3.16. Tree 1 Growth Rings at 3-Feet and 39-Feet

Moisture content and durometer hardness were measured at each fifth-year early-wood portions of the annual ring and one-foot of height. Earlywood was chosen because it was difficult to consistently hit the narrower latewood region with the tip of the indenter. An E-59820-08 Delmhorst moisture meter and a Shure type D durometer were

used. Figure 3.17 shows the relatively uniform relationship between moisture content at the pith and height along the majority of the trunk and a slight increase near the base of the trunk. Figure 3.18 shows the variable relationship between durometer hardness and height. While Kretschmann et al. (2002) state that "in a majority of cases earlywood and latewood properties increased going from pith to bark," an age-related trend for durometer hardness cannot be deduced from this data.

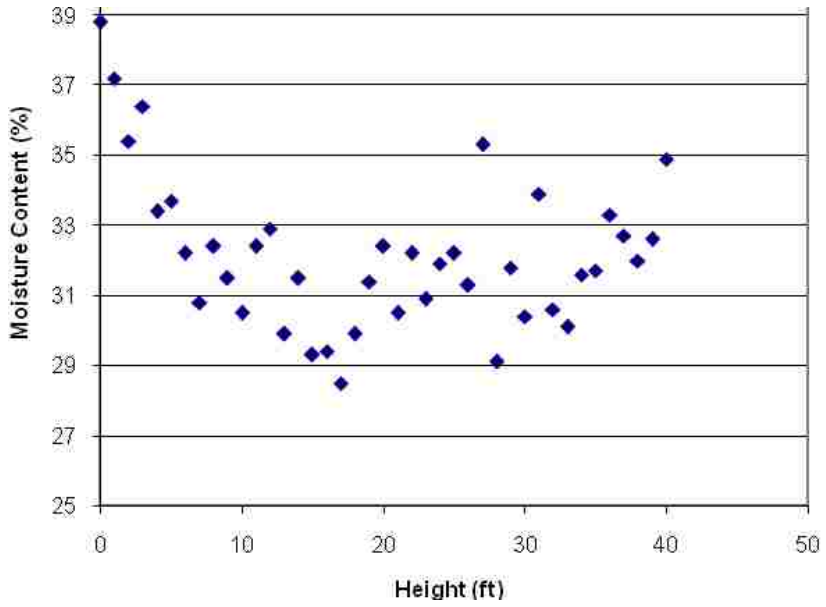

Figure 3.17. Tree 1 Moisture Content Versus Height

Tree 2, shown in Figure 3.19, was over 53-feet tall and approximately 32-years old and was processed in a similar manner to the first. Figure 3.20 shows how its diameter decreased with height. Figure 3.21 shows the relatively uniform relationship between moisture content at the pith and height along the majority of the trunk. Figure 3.22 shows the relationship between durometer hardness and height. In this case there appears to be a slight decrease in hardness with increasing height.

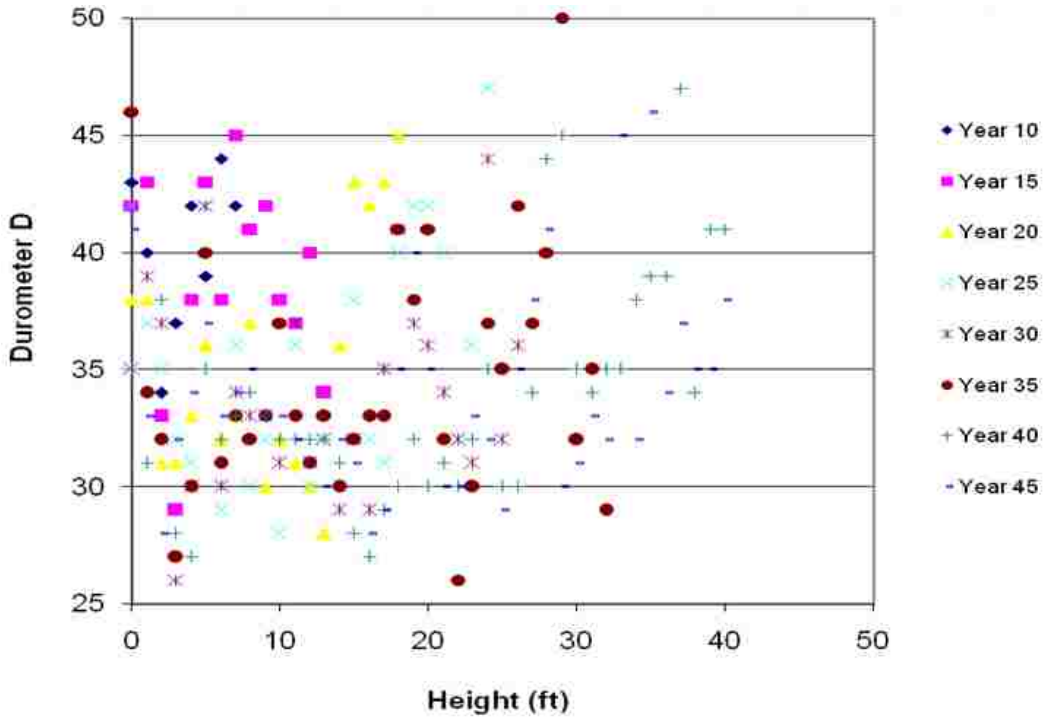

Figure 3.18. Tree 1 Durometer Hardness Versus Height

Figure 3.19. Tree 2 Processing

Tree 3, shown in Figure 3.23, was over 43-feet tall and approximately 36-years old. It was processed in a different manner than the first two. It was marked and cut transversely every one-inch along its length to create over 500 disks.

The disks were laid out in order and photographed. It was observed from these one-inch slices through the tree's history that new limbs were formed on average every seven inches through the height of the tree. Figures 3.24 and 3.25 show how these limbs appear in the sequence of disks. The left-most image corresponds to the lowest disk of the four.

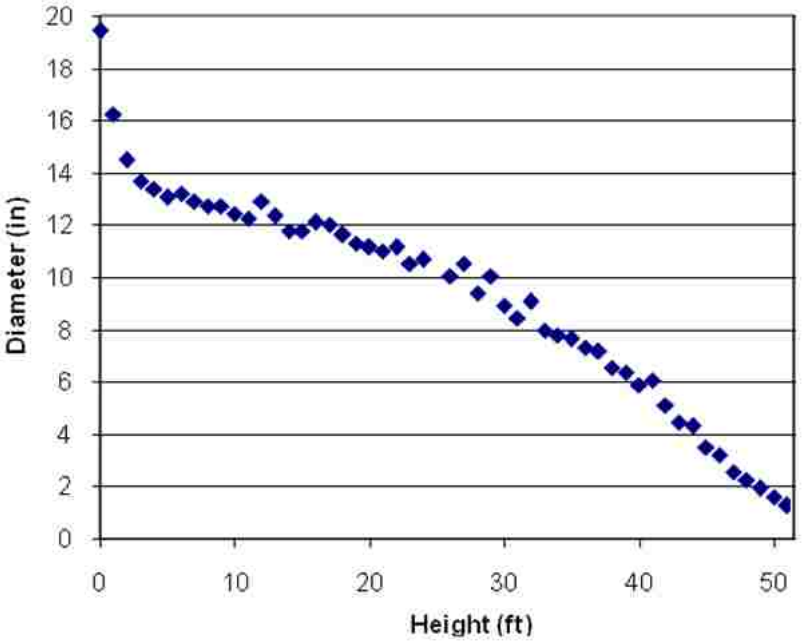

Figure 3.20. Tree 2 Diameter versus Height

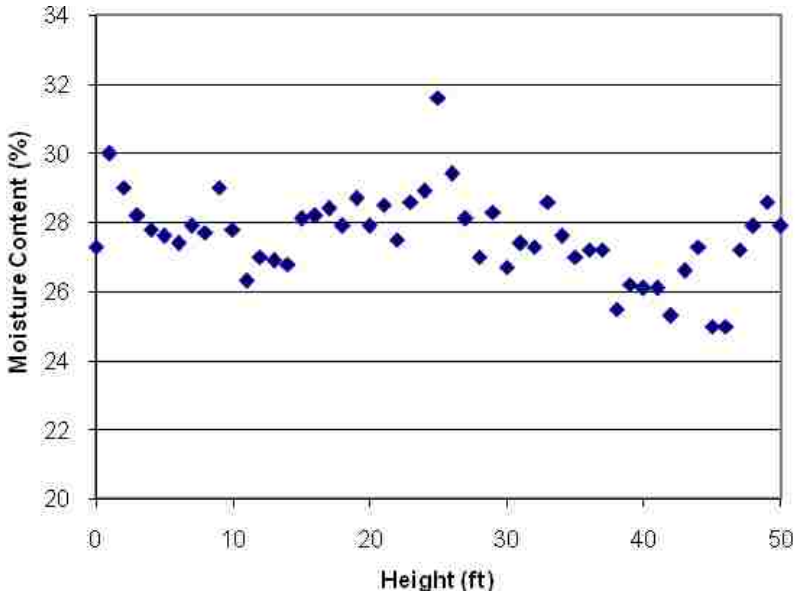

Figure 3.21. Tree 2 Moisture Content versus Height

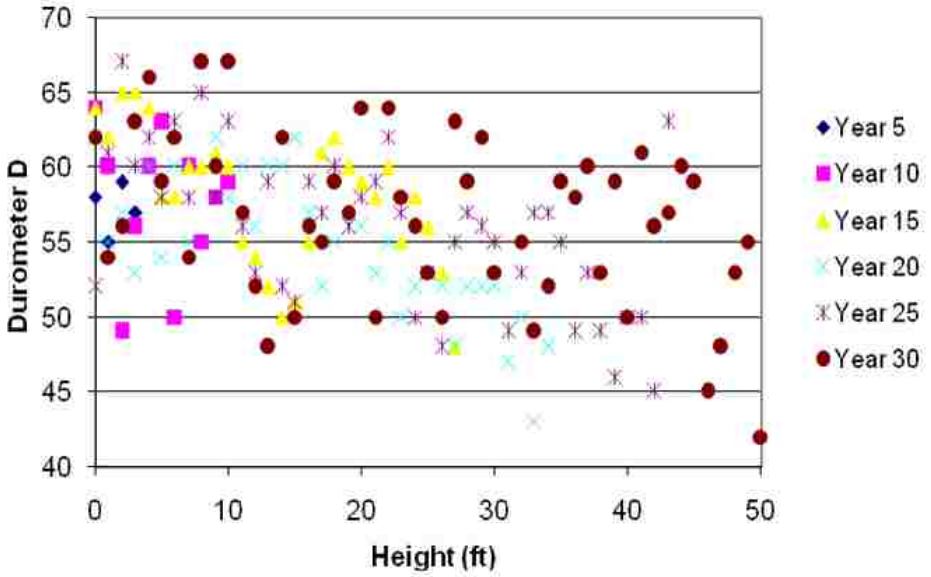

Figure 3.22. Tree 2 Durometer Hardness versus Height

Figure 3.23. Tree 3 Processing

Figure 3.26 shows that the limbs were arranged as a left-handed helix going from the base of the tree to the top. Figure 3.27 shows a similar arrangement in a trunk, given to the author by Tom Bryson, which has been hollowed out by termites.

3.3.2. Future Mapping Efforts. If further investigations are to be made, the following plan may be utilized.

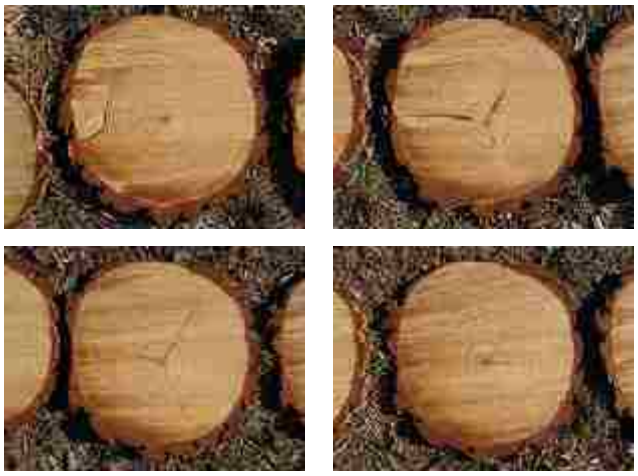

Figure 3.24. Tree 3 Disks 15 through 18

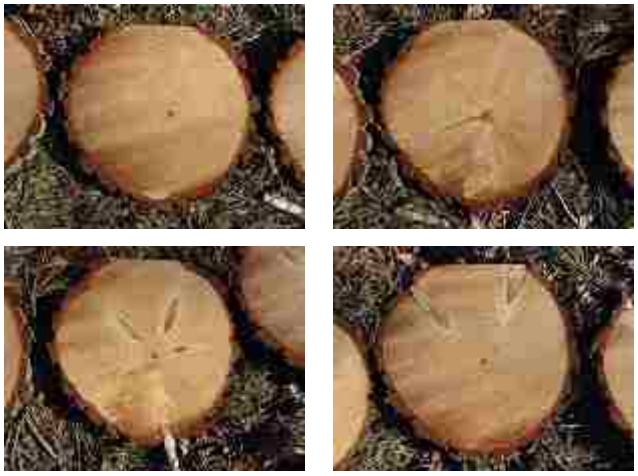

Figure 3.25. Tree 3 Disks 106 through 109

3.3.2.1 Specimen selection and harvest. The author will personally select and harvest two trees matching each of the following three categories.

1. symmetrical crown and vertical trunk (bending due to wind loads).
2. asymmetrical crown and vertical trunk (bending and torsion due to wind loads).
3. symmetrical crown and leaning trunk (bending due to wind loads and gravity, typically resulting in a large percentage of compression wood).

According to the developed trunk-loading models for wind, gravity, snow and ice, and physical contact with adjacent objects (Mattheck, 1991; Stathers, Rollerson, and

Figure 3.26. Tree 3 Phyllotaxis of Limbs

Mitchell, 1994; Guitard, 1995; Sakaguchi and Ohya, 1999; Coder, 2000; Jirasek, 2000), careful selection of crown geometry and trunk orientation will simplify the historical stress distribution on the trunk surface.

Specimens matching the first category are commonly found in the middle of an evenly aged stand. Here, primary solar contact occurs at a canopy of roughly equal height as the stand matures, and heliotropism results in strictly vertical trunk growth. Trees matching the second category are more commonly found at the stand border, where sunlight bathes one full side of the tree resulting in reduced limb shedding on that side. Trees of the third category are more difficult to locate but typically result from wind damage, direct contact with another object, or an unevenly aged stand, where younger trees lean as they seek sunlight in canopy gaps. A tree that divides relatively close to the ground or two trees growing in direct contact with each other at their bases may also match this category, because their trunks tend to lean away from each other. Trunks leaning due to wind damage or direct contact will be avoided in this study, because they will have had a inconsistent load history. However, they may make interesting candidates for alternative studies.

Once the six trees have been selected, the author will follow portions of ASTM International D5536: Standard Practice for Sampling Forest Trees for Determination of Clear Wood Properties (ASTM International, 2004i) during harvest. Cardinal point

Figure 3.27. Limbs Exposed by Termites

orientation will be field marked according to D5536 Section 5.6, and field documentation will follow D5536 Section 5.7.2. Following felling and limbing operations, trunk circumference will be measured every five feet along its length, beginning at the base, for comparison to stem form and taper models by Sharma and Oderwald (2001).

According to D5536 Section 5.1.2, deviations from standard specimen geometries are allowed for studies on radial and longitudinal property gradients, so a simplified version, matching the goals of this study, has been devised. One-foot long sections of the trunk will be cut at five-foot intervals, with the lower-most cylinder being taken directly at ground level, and proceed through the full height of the tree. To retard checking in these short sections, bark will be kept intact and the ends painted, according to D5536 Section X2.3.1. These short logs will then be transported back to the laboratory for moisture/temperature conditioning.

The portions of trunk between these logs will be longitudinally cut, along the east-west axis, and planed so the vertical ring progression can be tracked and recorded. Doing so will allow the absolute age of individual rings to be determined, instead of the customary method of dating rings relative to the pith at equal height. These portions of

the trunk will be discarded at this point, greatly reducing the volume of material to be stored in the laboratory.

3.3.2.2 Specimen preparation and testing. The final portion of the study will focus on sample preparation and testing. First, the conditioned short logs will be further reduced in size. A middle two-inch disk will be removed and sectioned, beginning along the cardinal axes, into eight equal pie-shaped pieces. If knots are present on the disk surface, another disk will be obtained from immediately adjacent material until a knot-free surface is obtained. A one-inch strip will be cut from the side of each pie-shaped piece, and then this strip will be further divided such that the growth ring corresponding to every fifth year of absolute age can be probed in the longitudinal, radial and transverse (L, R, and T) directions. In this manner, the growth for every fifth year, every 5-feet above the ground will be probed eight times in the three orthotropic directions. Indentation variables will be fixed throughout this phase and correspond to those used in efforts related to property scaling. Specimen density, percent latewood, and ring density will also be recorded.

A modified version of the specimen naming convention found in D5536 appendix X2 will be used to identify each specimen block. A label may look something like A05NW30, representing that the specimen's original location was in tree A, 5-feet above the ground, on the north-west side of the pith, and encompassing the growth ring of year 30.

The ends of the short logs remaining after the 2"-disks have been removed will be longitudinally sectioned to complete the tracking process for each ring. They will then be further reduced to estimate the years at which limbs at the corresponding elevation both died and were eventually shed. This is a rather simple process, as knots can be easily identified on the cut surfaces and then traced from the pith outwards using a band saw. This data will help to determine whether the transition in properties from juvenile to mature wood is influenced by limb vitality and the associated limb-induced stresses.

A contour map of L, R, and T properties will be prepared to overlay photographs of the standing tree and individual disks.

3.4. POTENTIAL FOLLOW-UP PROJECTS

In the author's mind, these investigations will serve as the foundation for a variety of other studies. Of course, the proposed approach, combined with improvements discovered in its execution, could be immediately applied to other softwood species – both virgin and preservative-treated. Modifications to account for differences in anatomy (ring density, cell types and sizes, tension wood, etc.) would allow its use with hardwoods. Also, with an established link between macro and meso properties, models linking to the cellular level and relationships to civil engineering design factors (timber beam size, depth, etc.) could be explored.

Limbs have an altered anatomy from that of the trunk (Bowyer, Shmulsky, and Haygreen, 2003), so an examination of their properties may prove insightful. Using the Rapoff et al. (2001) study of the stress concentrations at the long-bone nutrient foramen and the subsequent strength optimization studies for plates with holes (Venkataraman et al., 2001) as a role model, insights into stress concentration management at fiber-reinforced, cantilevered connections could possibly be achieved through examination of ring orientations (Mosbrugger, 1990) and properties at transitions between trunk and primary, secondary and tertiary limbs. Recent studies have also shown that root systems exhibit a thigmomorphogenic response (Mickovski and Ennos, 2003), so similar work could be carried out with roots and perhaps linked to mining and drilling applications.

4. HELICAL FORCE FLOW HYPOTHESIS

"Wilhelm Ritter...encouraged his students to visualize the flow of forces within a structure, as well as the ways in which different forms could change that flow." – D. P. Billington (2003)

In this section the author presents the concepts of *unit maps*, *unit mechanics*, *force flow* and *close-packed helices*. Levesque (2001) describes the creativity technique commonly employed by the author to develop such ideas as the role of a *navigator*. In this role the creative individual observes and adapts information from a wide variety of sources in order to *map* out new territories. Source material for the author comes from engineering, physics, materials science, biology, biomimetics, dimensional analysis, etc. His unit-mechanics concept can be used to classify mechanics models that span multiple levels of structural hierarchy and spatial dimension. Unit maps are more general and provide the framework for systematic searching of innovative ideas in science and engineering. As an example concept, the author explores the idea of *force per time* or *force flow*, where photons follow helical paths through a material's structure. He also presents the concept of *close-packed helices* in crystal lattices.

4.1. UNIT MECHANICS

As previously noted, "[biological] cells actively respond to mechanical signals through changes in morphology, signaling, and biochemical response" (Lang, 2007) and "hierarchical structures in biological materials span many orders of magnitude" (Elices, 2000). Antonietti and Mohwald (2001) describe how this plays into the overall optimization of the natural structure.

> The superb performance of biological material such as bone, seashell, wood, tendon, hair, or spider's silk is due to a hierarchical superstructure of the materials where structure control is exerted at every level of hierarchy. In addition, it must be pointed out that those materials are

> created around room temperature, represent in many cases optimal cases of lightweight design, are made of simple components such as calciumcarbonate or polypeptides, and are recyclable and sustainable. ... Previous work on self assembly has shown that the complexity of the resulting superstructures is restricted to rather simple shapes, which is due to the high symmetry of the starting objects and the connected building blocks with broken symmetry such as "Janus spheres" or "Janus coins" are objects with non-centrosymmetric fields which can line up in more interesting (and useful) superstructures, as they are for instance found in living nature. This would allow self-assembly to go "around the corner".

Ingber (1998) suggested that, "…tensegrity is the most economical and efficient way to build—at the molecular scale, at the macroscopic scale and at all scales in between," but few other approaches boast such versatility. The mechanical approaches used successfully for engineered materials and structures are not as well suited for natural ones, and, while natural materials are plentiful and easily observable, alternative approaches that accurately describe the behavior of biological materials are still being sought.

Lakes and Wang (2004) provide a bit of history on modeling efforts.

> …during the development of the theory of elasticity, it was by no means obvious how much freedom was necessary to describe materials. For example, the early uniconstant theory of Navier is based upon the assumption that forces act along the lines joining pairs of atoms and are proportional to changes in distance between them. This theory entails a Poisson's ratio of 1/4, for all materials. Experimental measurements (about a century ago) of Poisson's ratio of about 1/3 in common materials led to the replacement of uniconstant elasticity by the more general classical elasticity, following the continuum view of Green, which allows Poisson's ratios between -1 and 1/2.

Butchner and Lakes (2003) point out that, "…the classical continuum representation of a material depends on the structure size to be much smaller than the specimen size." Lakes (1995) continues the history lesson in the following.

> Microstructure elasticity includes Cosserat elasticity and the theory of voids as special cases. Classical elasticity is a special case of Cosserat elasticity and of void theory. Uniconstant elasticity is a special case of

> classical elasticity. … Continuum theories make no reference to structural features, however they are intended to represent physical solids which always have some form of structure.
>
> The ultimate origin of elastic behavior is the electromagnetic force between atoms in a solid. …
>
> One may distinguish the continuum view from the structural view. The continuum view is useful for making engineering predictions and for visualizing global response of materials. The structural view is relevant to the underlying causes of the behavior. One may link these views by developing an analytical model of the material microstructure, and obtaining approximations in order to obtain average values. Retention of only the lowest order terms in such analysis gives classical elasticity as a continuum representation. When higher order terms are retained, a generalized continuum representation is obtained. In either case the predicted elastic constants are functions of the structure and properties of the constituents. This is how the microphysics is introduced. …
>
> As for microstructure elasticity, little comparison has been made with experiment since few analytical solutions are available for this theory.

Kremer (2001) points at some alternative approaches that start further down the spatial ladder and try to work their way back up.

> Classical materials science activities in the past largely focused on bulk properties of different materials by characterizing them experimentally and analyzing them theoretically in terms of continuum mechanics models. Condensed matter physics and chemistry, on the other hand, focused on fundamental physical and chemical properties of systems in the condensed phase. Surface and interface science was traditionally located somewhere in between these two fields.

To better visualize the spatial ladder and how some of the modeling efforts related to ceramic materials–as an example–fit into this ladder, Table 4.1 was prepared. Some of the theories that would accompany the simulation techniques mentioned in the table are quantum physics, solid state chemistry, solid mechanics, fluid mechanics, fracture mechanics, pecolation theory, thermodynamics, and rheology (Fisher, 2001).

Here the author uses the word *unit* to mean "a single thing, person, or group that is a constituent of a whole" (Webster.com) and thinks of structural hierarchy in terms of *repeating units*. Depending on the material or structure in question, additional units

Table 4.1. Repeating Units and Simulation Methods

Size (m)	Unit	Ceramic Simulations (Fisher, 2001)
10^{-35}	Planck length, string length	
10^{-22}	electron (Dehmelt, 1988)	
10^{-19}	quark	
10^{-15}	proton, neutron	
10^{-14}	nucleus	
10^{-10}	atom	*Atomistic Modeling*
10^{-9}	molecule	Ab initio Molecular statics
10^{-8}	protein	Molecular dynamics Quantum mechanical Monte Carlo MD/MC hybrids Lattic dynamics
10^{-7}		*Microstructure Modeling*
10^{-6}	organelle	Potts Modell Monte Carlo Cellular Automata
10^{-5}		Diffuse-interface model
10^{-4}	cell	Phase Field models Voronoi methods Population Balance models
10^{-3}	tissue	*Macro-scale Modeling*
10^{-2}	organ	Finite Element Methods Densification models
10^{-1}	organ system	Computational thermodynamics
10^{0}	organism	
10^{2}	ecosystem	
10^{7}	planet	
10^{9}	star	
10^{16}	solar system	
10^{20}	galaxy	
10^{26}	universe	

could be added to this generic list and others deleted. For example, city, building, floors, rooms, and studs could be introduced between *organism* and *ecosystem* if one were focusing on wood and the forces applied to a building. Several of the biological references would be replaced with references to fiber, lamina, laminate, and product for fiber-reinforced laminated composites. One might even stretch the convention to include non-physical systems, such as poetry units of library, book, passage, paragraph, line, word, syllable, prosody, etc. when describing non-engineering topics.

Combining the words *unit* and *mechanics* – "a branch of physical science that deals with energy and forces and their effect on bodies" (Webster.com) – one could concoct a phrase that describes mechanics techniques that attempt to span multiple units. Ingber's (1998) ideas on tensegrity would be such an example. With continuum theories typically being limited to one unit at a time, the study of a fiber-reinforced laminated composite would attempt to follow the behavior through successive units. Tradeoffs between accuracy and computational efficiency are obviously associated with the method one chooses to move between units.

One might even view *interactions* between atomic and subatomic entities and *forces* in macro- or micro-level entities as concepts specific to certain sets of units, instead of the traditional and often confusing attempts to use *force* at all the spatial levels. Scholberg (2005) provides an example.

> Fundamental matter is made up of only two main types of particles, quarks and leptons, which come in three successively heavier generations. These constituents interact with one another in only four ways, determined by the four forces: gravity, electromagnetism, the strong (or nuclear) force and the weak force. For the latter three, we now know what the associated force transfer particles are: the photon (electromagnetism), the gluon (the strong force) and the W and Z bosons (the weak force). ... We believe that at high energy, electromagnetic, weak and strong forces have the same strength: they unify. But how exactly does the unification happen? Even murkier are questions of whether and how gravity, the weakest force, merges with the other three. ... Another idea that may be tested in the short term in collider experiments is the possibility that spatial dimensions beyond our familiar three may exist, allowing gravity to partially "leak away," which would account for its extreme feebleness compared with the other forces.

To non-physicists, *particles* of force seem odd, to say the least. With the electromagnetic force carrying particle being a photon, which behaves as both a particle and a wave, has zero (rest) mass, carries all wave lengths of electromagnetic radiation instead of what would normally be considered a *force*, and as all school children know is what their eyes recognize as light, one feels certain that physicists could learn a thing or two about taxonomy from their biologist cousins.

4.2. UNIT MAPS

In this section, the author will use the word *unit* to have perhaps the more expected meaning of, "a determinate quantity (as of length, time, heat, or value) adopted as a standard of measurement" (Webster.com).

Berkson (1974), as previously mentioned, suggested that volume forces might better represent the concept of force and force fields that Faraday had. What other options might there be? When touching a piece of ice or a hot mug, does one feel temperature? Or, instead, does one sense an energy flow rate, where *hot* and *cold* are simply used to describe the directions of the flow? While Faraday seemed to have a wide definition for *force* and sought a conservation law for it, his contemporaries turned their attentions to *energy* and alternative conservation laws.

Energy seems more robust a concept than force. But why? If one integrates Newton's second law of motion with respect to position, one arrives at the principle of work and energy. If one integrates it with respect to time, one arrives at the principle of linear impulse and momentum. Both of these alternatives have associated conservation laws. So why not force? Or power? Or other measurable quantities?

To start the search, one could integrate Newton's second law with respect to some other variable or integrate additional times with respect to position and time. Quickly the number of possible alternatives grows.

Another approach would be to entertain concepts from neighboring areas, just as Cauchy used the idea of pressure from fluid mechanics to describe stresses in solids. As previously mentioned, an analogy of force density from fluid mechanics in solids might

be fruitful. Or maybe power per unit volume used to describe the mass/energy transfer in multiphase systems would prove insightful for just solids.

What about random searches, or semi-random searches? One could quickly ponder whether concepts of energy flux density, energy per volume and time, power density, power dissipation/absorption, energy per unit space-time, power density direction, power flux density, etc. might provide a better understanding of force and how it *flows* through structures.

It can be assumed that most of these ideas have been tried, but it is hard to find publications of unsuccessful attempts. Few people want to discuss their failures. So how does one efficiently search for an alternative view of force? What is described next might provide the means for a more systematic approach.

4.2.1. A Unit Map. To better understand the relationship between physical quantities, the author crafted a polar coordinate system to visually represent the International System of Units (SI) based units of each quantity. Figure 4.1 shows a blank grid.

The angular coordinates in the upper half of the grid are used to plot units for length, mass, time, electric current, thermodynamic temperature, amount of substance, and luminous intensity (starting at the polar axis and going counterclockwise) found in a quantity's numerator. Angular coordinates in the lower half were used for units found in a quantity's denominator. The radial coordinate corresponds to the power of the unit, with the pole representing unity. Figure 4.2 shows an example for length (m^1), area (m^2) and volume (m^3).

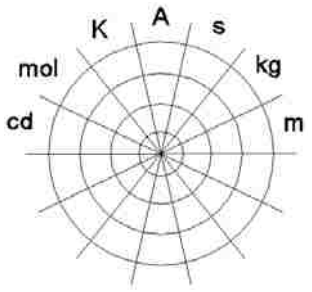

Figure 4.1. Blank Unit Chart

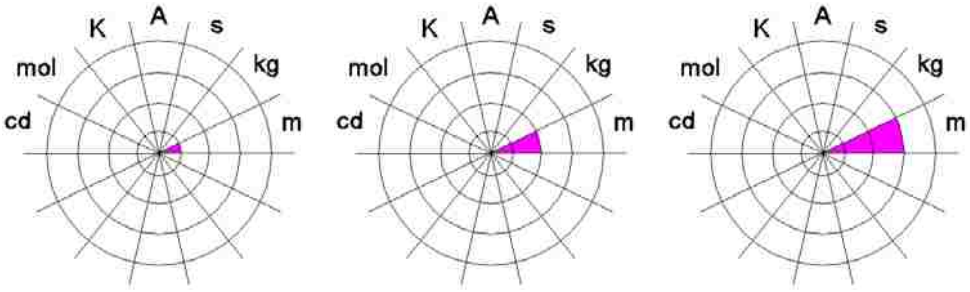

Figure 4.2. Unit Charts for Length, Area and Volume

Figure 4.3 shows some other common quantities. Note that strain (m/m or m^1m^{-1}), which might be considered dimensionless, could be represented as having the first radial coordinate on both the upper and lower halves shaded, where the corresponding units are reflected through the pole. This way the strain chart would not appear blank. The author chose to only represent dimensionless quantities this way. All other quantities were represented in terms of the simplest version of base units. For example, energy, work, heat, and torque were represented by the same chart (kg m^2 s^{-2}) even though their physical significance is quite different.

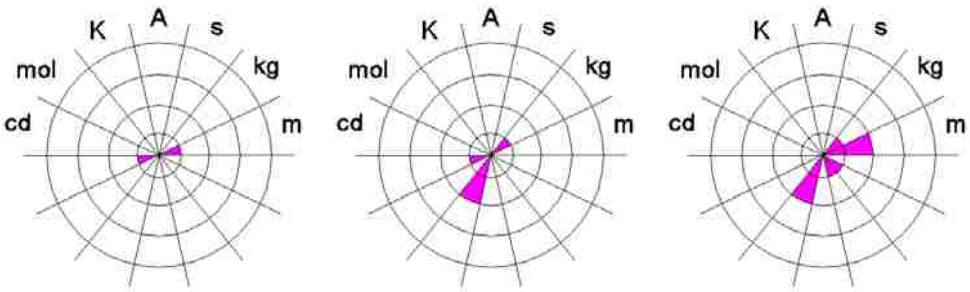

Figure 4.3. Unit Charts for Strain, Stress, and Molar Heat Capacity

The charts can now be used as points on a Cartesian coordinate system, where each of the axes is divided into regions corresponding to unity, for dimensionless quantities, and the seven base units. Figure 4.4 shows a three-dimensional view of the coordinate system and mapped quantities, and Table 4.2 (derived from

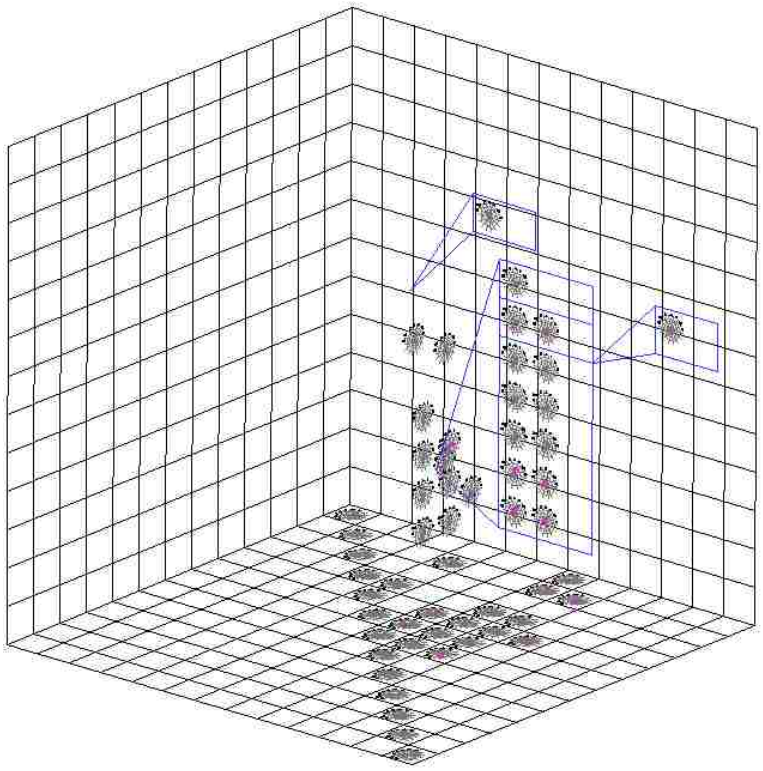

Figure 4.4. First Unit Map

en.wikipedia.org/wiki/SI_derived_unit) lists the quantities in more detail. Note that quantities involving only one base unit, such as length and volume, are plotted along the diagonal of the bottom plane. Quantities involving two base units, such as velocity and acceleration, are plotted on one side of this diagonal. Quantities with three base units, such as force and momentum, are plotted above the previous *planar* quantities. Quantities involving four and five base units are shown as extending out from the quantities with three base units. An interesting observation is that most of the quantities involving two or more base units are clustered in the same region of this space, with only a few outliers.

Figure 4.5 shows the bottom plane of the unit map with the one-base-unit quantities along the diagonal and the two-base-unit quantities to the right of the diagonal. It also shows that the largest grouping of quantities is at the intersection of length, mass and time, which is perhaps not surprising since historically these are the most familiar and commonly measured items.

Table 4.2. Physical Quantities in First Unit Map

Number of base units	Physical quantity	Unit name	SI base units
1	plane angle	radian, rad	m · m-1
	solid angle	steradian, sr	m2 · m-2
	wavenumber	reciprocal meter	m-1
	length	meter, m	m
	area	square meter	m2
	volume	cubic meter	m3
	mass	kilogram	kg
	time	second	s
	frequency	hertz, Hz	s-1
	activity (radioactive)	becquerel, Bq	s-1
	angular velocity	radian per second	s-1
	electrical current	ampere, A	A
	thermodynamic temperature	degree kelvin	K
	amount of substance	mole	mol
	luminous flux	lumen, lm	cd
2	density, mass density	kilogram per cubic meter	kg · m-3
	specific volume	cubic meter per kilogram	kg-1 · m3
	acceleration	meter per second squared	m · s-2
	speed, velocity	meter per second	m · s-1
	heat flux density, irradiance	watt per square meter	kg · s-3
	absorbed dose rate	gray per second	m2 · s-3
	specific energy, absorbed dose	joule per kilogram	m2 · s-2
	kinematic viscosity, diffusion coefficient	square meter per second	m2 · s-1
	surface tension	newton per meter	kg · s-2
	electric current density	ampere per square meter	A · m-2
	magnetic field strength	ampere per meter	A · m-1
	electric charge	coulomb, C	A · s
	amount concentration	mole per cubic meter	m-3 · mol
	molar volume	cubic meter per mole	m3 · mol-1
	catalytic activity	katal, kat	mol · s-1
	luminance	candela per square meter	cd · m-2

Figure 4.6 shows the three-base-unit quantities that appear above the two-base-unit quantities in the full map. Figure 4.7 shows the four- and five-base-unit quantities and how they extend out from points in the three-dimensional map.

With a map similar to this in hand, one is tempted to explore the space surrounding the most dense portions of the map in hopes of identifying new, as yet unnamed physical quantities. However, before one invests the time and effort, it might

Table 4.2 continued. Physical Quantities in First Unit Map

Number of base units	Physical quantity	Unit name	SI base units
3	pressure, stress, energy density dynamic viscosity force, weight momentum power, radiant flux energy, work, heat, moment of force angular momentum electric charge density magnetic flux density, magnetic inductivity exposure (X and gamma rays) specific heat capacity or entropy	pascal, joule per cubic meter pascal second newton, N newton second watt, W joule, J newton meter second coulomb per cubic meter tesla, T coulomb per kilogram joule per kilogram kelvin	kg · m-1 · s-2 kg · m-1 · s-1 kg · m · s-2 kg · m · s-1 kg · m2 · s-3 kg · m2 · s-2 kg · m2 · s-1 m-3 · s · A kg · s-2 · A-1 kg-1 · s · A m2 · s-2 · K-1
4	conductivity permittivity electric conductance electric capacitance electrical resistance, impedance, reactance electric potential, electromotive force inductance magnetic flux electric field strength permeability thermal conductivity heat capacity, entropy molar energy molar conductivity	siemens per meter farad per meter siemens, S farad, F ohm, Ω volt, V henry, H weber, Wb volt per meter henry per meter watt per meter kelvin joule per kelvin joule per mole siemens meter2 per mole	kg-1 · m-3 · s3 · A2 kg-1 · m-3 · s4 · A2 kg-1 · m-2 · s3 · A2 kg-1 · m-2 · s4 · A2 kg · m2 · s-3 · A-2 kg · m2 · s-3 · A-1 kg · m2 · s-2 · A-2 kg · m2 · s-2 · A-1 kg · m · s-3 · A-1 kg · m · s-2 · A-2 kg · m · s-3 · K-1 kg · m2 · s-2 · K-1 kg · m2 · s-2 · mol-1 kg-1 · s3 · mol-1 · A2
5	molar heat capacity, molar entropy	joule per kelvin mole	kg · m2 · s-2 · K-1 · mol-1

be best to refine the mapping system and expand it to include less common but already claimed quantities. This is described next.

4.2.2. A Refined Unit Map. The preceding unit map was first published by the author in a classroom setting on February 7, 2006. The following, as yet unpublished, map was developed in August and September of 2008. In this technique a more refined method for dividing up the coordinate axes was introduced, and a few more physical quantities were included. Table 4.3 highlights the major axis divisions.

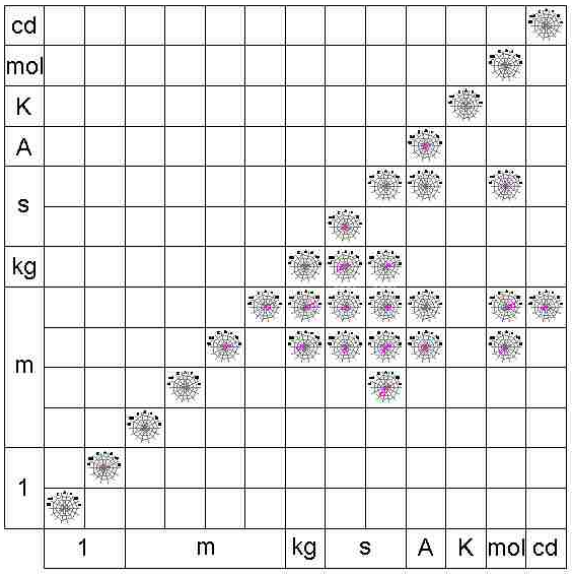

Figure 4.5. One- and Two-Base-Unit Quantities

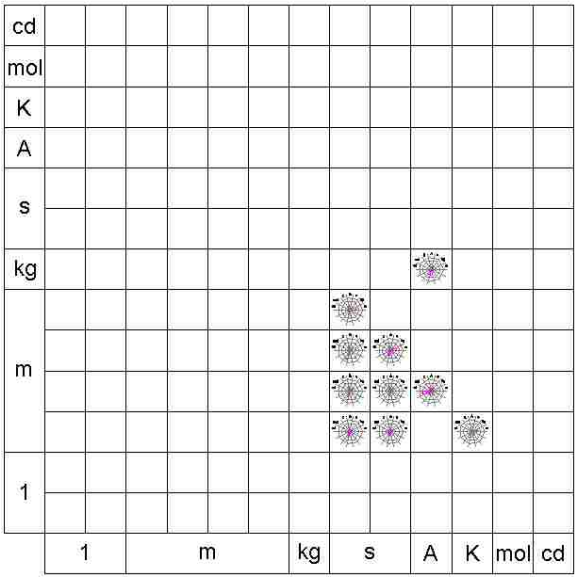

Figure 4.6. Three-Base-Unit Quantities

One will quickly note that mass is left out of the table. To reduce the number of required dimensions from five to four it was decided to plot quantities with no reference to mass in one color, quantities with kilograms in the numerator in another color, and quantities with kilograms in the denominator in a third color. A similar approach could

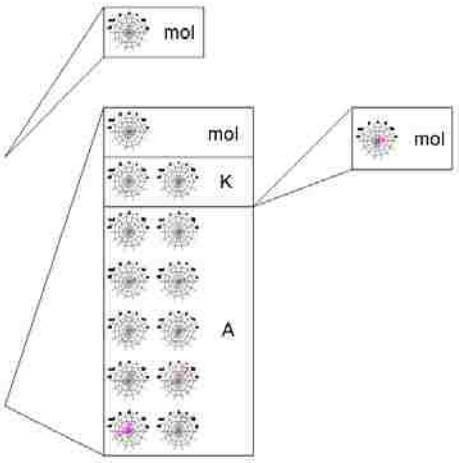

Figure 4.7. Four- and Five-Base-Unit Quantities

Table 4.3. Major Divisions

0-10	unity
11-20	meter
21-30	second
31-40	Ampere
41-50	mole
51-60	Kelvin
61-70	candela

have been used with mole or Kelvin units, since these too only have exponents of -1, 0 and +1 for the quantities used. Kilogram was chosen because it showed up in more of the physical quantities.

It is worth noting that there was only one quantity, molar heat capacity/entropy, used in the first map that had five base units. After deciding to describe mass using colors, it was a simple decision to plot this single quantity in the three-dimensional map using its own unique color. This way all of the quantities could be mapped within a three-dimensional space.

Table 4.4 shows how the axes were further divided. Using the major and minor divisions and some simple rules to prevent a quantity from appearing in multiple places,

quantities were assigned three coordinate values. For example, length was given coordinates of (16, 5, 5). The sixteen represents *meters to the first power on the first axis*, and the fives represent *unity* on the second and third axes. While unity raised to any power is still unity, five was used for any reference to unity because it represented unity in all of the major divisions, not just in the region from one to ten.

Table 4.4. Minor Divisions

1	X^{-4}
2	X^{-3}
3	X^{-2}
4	X^{-1}
5	X^{0}
6	X^{1}
7	X^{2}
8	X^{3}
9	X^{4}
10	unused

Figure 4.8 shows all of the quantities used by the author with one, two and three base units on a single plane. Quantities with one base unit are aligned along the bottom of the graph, with unity as their second coordinate. Figure 4.9 highlights the region where length and time intersect and several quantities are located.

Table 4.5 describes the quantities signified by the spheres in Figure 4.9. One should note that some locations have a single sphere and others have two. The leftmost of the paired spheres in Figure 4.9 represents quantities that have kilogram as one of the base units. The rightmost sphere represents quantities without kilogram. With this region being so well populated, it seems natural to ponder whether investigating locations around the periphery would reveal useful new quantities. For example, would position (12, 24), which is between sound resistance and sound impedance, represent a significant

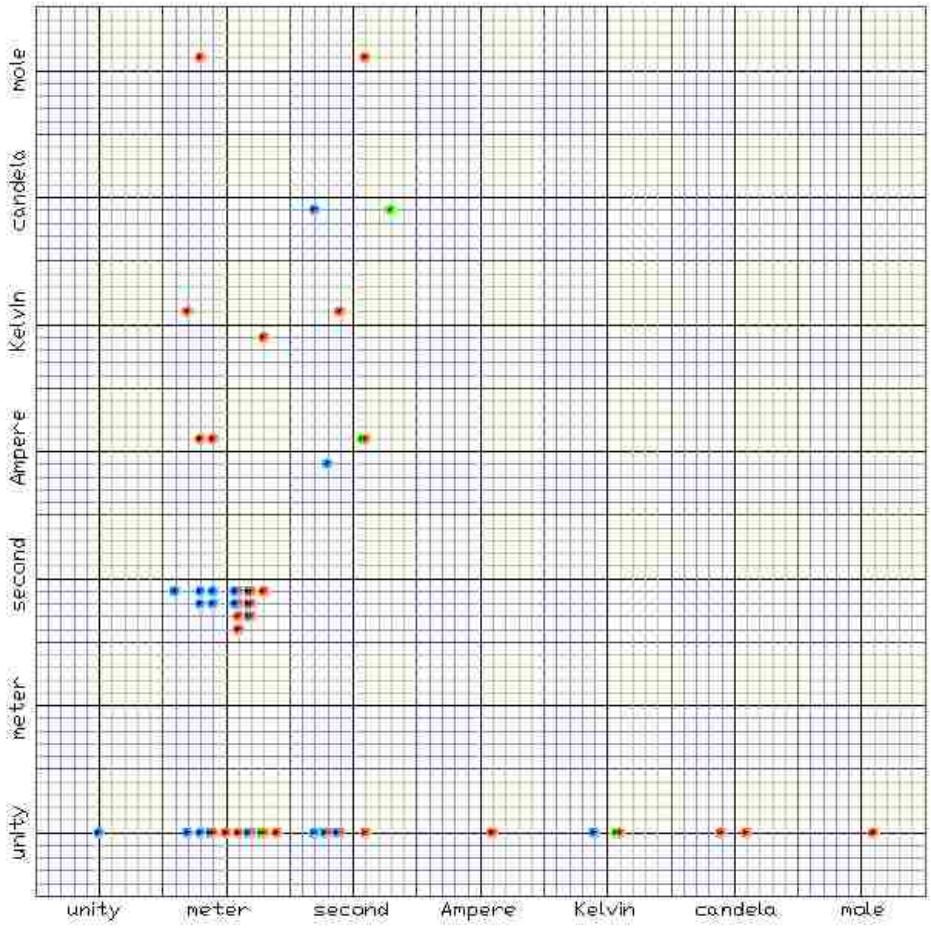

Figure 4.8. Bottom Plane of Second Unit Map

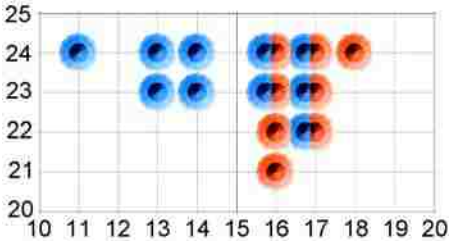

Figure 4.9. Length-Time Detail

new quantity related to the study of sound? Perhaps it already does but the author simply did not know about the quantity?

Recalling the earlier discussion about Newton's second law, energy and momentum, it is interesting to note that force and acceleration are at the same coordinate

Table 4.5. Quantities in Length-Time Detail

Coordinates	Physical quantity with mass	Physical quantity without mass
(11, 24)	sound resistance ($kg \cdot m^{-4} \cdot s^{-1}$)	*none*
(13, 23)	force density ($kg \cdot m^{-2} \cdot s^{-2}$)	*none*
(13, 24)	sound impedance ($kg \cdot m^{-2} \cdot s^{-1}$)	*none*
(14, 23)	pressure, stress, energy density ($kg \cdot m^{-1} \cdot s^{-2}$)	*none*
(14, 24)	dynamic viscosity ($kg \cdot m^{-1} \cdot s^{-1}$)	*none*
(16, 21)	*none*	snap ($m \cdot s^{-4}$)
(16, 22)	*none*	jerk, jolt ($m \cdot s^{-3}$)
(16, 23)	force, weight ($kg \cdot m \cdot s^{-2}$)	acceleration ($m \cdot s^{-2}$)
(16, 24)	momentum, impulse ($kg \cdot m \cdot s^{-1}$)	speed, velocity ($m \cdot s^{-1}$)
(17, 22)	power ($kg \cdot m^{2} \cdot s^{-3}$)	absorbed dose rate ($m^{2} \cdot s^{-3}$)
(17, 23)	energy, work, heat, moment of force ($kg \cdot m^{2} \cdot s^{-2}$)	Specific energy, specific latent heat, absorbed dose, dose equivalent ($m^{2} \cdot s^{-2}$)
(17, 24)	angular momentum ($kg \cdot m^{2} \cdot s^{-1}$)	kinematic viscosity, diffusion coefficient ($m^{2} \cdot s^{-1}$)
(18, 24)	*none*	volumetric flow ($m^{3} \cdot s^{-1}$)

location in Figure 4.9 while energy and momentum are in adjacent locations. This relationship is not so obvious in Table 4.5. If one ignores the separation due to the unity line, stress is also adjacent to force. The fourth adjacent location is home to jerk (or jolt) but does not have a corresponding mass-related quantity. This quantity would perhaps be force per time (or *yank* as some have proposed).

Figure 4.10 includes quantities with four and five base units. Interestingly, a large number of these units are directly above the region highlighted in Figure 4.9. Figure 4.11 highlights the most densely populated region where length, time, and electric current intersect. All but one of the quantities on the left side have mass in the numerator, the quantities on the right side have mass in the denominator, and the middle two quantities do not involve mass.

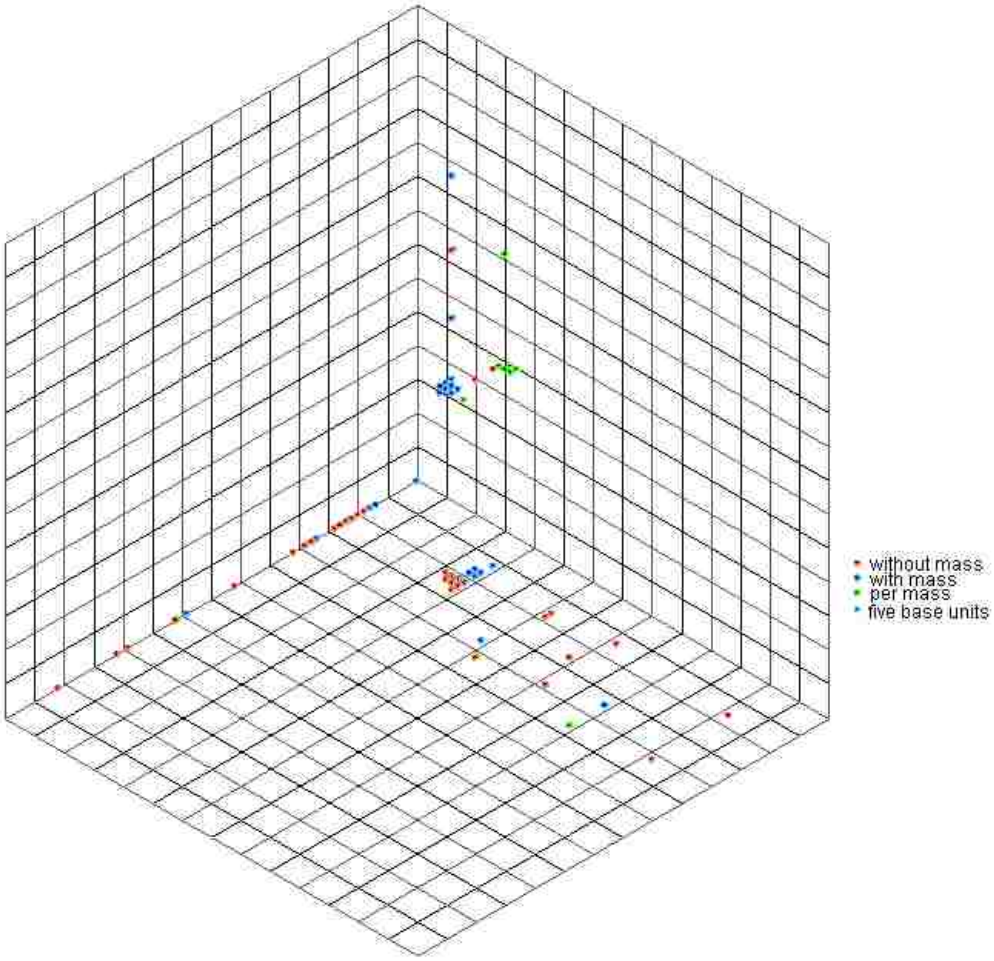

Figure 4.10. Full Unit Map

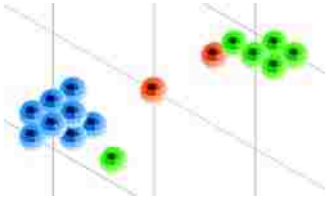

Figure 4.11. Length, Time and Electric Current Detail

One would wonder whether the proximity of these quantities indicates that this region has unique significance in nature, is simply the most studied or easily measured, is an artifact of the mapping technique, or is just a coincidence. Obviously, the result tempts further investigation and possibly new discoveries.

It may be worth noting that permeability lies in this space directly above force. Heat capacity, entropy, molar energy, magnetic flux, and inductance are above energy. Thermal conductivity and electric field strength lie above the spot for force per time. The next section offers speculations on a new quantity for this location.

Tables 4.6, 4.7 and 4.8 list all of the mapped quantities according to the mass exponents of 0, +1 and -1, respectively.

One may find it worthwhile to expand the presented technique to include a map of dimensionless numbers. While in the maps described above such items would appeared in the unity-cubed region, using the non-simplified version of the base units (recall strain in the first map) might give these quantities a unique coordinate location. In fact, it might be useful to replot all of the physical quantities this way so that entries like energy and torque show up at distinct locations.

4.3. FORCE FLOW

From today's perspective, the extension of Archimedes' fulcrum and lever to that of a helical lever called the Archimedes screw seems an obvious step. The helical nature of nuts and bolts, coil springs, fans, pumps, etc. is now taken for granted.

In the late nineteenth century William Thompson (1824-1907) and others attempted to describe matter as *vortex atoms* in a *vortex sponge* ether (Berkson, 1974; Silver, 2006). While this and most ether theories were eventually abandoned, Dmitriyev (2007) has worked for the last ten or more years on an analogy between fluid flow and electromagnetic fields and particles that is reminiscent of the vortex-atom theory. He represents the electromagnetic field as a turbulent, perfect fluid and the particles and charges as discontinuities in the fluid, such as a vapor bubble being representative of a neutron. He points out that, "particles should be properly considered waves of the turbulence energy." In particular he describes *wave packets* as right- and left-handed screw helices with the "ideal fluid pierced in all directions by the vortex filaments," where "microscopically the turbulent substratum is seen as the vortex sponge" (Dmitriyev, 2002).

Table 4.6. Physical Quantities without Mass

Number of base units	Physical quantity	SI base units	kg	m	s	A	K	cd	mol	Coordinates
1	wavenumber	m^{-1}	0	-1	0	0	0	0	0	(14, 05, 05)
	plane angle,	$m \cdot m^{-1}$	0	0	0	0	0	0	0	(15, 05, 05)
	solid angle	$m^2 \cdot m^{-2}$	0	0	0	0	0	0	0	(15, 05, 05)
	length	^{m}	0	1	0	0	0	0	0	(16, 05, 05)
	area	m^2	0	2	0	0	0	0	0	(17, 05, 05)
	volume	m^3	0	3	0	0	0	0	0	(18, 05, 05)
	area moment of inertia	m^4	0	4	0	0	0	0	0	(19, 05, 05)
	angular acceleration	$rad \cdot s^{-2}$	0	0	-2	0	0	0	0	(23, 05, 05)
	frequency, activity, angular velocity	s^{-1}	0	0	-1	0	0	0	0	(24, 05, 05)
	time	s	0	0	1	0	0	0	0	(26, 05, 05)
	electric current	A	0	0	0	1	0	0	0	(36, 05, 05)
	amount of substance	mol	0	0	0	0	0	0	1	(46, 05, 05)
	coefficient of linear expansion	K^{-1}	0	0	0	0	-1	0	0	(54, 05, 05)
	temperature	K	0	0	0	0	1	0	0	(56, 05, 05)
	luminous flux or intensity	cd	0	0	0	0	0	1	0	(66, 05, 05)
2	snap	$m \cdot s^{-4}$	0	1	-4	0	0	0	0	(16, 21, 05)
	jerk, jolt	$m \cdot s^{-3}$	0	1	-3	0	0	0	0	(16, 22, 05)
	acceleration	$m \cdot s^{-2}$	0	1	-2	0	0	0	0	(16, 23, 05)
	speed, velocity	$m \cdot s^{-1}$	0	1	-1	0	0	0	0	(16, 24, 05)
	absorbed dose rate	$m^2 \cdot s^{-3}$	0	2	-3	0	0	0	0	(17, 22, 05)
	specific energy, specific latent heat, absorbed dose, dose equivalent	$m^2 \cdot s^{-2}$	0	2	-2	0	0	0	0	(17, 23, 05)
	kinematic viscosity, diffusion coefficient	$m^2 \cdot s^{-1}$	0	2	-1	0	0	0	0	(17, 24, 05)
	volumetric flow	$m^3 \cdot s^{-1}$	0	3	-1	0	0	0	0	(18, 24, 05)
	electric current density	$m^{-2} \cdot A$	0	-2	0	1	0	0	0	(13, 36, 05)
	magnetic field strength	$m^{-1} \cdot A$	0	-1	0	1	0	0	0	(14, 36, 05)
	amount (-of-substance) concentration	$m^{-3} \cdot mol$	0	-3	0	0	0	0	1	(12, 46, 05)
	molar volume	$m^3 \cdot mol^{-1}$	0	3	0	0	0	0	-1	(18, 44, 05)
	luminance, illuminance, illumination	$m^{-2} \cdot cd$	0	-2	0	0	0	1	0	(13, 66, 05)
	electric charge	$s \cdot A$	0	0	1	1	0	0	0	(26, 36, 05)
	catalytic activity	$s^{-1} \cdot mol$	0	0	-1	0	0	0	1	(24, 46, 05)
	luminous energy	$s \cdot cd \cdot sr$	0	0	1	0	0	1	0	(26, 66, 05)
3	electric charge density	$m^{-3} \cdot s \cdot A$	0	-3	1	1	0	0	0	(12, 26, 36)
	dielectric polarization, displacement, surface charge density	$m^{-2} \cdot s \cdot A$	0	-2	1	1	0	0	0	(13, 26, 36)
	electric dipole moment	$m \cdot s \cdot A$	0	1	1	1	0	0	0	(16, 26, 36)
	specific heat capacity, specific entropy	$m^2 \cdot s^{-2} \cdot K^{-1}$	0	2	-2	0	-1	0	0	(17, 23, 54)

We consider a vortex tube in an ideal fluid. It can be imagined in the following way. Let a viscous fluid be pierced by a pin than spins about its axis, causing a circular motion in the fluid. The motion persists if we withdraw the pin and the fluid viscosity is removed. A very thin vortex

Table 4.7. Physical Quantities with Mass

Number of base units	Physical quantity	SI base units	kg	m	s	A	K	cd	mol	Coordinates
2	mass	kg	1	0	0	0	0	0	0	(05, 05, 05)
	density, mass density	$kg \cdot m^{-3}$	1	-3	0	0	0	0	0	(12, 05, 05)
	mass per unit area	$kg \cdot m^{-2}$	1	-2	0	0	0	0	0	(13, 05, 05)
	mass per unit length	$kg \cdot m^{-1}$	1	-1	0	0	0	0	0	(14, 05, 05)
	mass moment of inertia	$kg \cdot m^{2}$	1	2	0	0	0	0	0	(17, 05, 05)
	heat flux density, irradiance	$kg \cdot s^{-3}$	1	0	-3	0	0	0	0	(22, 05, 05)
	surface tension	$kg \cdot s^{-2}$	1	0	-2	0	0	0	0	(23, 05, 05)
	mass flow rate	$kg \cdot s^{-1}$	1	0	-1	0	0	0	0	(24, 05, 05)
	molar mass	$kg \cdot mol^{-1}$	1	0	0	0	0	0	-1	(44, 05, 05)
3	sound resistance	$kg \cdot m^{-4} \cdot s^{-1}$	1	-4	-1	0	0	0	0	(11, 24, 05)
	force per volume	$kg \cdot m^{-2} \cdot s^{-2}$	1	-2	-2	0	0	0	0	(13, 23, 05)
	sound impedance	$kg \cdot m^{-2} \cdot s^{-1}$	1	-2	-1	0	0	0	0	(13, 24, 05)
	pressure, stress, energy density	$kg \cdot m^{-1} \cdot s^{-2}$	1	-1	-2	0	0	0	0	(14, 23, 05)
	dynamic viscosity	$kg \cdot m^{-1} \cdot s^{-1}$	1	-1	-1	0	0	0	0	(14, 24, 05)
	force, weight	$kg \cdot m \cdot s^{-2}$	1	1	-2	0	0	0	0	(16, 23, 05)
	momentum, impulse	$kg \cdot m \cdot s^{-1}$	1	1	-1	0	0	0	0	(16, 24, 05)
	power, radiant flux	$kg \cdot m^{2} \cdot s^{-3}$	1	2	-3	0	0	0	0	(17, 22, 05)
	energy, work, heat, moment of force	$kg \cdot m^{2} \cdot s^{-2}$	1	2	-2	0	0	0	0	(17, 23, 05)
	angular momentum	$kg \cdot m^{2} \cdot s^{-1}$	1	2	-1	0	0	0	0	(17, 24, 05)
	coefficient of heat transfer	$kg \cdot s^{-3} \cdot K^{-1}$	1	0	-3	0	-1	0	0	(22, 54, 05)
	magnetic flux density, magnetic inductivity	$kg \cdot s^{-2} \cdot A^{-1}$	1	0	-2	-1	0	0	0	(23, 34, 05)
4	electric field strength	$kg \cdot m \cdot s^{-3} \cdot A^{-1}$	1	1	-3	-1	0	0	0	(16, 22, 34)
	permeability	$kg \cdot m \cdot s^{-2} \cdot A^{-2}$	1	1	-2	-2	0	0	0	(16, 23, 33)
	electrical resistance, impedance, reactance	$kg \cdot m^{2} \cdot s^{-3} \cdot A^{-2}$	1	2	-3	-2	0	0	0	(17, 22, 33)
	electric elastance	$kg \cdot m^{2} \cdot s^{-4} \cdot A^{-2}$	1	2	-4	-2	0	0	0	(17, 21, 33)
	electric potential, electromotive force	$kg \cdot m^{2} \cdot s^{-3} \cdot A^{-1}$	1	2	-3	-1	0	0	0	(17, 22, 34)
	inductance	$kg \cdot m^{2} \cdot s^{-2} \cdot A^{-2}$	1	2	-2	-2	0	0	0	(17, 23, 33)
	magnetic flux	$kg \cdot m^{2} \cdot s^{-2} \cdot A^{-1}$	1	2	-2	-1	0	0	0	(17, 23, 34)
	resistivity	$kg \cdot m^{3} \cdot s^{-3} \cdot A^{-2}$	1	3	-3	-2	0	0	0	(18, 22,33)
	magnetic dipole moment	$kg \cdot m^{3} \cdot s^{-2} \cdot A^{-1}$	1	3	-2	-1	0	0	0	(18, 23, 34)
	molar energy	$kg \cdot m^{2} \cdot s^{-2} \cdot mol^{-1}$	1	2	-2	0	0	0	-1	(17, 23, 44)
	thermal conductivity	$kg \cdot m \cdot s^{-3} \cdot K^{-1}$	1	1	-3	0	-1	0	0	(16, 22, 54)
	heat capacity, entropy	$kg \cdot m^{2} \cdot s^{-2} \cdot K^{-1}$	1	2	-2	0	-1	0	0	(17, 23, 54)
5	molar heat capacity, molar entropy	$kg \cdot m^{2} \cdot s^{-2} \cdot K^{-1} \cdot mol^{-1}$	1	2	-2	0	-1	0	-1	(17, 23, 44, 54)

tube will be referred to as a vortex filament. … Vortex filaments are structural constituents of turbulence in a fluid. Perturbation waves on vortices represent a secondary formation known as soliton turbulence. A kink on a straight vortex filament [*wave packet*] evolves according to the nonlinear Schrödinger equation. Schrödinger dynamics was shown to be

Table 4.8. Per-Mass Quantities

Number of base units	Physical quantity	SI base units	kg	m	s	A	K	cd	mol	Coordinates
2	specific volume	$kg^{-1} \cdot m^3$	-1	3	0	0	0	0	0	(18, 05, 05)
	chemical concentration	$kg^{-1} \cdot mol$	-1	0	0	0	0	0	1	(46, 05, 05)
3	exposure (X and gamma rays)	$kg^{-1} \cdot s \cdot A$	-1	0	1	1	0	0	0	(26, 36, 05)
4	conductivity	$kg^{-1} \cdot m^{-3} \cdot s^3 \cdot A^2$	-1	-3	3	2	0	0	0	(12, 28, 37)
	permittivity	$kg^{-1} \cdot m^{-3} \cdot s^4 \cdot A^2$	-1	-3	4	2	0	0	0	(12, 29, 37)
	reluctance	$kg^{-1} \cdot m^{-2} \cdot s^2 \cdot A^2$	-1	-2	2	2	0	0	0	(12, 27, 37)
	thermal resistance	$kg^{-1} \cdot m^{-2} \cdot s^3 \cdot K^1$	-1	-2	3	0	1	0	0	(13, 28, 54)
	electric conductance	$kg^{-1} \cdot m^{-2} \cdot s^3 \cdot A^2$	-1	-2	3	2	0	0	0	(13, 28, 37)
	electric capacitance	$kg^{-1} \cdot m^{-2} \cdot s^4 \cdot A^2$	-1	-2	4	2	0	0	0	(13, 29, 37)
	molar conductivity	$kg^{-1} \cdot s^3 \cdot A^2 \cdot mol^{-1}$	-1	0	3	2	0	0	-1	(28, 36, 44)

> valid not only for an isolated vortex filament, but also for perturbation waves on vortex cores in general. So, the nonlinear Schrödinger equation can be used as a model of soliton turbulence. (Dmitriyev, 2005)

While the author does not claim to fully comprehend Dmitriyev's efforts, he does find the idea of modeling physical entities with helices intriguing. For a few years the author has toyed with the idea of using helices as a combined representation of force and the moment of force. The idea is similar to that of a *wrench* on a *screw* in that the force and moment are combined into a single mathematical representation but different in that the combination would be a pair of forces. If these forces were directed along antiphase helical paths with coincident screw axes, then one set of the vector components lying in the plane perpendicular to the screw axes can be shown to form a *couple* or pure moment, the other set of components can be shown to cancel out, and the remaining components parallel to the screw axes can be shown to retain the linear nature of a force.

Poinsot's theorem says that these forces would reduce to a wrench, so one may ask, "Why a helical path?" Well, the author speculates the utility may lie in relation to the helical structures so commonly found in nature and perhaps the concept of *force per time* mentioned in the previous section. In 1986 J. L. Gassenbeek (as cited in Adams, 2001) hypothesized that photons exit an atom along a helical path and that electromagnetic radiation is comprised of "double helix photon waves." While the

accuracy of this concept is questionable, it offers a tantalizing visual image. Mix with this the prevalence of helices found in natural structures and one has enough encouragement to at least entertain the idea of representing force and moment by helices moving through a material, reminiscent of Faraday's *lines of force*. At the very least, it may offer an intuitive, visual introduction to some physics concepts that are absent in engineering education.

4.3.1. The Helical Path. According to convention, light follows a straight trajectory, with deviations described by geometric optics, Rayleigh and Mie scattering, and Maxwell's equations. As previously mentioned, Gassenbeek (as cited in Adams, 2001) offered an alternative in that photons exit an atom along a helical path and that electromagnetic radiation is comprised of "double helix photon waves." Ashworth (1998) and Gauthier (2008) offer additional ideas on the possible helical nature of photons.

Atoms absorb and emit photons with energy matching the amount between electron levels. In the following, Shu (1982) describes how quantum mechanics relates this exchange to macro-level forces.

> ...the forces of nature, the pushes and pulls, are ultimately mediated by the exchange of bosons...exchanged photons are not real photons... Virtual photons are those emphemeral entities which are created (emitted) and destroyed (absorbed) within a time interval that is too short to allow their detection by any physical means.
>
> If the virtual photon has very little energy E (very long wavelength gamma), it may get very far from its source before being absorbed by another charge. Thus, charges may influence one another over very long distances...
>
> ...we may think of an electron as always being surrounded by a cloud of virtual photons. If the electron is violently accelerated by some external means, some of this cloud may be shaken loose and given enough energy to become real photons.

Hestenes (1990), Rodrigues et al. (1993), Pavsic et al. (1993), Salesia and Recami (1994 and 2000), and King (2001) offer some interesting speculations about electrons following a helical path. More recently, Reinhold (2007) described how "bumps and dips in the graphene sheet…have only a minor effect on electron transport" but that "strong

scattering is caused by missing carbon atoms in the crystal lattice." This result was described as "counterintuitive," but perhaps electrons (and photons) prefer to follow a helical path along close-packed directions and scatter when confronted by defects, thereby slowing electrical, thermal and force flows.

Suppose for the following discussion that the preferred photon path is along the periphery of an atom. In a crystal with simple lattice geometry this path might take the form of a circular helix as illustrated in Figure 4.12. If the helix diameter were (somehow) tied to the size of the atom, being a fraction to a few times the atomic diameter, and similar in size to the wavelength, then it might be considered a gamma ray.

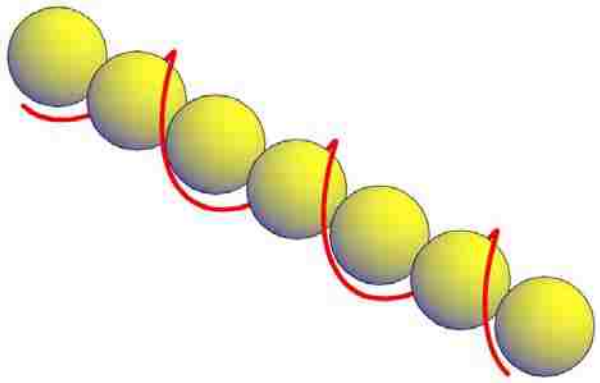

Figure 4.12. A Circular Helix

The position vector of a helix aligned with the z-axis of an orthogonal coordinate system would take the following form.

$$\bar{R}(t) = \begin{pmatrix} r(t)\cdot\cos\left[\theta(t)\right] \\ r(t)\cdot\sin\left[\theta(t)\right] \\ h(t) \end{pmatrix} \tag{1}$$

where in general terms,

$$r(t) = a_r t^2 + v_r t + r_o$$
$$\theta(t) = \alpha t^2 + \omega t + \theta_o$$
$$h(t) = a_h t^2 + v_h t + h_o \qquad (2)$$

In equation (2) the variables a_r, v_r and r_o represent acceleration, velocity and initial position, respectively, along the helix's radial axis. Likewise, a_h, v_h and h_o represent acceleration, velocity and initial position along the z-axis, and α, ω and θ_o represent the rotational acceleration, velocity and initial position about the z-axis.

Table 4.9 summarizes the shape the of position, velocity and acceleration curves when specific versions of radius *r(t)*, angular position *θ(t)* and distance *h(t)* are used. For example, in the first case, where *r(t)*, *θ(t)* and *h(t)* are all constant and represented by the letter *c*, the position would be a point and the velocity and acceleration would be zero. Trends for the rows shown in bold font are represented in Figure 4.13.

The simplest way to represent the idea of a photon moving along close-packed atoms of equal diameter would be to use the following parameters, which correspond to the *c-t-t* trends in Table 4.9, for a circular helix.

$$r(t) = r_o$$
$$\theta(t) = \omega t + \theta_o$$
$$h(t) = v_h t + h_o \qquad (3)$$

If photons were to follow this path, it might provide an alternative explanation to the tendency for metals to "deform along planes of atoms that are most tightly packed" (Askeland, 1989), because the photons would offer the energy necessary for deformation and eventually slip. It might also hint at the difference in mechanical properties for the various lattice arrangements. According to Askeland, "metals with FCC structures are normally soft and ductile, metals with BCC structures are much stronger, and metals with HCP structures tend to be relatively brittle."

Figure 4.14 shows a simple-cubic lattice populated with helices of various wavelengths. It also shows unobstructed pathways within the lattice (i.e. a negative image of the lattice) and an end-on view of the lattice so that one can clearly see the

Table 4.9. Trends for a Helical Path and its Derivatives

Radius	Theta	Height	Position	Velocity	Acceleration
c	c	c	point	zero	zero
c	c	t	line	point	zero
c	c	t^2	line	line	point
t	c	c	line	point at z=0	zero
t	c	t	line	point	zero
t	**c**	**t^2**	**curve**	**line**	**point**
t^2	c	c	curve	line at z=0	point at z=0
t^2	c	t	curve	line	point at z=0
t^2	c	t^2	curve	line	point
c	**t**	**c**	**circle**	**circle at z=0**	**circle at z=0**
c	t^2	c	circle	spiral at z=0	spiral at z=0
t	t	c	spiral	spiral at z=0	spiral at z=0
t^2	t	c	spiral	spiral at z=0	spiral at z=0
t	t^2	c	spiral	spiral at z=0	spiral at z=0
t^2	t^2	c	spiral	spiral at z=0	spiral at z=0
c	**t**	**t**	**helix**	**circle**	**circle at z=0**
t	**t**	**t**	**helix**	**spiral**	**spiral at z=0**
t^2	t	t	helix	spiral	spiral at z=0
c	t^2	t	helix	spiral	spiral at z=0
t	t^2	t	helix	spiral	spiral at z=0
t^2	t^2	t	helix	spiral	spiral at z=0
c	**t**	**t^2**	**helix**	**helix**	**circle**
t	t	t^2	helix	helix	spiral
c	t^2	t^2	helix	helix	spiral
t	t^2	t^2	helix	helix	spiral
t^2	t	t^2	helix	helix	spiral
t^2	t^2	t^2	helix	helix	spiral

space between the atomic *clouds*. Other lattice arrangements, such as the simple monoclinic, simple orthorhombic, rhombohedral, simple tetragonal and triclinic, would also have open corridors for helices to propagate. However, one may notice that these corridors only occur in the close-pack directions; diagonally oriented helices would pass into some of the atomic clouds and violate the assumed preference for remaining on the periphery.

Figure 4.15 shows the BCC lattice. The upper images offer the lattice and its negative. The lower images offer two candidate orientations (of seven) for helical passage (i.e. the close packed directions are into the page), but the alternating positions of

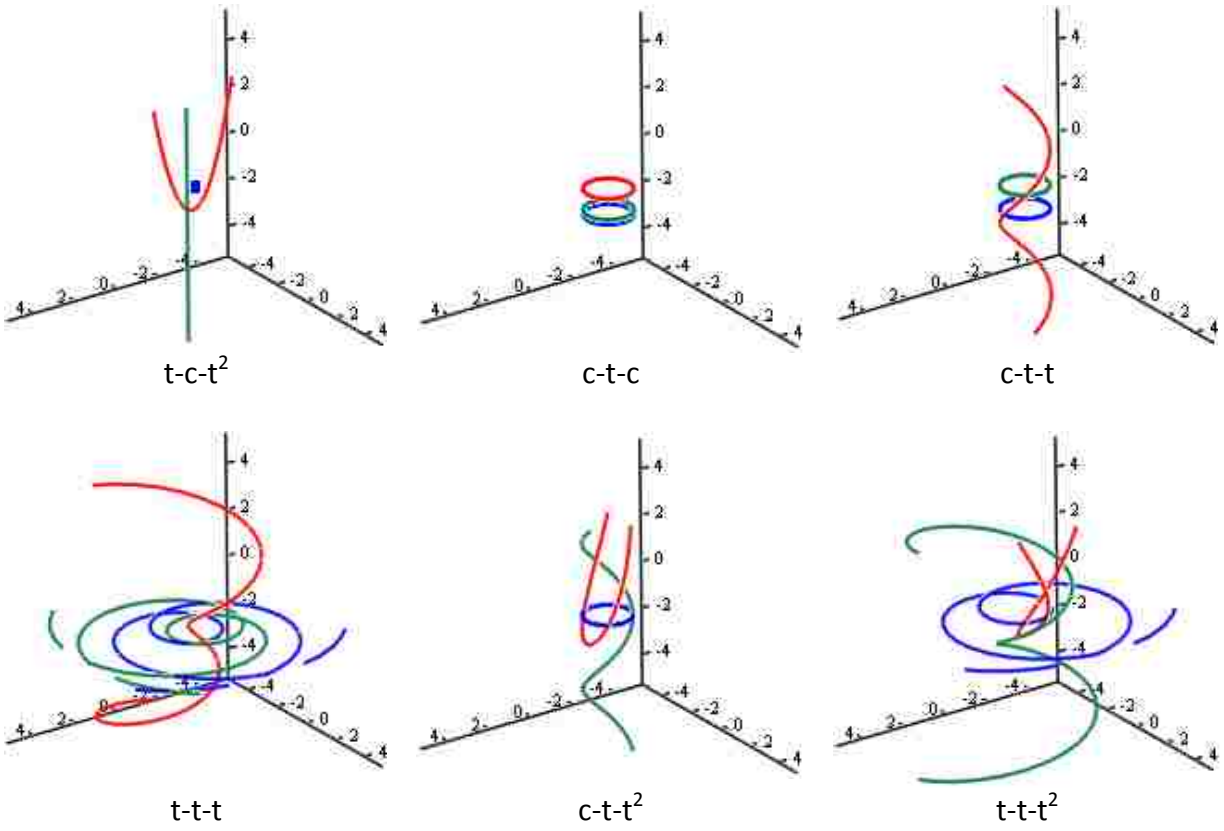

Figure 4.13. Plots of Helical Paths and their Derivatives

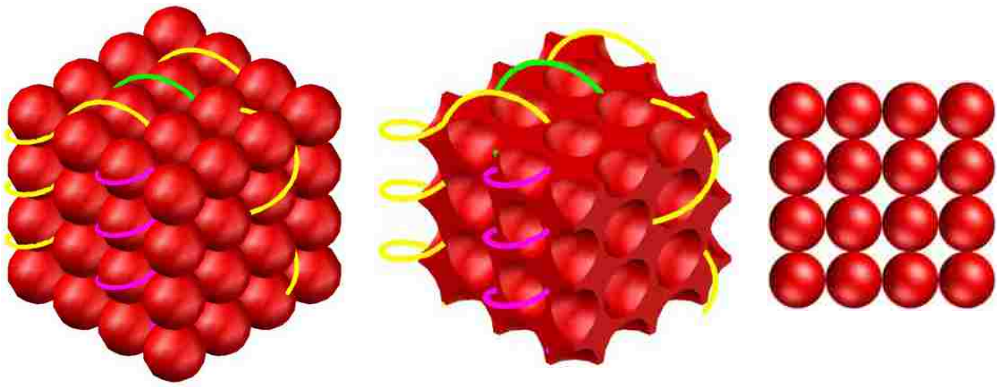

Figure 4.14. Simple Cubic

the atoms as one moves into or out of the page prevent this, unless the helical path either enters the atomic cloud of some of the atoms or simplifies to a straight line.

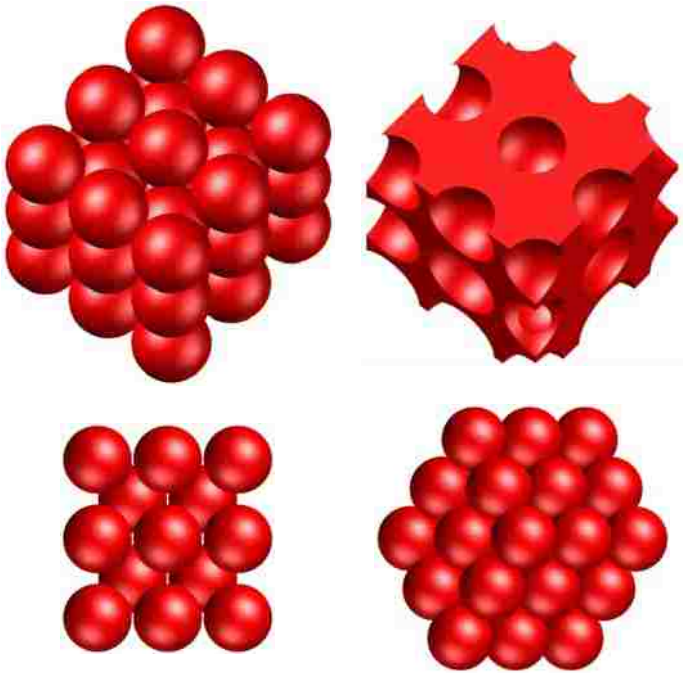

Figure 4.15. Body-Centered Cubic

Figure 4.16 shows the FCC lattice with similar views as to the BCC lattice. Here there are nine candidate orientations for helical passage, but the results are the same. Figure 4.17 shows the HCP lattice. Here there are three candidate corridors for helical passage, but, again, a helix would either enter the atomic cloud of some of the atoms or need to simplify to a straight line.

At this point, with the helical path being geometrically impossible for some of the common lattice structures of crystalline materials, the proposed model seems doomed. One could give up, cycle back to the unit maps of the previous sections and partake on a different exploration, or try some alternative paths to the simple, circular helix. A slightly more general form would be an elliptical helix. Or a more specific form would be a wave or line. Another, perhaps more interesting, alternative would be to vary the diameter (imagine a conical helix) or axis of rotation as the path moves through the lattice. Examples of elliptical and conic helices are shown in Figure 4.18.

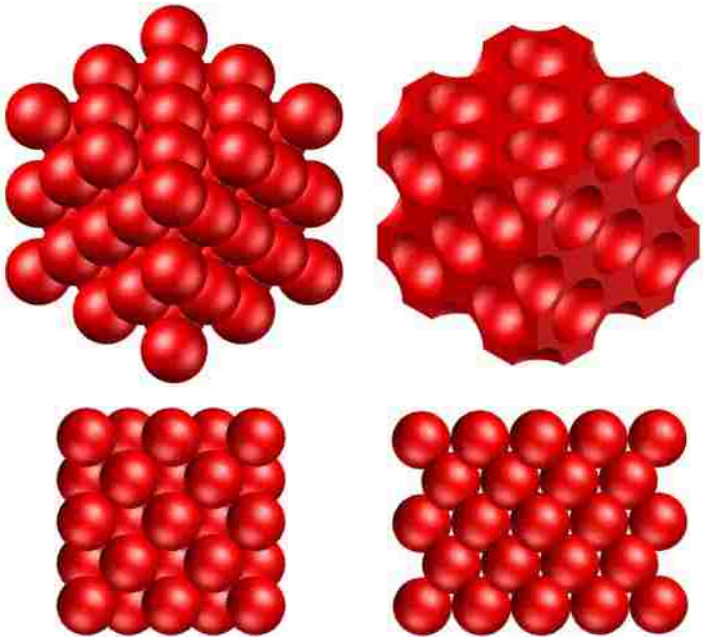

Figure 4.16. Face-Centered Cubic

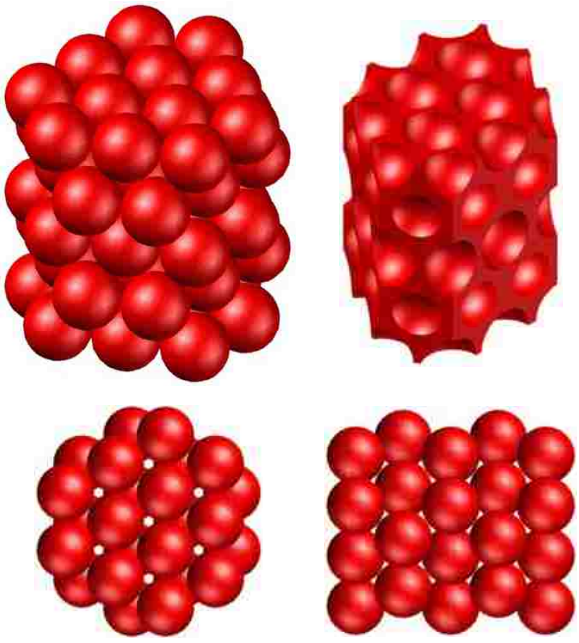

Figure 4.17. Hexagonal Close-Packed

The author spent a little time considering these alternatives. Borrowing from the geometry of wire and rope, one can imagine a path described as a *coiled coil* or *super*

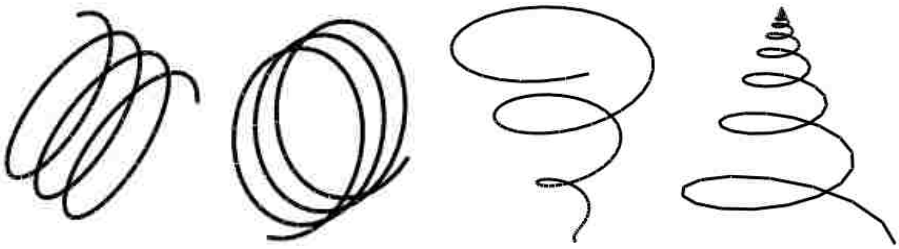

Figure 4.18. Elliptical and Conical Helices

helix. The circular helix so far considered would be a first-order helix. Instead, a second-order helix, or a helix wound around another helix, would resemble something as fundamental as DNA. Figure 4.19 shows sample plots of the second-order path defined by

$$\vec{R}(t) = \begin{pmatrix} \cos(t)\left[r_2 + r_1\cos(Nt)\right] - r_1\cos(\alpha)\sin(t)\sin(Nt) \\ \sin(t)\left[r_2 + r_1\cos(Nt)\right] + r_1\cos(\alpha)\cos(t)\cos(Nt) \\ ht - r_1\sin(\alpha)\sin(Nt) \end{pmatrix} \tag{4}$$

where r_1 is the radius of the first-order helix, r_2 is the radius of the second order helix, N is the number of first-order turns for each of the second-order turns, and α is the pitch angle of the first order helix ($\tan \alpha = r_1 / h$) (Benham, Brady and Fein, 1980).

This concept may not seem particularly useful until one takes a second look at the lattice structures. Figure 4.20 shows how a second-order helix may be able to pass through BCC, FCC and HCP lattices, whereas a first order would not. The wavelength of higher-order helices moving along the highlighted atoms would be 4.1, 5.7 and 9.8 times the atomic radius, respectively.

It would be interesting to see whether other helical paths can be found for lattice structures and none-crystalline materials. Perhaps a mixture of the path alternatives mentioned above, and even-higher-order helices, could be used to visualize helical paths through more detailed atomic and molecular orbitals, amorphous materials, polymers, biological structures, etc.

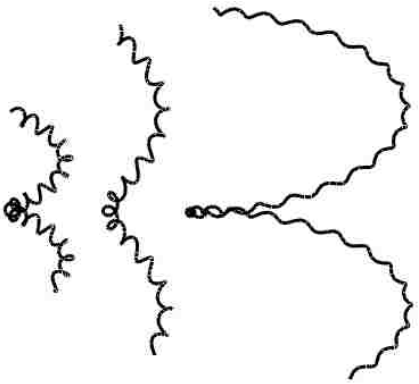

Figure 4.19. Second-Order Helices

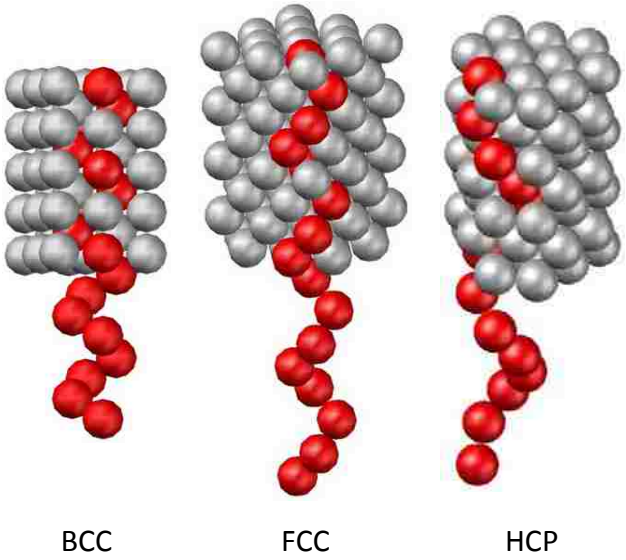

Figure 4.20. A Higher-Order Helical Path in Lattices

It would take a lot more development, that may at some point prove completely useless, but this concept *might* offer opportunities similar to that of Cosserat (or micropolar) elasticity with chiral materials (Lakes and Benedict, 1982). One may even go so far as to imagine that the helical architecture of plants, bone, etc. is adapted for carrying a variety of electromagnetic wavelengths in the form of different sized helices. Might the following tie into this idea?

> It is now well established that all living systems emit a weak but permanent photon flux in the visible and ultraviolet range. This biophoton emission is correlated with many, if not all, biological and physiological functions. There are indications of a hitherto-overlooked information channel within the living system. Biophotons may trigger chemical reactivity in cells, growth control, differentiation and intercellular communication, i.e. biological rhythms. (Chang, Fisch and Popp, 1998)

Merging information from Tables 1.1 and 4.1 and adding radiation wavelengths and a few matter-radiation interaction mechanisms, one obtains the information shown in Table 4.10. It is interesting to note that helices with diameters and wavelengths in relation to lattice dimensions, as described above, would probably fall in the gamma and x-ray ranges. The geometry of the sub-cellular architecture of wood coincides with the near-infrared, visible and ultraviolet ranges. The more macro-level architecture of wood coincides with the mid- and far-infrared, microwave and radio ranges.

It is also interesting to note that the human body senses information from several of the ranges given in Table 4.10. The eyes sense approximately 400-700 nm wavelengths, ears 20-20,000 Hz (0.017-17 m); mechanoreceptors in the skin 5-400 Hz. Thermoreceptors in the skin are commonly credited with sensing temperature, but it is more likely a thermal flow rate, because a person can readily perceive a difference between materials with high and low thermal conductivity (e.g. the metal legs and wood top of a classroom desk). This means that the thermoreceptors might be also be thought of as sensing a range of wavelengths (i.e. molecular vibrations).

4.3.2. Relation to Forces and Moments. To make the idea of force flow more meaningful to engineering, the author made an attempt to tie the first-order helical path equation given above to macro-level forces and moments. Now, suppose that in place of a photon following a first-order helix sits a force vector. This vector would move along the same helical path and align itself with the path.

The derivative of the path equation with respect to time provides a velocity vector that is tangent to the path. Turning this vector into a unit vector and multiplying by a force magnitude will provide the following force vector.

Table 4.10. Matter-Radiation Interactions and Wood Architecture

Size (m)	Repeating Unit	Radiation Wavelength	Interaction	Wood Architecture
10^{-10}	atom	gamma-ray		
10^{-9}	molecule	x-ray	ionization	
10^{-8}	protein	ultraviolet	chemical bonds broken	protofibrils
10^{-7}	organelle	visible	electron level change	microfibrils
10^{-6}	organelle	near infrared	electron level change	cellulose fibers
10^{-5}				laminated cell walls
10^{-4}	cell	mid (thermal) infrared	molecular vibration	cell diameter
10^{-3}	tissue	far infrared	phonon	cell length
10^{-2}	organ	microwave	molecular rotation	growth rings
10^{-1}	organ	microwave		
10^{0}	system	radio		trunk
10^{4}	organism	audible		

$$\overline{F}(t) = \frac{F}{\sqrt{r_o^2\omega^2 + v_h^2}} \cdot \begin{pmatrix} -r_o\omega\sin(\omega t + \theta_o) \\ r_o\omega\cos(\omega t + \theta_o) \\ v_h \end{pmatrix} \tag{5}$$

In the classical approach for particle dynamics, force would be equal to the particle's mass times the acceleration vector, but considering that our starting idea was of a massless photon and a moving force, this scheme seems a somewhat reasonable trial.

One will notice that the value of the force parallel to the *z*-axis given in Equation (5) is fixed, whereas the components in the *x*-*y* plane vary according to position along the circular path in this plane. This is similar to the force and moment of a wrench, but the only way to balance the oscillating *x*-*y* components is to make either the r_o or ω equal to zero, which ruins the idea of a helix and requires that the moment be zero. Instead, a second helical path and force vector that is 180-degrees out of phase from the first, but the same handedness, will be added. This arrangement is shown in Figure 4.21.

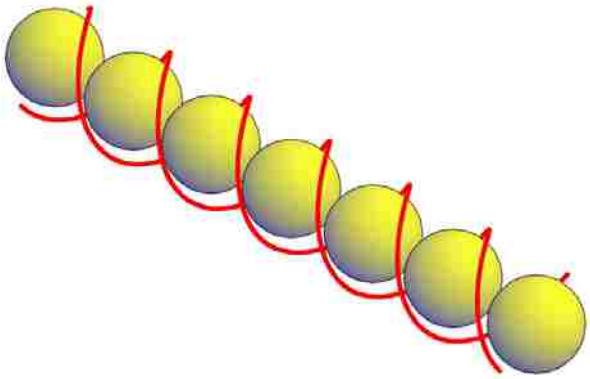

Figure 4.21. Dual Helices

Figure 4.22 provides an alternative view, looking down the z-axis at the first sphere (atom) and the force vectors (photons) that are passing by the sphere at that instant.

Figure 4.22. Individual Forces Passing a Sphere

The two forces would now appear as the following.

$$\overline{F}_1(t) = \frac{F_1}{\sqrt{r_1^2 \omega_1{}^2 + v_1^2}} \cdot \begin{pmatrix} -r_1\omega_1 \sin(\omega_1 t + \theta_1) \\ r_1\omega_1 \cos(\omega_1 t + \theta_1) \\ v_1 \end{pmatrix} \tag{6}$$

$$\overline{F}_2(t) = \frac{F_2}{\sqrt{r_2^2 \omega_2{}^2 + v_2^2}} \cdot \begin{pmatrix} -r_2\omega_2 \sin(\omega_2 t + \theta_2) \\ r_2\omega_2 \cos(\omega_2 t + \theta_2) \\ v_2 \end{pmatrix} \tag{7}$$

Setting $F_1 = F_2 = F$, $r_1 = r_2 = r$, $\omega_1 = \omega_2 = \omega$, $v_1 = v_2 = v$ and $\theta_2 = \theta_1 + \pi$ and summing forces and moments around the origin results in the following, which has a similar form to that of a wrench.

$$\Sigma\overline{F}(t) = \begin{pmatrix} 0 \\ 0 \\ \dfrac{2vF}{\sqrt{r^2\omega^2 + v^2}} \end{pmatrix} \tag{8}$$

$$\Sigma\overline{M}(t) = \Sigma\left[\overline{R}(t) \times \overline{F}(t)\right] = \begin{pmatrix} 0 \\ 0 \\ \dfrac{2r^2\omega F}{\sqrt{r^2\omega^2 + v^2}} \end{pmatrix} \tag{9}$$

If $v = 0$, then $\Sigma\boldsymbol{F} = \mathbf{0}$ and $\Sigma\boldsymbol{M} = 2rF\boldsymbol{k}$ which can be visualized as two forces following a circular path, just as a *couple*. If ω or $r = 0$, then $\Sigma\boldsymbol{F} = 2F\boldsymbol{k}$ and $\Sigma\boldsymbol{M} = \mathbf{0}$, which can be visualized as two forces parallel or coincident, respectively, to the *z*-axis. If $F = 0$, then $\Sigma\boldsymbol{F} = \Sigma\boldsymbol{M} = \mathbf{0}$. Unlike a true wrench, the wrench-force and wrench-moment provided by this double-helix model are not independent. Modifying any of the variables modifies both of the summations. Table 4.11 summarizes the effect on the wrench-force and wrench-moment by altering the variables. For example, increasing *F* increases both the wrench-force and wrench-moment.

Table 4.11. Influence of Variables on Wrench Components

Variable change	Wrench-force change	Wrench-moment change
↑ F	↑	↑
↑ r	↓	↑↑
↑ ω	↓	↑
↑ v	↑	↓

Cylindrical coordinates may offer a more convenient mathematical description. The helix position vector would be defined as

$$\overline{R}(t) = r(t)\hat{e}_r + h(t)\hat{e}_z \tag{10}$$

and a force vector defined as

$$\overline{F}(t) = -F_r(t)\hat{e}_r + F_\theta(t)\hat{e}_\theta + F_z(t)\hat{e}_z \tag{11}$$

One will note that F_r must be zero to match the rectangular definition of force already provided, since the theta-direction is perpendicular to the path. Even if this component were not zero, it would be balanced by F_r of the second force and result in the same summation of force and moment as above.

What about adding more forces (or helices)? Figure 4.23 shows a few arrangements that would behave similarly to the two-helix model just described.

Several situations can be imagined that would unbalance the forces in the x-y plane. For the simple two-helix case, a few examples would be $F_1 \neq F_2$, $r_1 \neq r_2$, $\omega_1 \neq \omega_2$, $v_1 \neq v_2$, $\theta_2 \neq \theta_1 + \pi$, opposite handedness, or opposite velocity directions along the z-axis. Figure 4.24 shows a few unbalanced cases.

If this proposed system has any legitimacy, one might speculate that unbalanced conditions would cause the photons to scatter, be absorbed, and/or cause vibrations in the crystal structure. Similarly, irregularities in the crystal structure would cause the photon

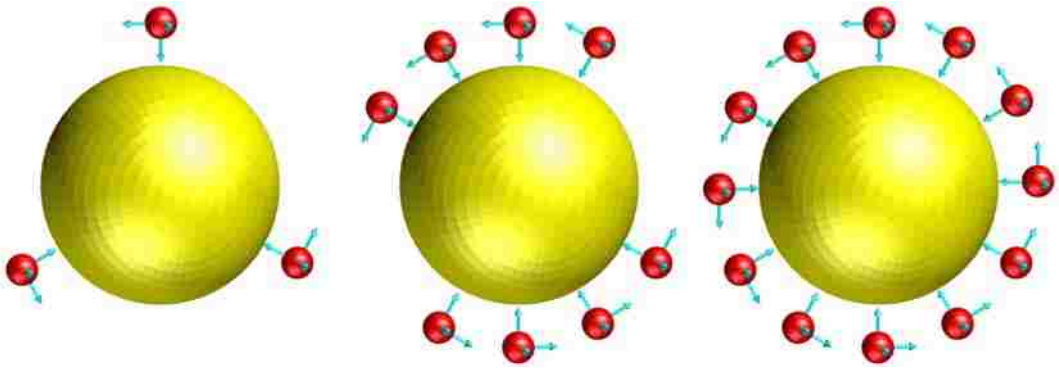

Figure 4.23. Balanced Helices

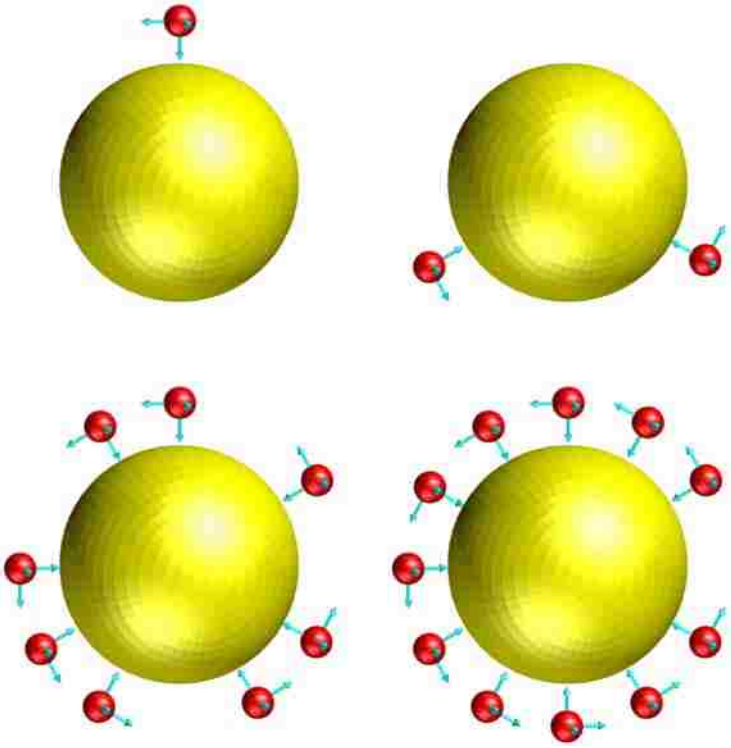

Figure 4.24. Unbalanced Helices

flow to deviate, perhaps into one of these unbalanced cases. Figure 4.25 shows a simple-cubic lattice with multiple, parallel helix pairs. Since the Pauli Exclusion Principle does not apply to photons, perhaps one could ignore the obvious problem of overlapping or interfering paths (Stanford Linear Accelerator Center [SLAC], 2008a).

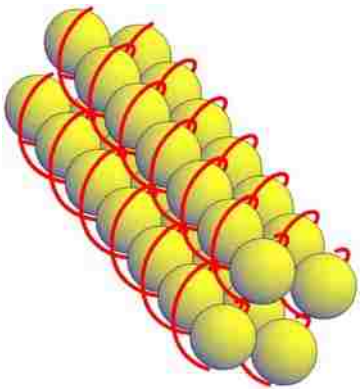

Figure 4.25. Multiple Force Streams

Moving to larger spatial geometries, one might consider the possibility of merging the photon flows into force *streams* akin to liquid moving through a sponge or photoelastic stress patterns. Figures 4.26 and 4.27 show a series of changing stress patterns in simply-supported and cantilever beams, respectively, that the author commonly uses to discuss force flow in the classroom.

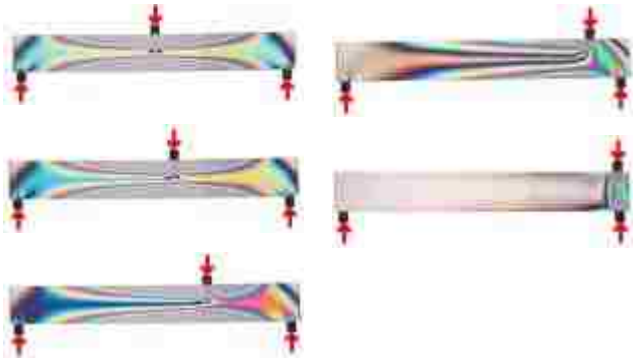

Figure 4.26. Photoelastic Simply-Supported Beam

In Figure 4.26 the upper arrow represents the *applied* load and can be thought of as an *inlet* for liquid to the sponge. The lower *support* arrows can be thought of as *outlets* or *drains* for the liquid. With the inlet exactly between the drains, the liquid flow is symmetric. As the inlet moves closer to one drain and further from the other, there is a

preferential flow to the closer drain. With the inlet directly above a drain, the liquid passes straight across to that drain

In Figure 4.27 the arrow and dark block on the left side clamp the cantilever beam in place and can be thought of as the drain. As the inlet changes position around the beam, different photoelastic patterns appear. Portions of the beam to the right of the inlet remain clear and can be considered *dry* or stagnant, as there is no drain on that side.

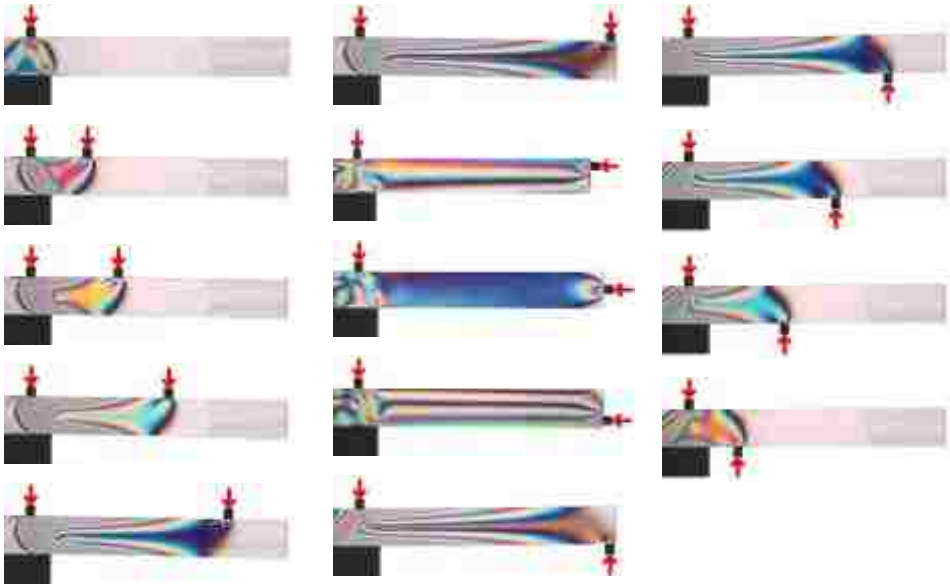

Figure 4.27. Photoelastic Cantilever Beam

Kelly and Tosh (2000) offer the following on *load paths*.

> Design engineers use the term load path to describe, in general terms, the way in which loads path through a structure from the points of application to the points where they are reacted. In contrast, stress trajectories are more clearly identified by the direction of the principal stress vectors at a point.

In the following, Bolton (2000) describes the load path in granular material and the relationship to stress.

> … so in granular media we need to accept that stress is extremely high at points of loaded contact, rather small away from such points, and equal to the pore pressure in the voids between particles. If micro-mechanisms are to be understood, it must first be accepted that the effective stress tensor devolves to some pattern of inter-granular contact forces. Research by de Josselyn de Jong and Verruijt on the photoelastic analysis of glass balls has shown that the major stress is carried in strong load paths through chains of particles which happen to enjoy favorable contact normals. … These strong load paths switch around suddenly as the deviatoric stress is increased, so that many particles may take turns in carrying an unfair proportion of the overall load."

With engineered materials and structures growing progressively more complex, the work required to model their mechanical behavior also grows. In biological structures, where the engineer has little or no control over the material architecture, the utility of stress and strain diminishes. The real power of these concepts lies in the ability to optimize component geometries prior to manufacture. Without that ability it is tempting to bypass these tools and go for a more direct link between load and deformation, relying more on experimental investigations. Perhaps, instead of the scalable stress elements, one could have a scalable definition of force in progressively larger load streams that coincide with hierarchical elements of the material architecture?

Using a very simple version of Dmitriyev's vortex sponge (2002, 2005, 2007), it is easy to imagine atoms, given a framework by the strong and weak nuclear forces, as a sponge and photons as the liquid in the sponge. Squeezing the sponge would both distort the sponge's geometry and cause the liquid to relocate. It's an interesting analogy, because the liquid would move through all of the hierarchical levels in the sponge's geometry – small pores, big pores, channels, etc. – as it responds to the squeeze. The liquid could evaporate, condense, and pass from/to neighboring sponges. The envisioned evaporation and condensation could be thought of as body forces, like gravity and magnetism, and neighboring sponges could be used to describe other bodies or ground connections.

In this framework, perhaps Newton's static equilibrium could be considered a steady-state flow, versus the conventional stagnant pressure. But would a sponge that allows for easy transport be considered high strength or low? Would channels in the

sponge be similar to the load-carrying fibers in a fiber-reinforced polymer or the cellulose of a tree's cell walls? Would the expansion of the sponge as it absorbs liquid be similar to an atom with excited electrons? Is there a limit to the flow capacity or flow rate of the sponge? What happens if these are exceeded?

According to thermoelastic experiments, where a detector registers infrared emission, a body warms slightly in response to tensile stress and cools with compressive stress. The temperature change is proportional to the "change in the sum of principal stresses on the component surface" (Cloud, 2006). In view of a flowing force, could one consider tensile stress an outflow and compressive stress an inflow?

Obviously a lot more work is required to develop this concept of force flow. At this point there are more questions than answers.

4.4. CONCLUSION

The author has long speculated that the prevalence of helical structures in botany and zoology hint to an optimized pathway for force or energy or *something* related to the structure's mechanical function, along with a host of other non-mechanical functions. His long-range goal has been to realize an alternative approach to the standard stress analysis used in engineering in order to more efficiently and accurately deal with biomaterials. Biomaterials are readily available for experimentation, at least on the botany side, and a better understanding of their mechanical behavior would have far reaching consequences—both for biological and non-biological materials.

Unit maps offer a unique framework for systematic scientific exploration and discovery. In relation to the author's interests, he chose to explore the *force per time* location in his second unit map. Ideas on helical photon movement were considered because photons are tied to what is interpreted as force at the macro level and because, as an elementary item, they would be fundamental to all hierarchical levels and material phases. As part of future explorations, alternative helical equations can be considered. The second order helix in Equation (4) does not lend itself to an easy, succinct definition of force like Equation (5), but it is probably worth some attention.

The idea of close packed helices in lattices is interesting and will likely receive more of the author's attention. Even without photons following a helical path, there may be preferential transfer along such lattice helices.

The topics discussed in this document cross a variety of traditional fields. The author has always been more interested in system-level topics than the depth of any single field. However, the common link between the author's varied interests is the mechanical behavior of materials and structures.

The author will probably continue to work with biological materials. He considers probe-based experiments to offer unrealized potential, especially with these materials. Although the stress pattern under a probe tip is complex, the technique requires less specimen preparation than conventional mechanical tests. One can also probe the same sample from multiple directions, with different size probes, and a variety of probe actions.

As his primary motives, the author hopes to continue learning about the physical environment and inspiring engineering students to see things in new ways.

"Like the wheel of a cart is the mind of a fool;
his thoughts revolve in circles." – Sirach 33:5 NAB

BIBLIOGRAPHY

Adams, A. (2001). The helical particle wave, Summary and speculations by Ali Adams. Retrieved from www.geocities.com/aliadams/helicalwave.htm

Aizenberg, J., Weaver, J. C., Thanawala, M. S., Sundar, V. C., Morse, D. E., and Fratzl, P. (2005). Skeleton of Euplectella sp.: Structural hierarchy from the nanoscale to the macroscale. *Science 309*, 275.

Agarwal, B. D., Broutman, L. J., and K. Chandrashekhara (2006). *Analysis and performance of fiber composites* (3rd ed.). Wiley and Sons.

AlexanderDesign (2008). The periodic table. Available from allperiodictables.com/aptpages/gridlink/grid02_table.htm

Antonietti, M., and Mohwald, H. (2001). Colloid physics and chemistry. In European white book on fundamental research in materials science (section 5.6, pp. 180-182). Munich: Max Planck Society for the Advancement of Science.

Ashworth, R. A. (1998) Confirmation of helical travel of light through microwave waveguide analyses. *Physics Essays 11(3)*. Available from www.omsriram.com/Helical%20Travel%20of%20Light.htm

Askeland, D. R. (1989). *The science and engineering of materials* (2nd ed.) (pp. 50-103). Boston: PWS-Kent.

ASM (1995). *ASM handbook, volume 8, mechanical testing*. ASM International.

ASTM International. (2004a). WK382 Practice for Instrumented Indentation Testing.

ASTM International. (2004b). WK381 Standard test methods for automated ball indentation testing of metallic samples and structures to determine stress-strain curves and ductility at various test temperatures.

ASTM International. (2004c). D1037-99 Standard test methods for evaluating properties of wood-base fiber and particle panel materials.

ASTM International. (2004d). D2240-04 Standard test method for rubber property – durometer hardness.

ASTM International. (2004e). D143-94(2000)e1 Standard test methods for small clear specimens of timber.

ASTM International. (2004f). D4444-92(2003) Standard test methods for use and calibration of hand-held moisture meters.

ASTM International. (2004g). D4933-99(2004) Standard guide for moisture conditioning of wood and wood-base materials.

ASTM International. (2004h). E104-02 Practice for maintaining constant relative humidity by means of aqueous solutions.

ASTM International. (2004i). D5536-94(2004) Standard practice for sampling forest trees for determination of clear wood properties.

Bartel, D. L., Davy, D. T., and Keaveny, T. M. (2006). *Orthopaedic biomechanics – mechanics and design in musculoskeletal systems*. New Jersey: Pearson Prentice Hall.

Benham, C. J., Brady, G. W. and Fein, D. B. (1980). X-ray scattering from randomly oriented superhelices, Circular superhelical DNA. *Biophysical Journal, 29(3)*, 351-366.

Benyus, J. M. (2002). *Biomimicry: Innovation inspired by nature*. Harper Perennial.

Berkson, W. (1974). *Fields of force, the development of a world view from Faraday to Einstein* (pp. 105,117, 119,317-318,322-323,332). Wiley and Sons.

Biblis, E. J. (1969). Transitional variation and relationships among properties within loblolly pine growth rings. *Wood Science and Technology, 3*, 14-24.

Billington, D. P. (2003). The art of structural design, A Swiss legacy. Available from mcis2.princeton.edu/swisslegacy/engineers_2.html

Biophotonics International (2005, April). Mechanical loads influence cardiac muscle wall architecture: Confocal microscopy used to study heart development (p. 50). Biophotonics International.

Bolton, M. D. (2000). The role of micro-mechanics in soil mechanics. Available from www-civ.eng.cam.ac.uk/geotech_new/publications/TR/TR313.pdf

Boresi, A. P., Schmidt, R. J., and Sidebottom, O. M. (1993). *Advanced mechanics of materials* (5th ed.) Wiley and Sons.

Bourne, M .C. (2002). *Food texture and viscosity: concept and measurement* (2nd ed.) (pp. 113-127). New York: Academic Press.

Bowyer, A. (2008, October 5) Biomimetics: Picking things up, robots and animals. Available from people.bath.ac.uk/ensab/Teaching/Grip/

Bowyer, J. L., Shmulsky, R., and Haygreen, J. (2003). *Forest products and wood science: an introduction* (4th ed.). Iowa State Press.

Brown, E. N., Peterson, M. L., and Grande-Allen, K. J. (2006). Biological systems and materials: A review of the field of biomechanics and the role of the society for experimental mechanics (p. 26). *Experimental Techniques 30(2)*, 21-29.

Butchner, P. M., and Lakes, R. S. (2003). Size effects in the elasticity and viscoelasticity of bone. *Biomech Model Mechanobiol 1(4)*, 295-301.

Cajori, F. (1899). *A history of physics, in its elementary branches including the evolution of physical laboratories* (pp. 30-31, 52-55). MacMillan.

Campbell, N. A., Mitchell, L. G., and Reece, J. B. (1997). *Biology: concepts and connections* (2nd ed.) (p. 36). Addison Wesley.

Carlsson L. A., Pipes R. B. (1987). *Experimental characterization of composite materials*. Prentice-Hall.

Chang, J. J., Fisch, J., Popp, F. A. (1998). *Biophotons*. Springer.

Cipollini, D. F. (1999). Costs to flowering of the production of a mechanically hardened phenotype, *Brassica Napus L. International Journal of Plant Sciences, 160*, 735.

Cloud, G. L. (2006). Experimental stress and strain analysis. In E. A. Avallone, T. Baumeister, A. Sadegh and L. S. Marks (Ed.), *Marks' standard handbook for mechanical engineers* (p. 5-71). McGraw-Hill.

Coder, K. D. (2000). Tree biomechanics series. *Extension publications FOR 00-13 to 32*. University of Georgia School of Forest Resources.

Conza, N. (2005). Part 3: Tissue preconditioning. *Experimental Techniques 29(2)*, 43-46.

Cowin, S. (2001). *Bone mechanics handbook* (2nd ed.) (p. 7.17-21). New York: CRC Press.

Cox, A. (1997). Making Missouri green: The George O. White State Forest Nursery celebrates 50 years of tree production. Missouri Department of Conservation.

Cramer, S., Kretschmann, D., Lakes, R., and Schmidt, T. (2003). Mesostructure elastic properties in loblolly pine. *Proceedings of the 4th plant biomechanics conference: 2003 Jul 21-25*. East Lansing, MI.

Dao, M., Chollacoop, N., Van Vliet, K. J., Venkatesh, T. A., and Suresh, S. (2001). Computational modeling of the forward and reverse problems in instrumented indentation. *Acta Materialia 49*, 3899-3918.

Davis, H. E., Troxell, G. E., and Wiskocil, C. T. (1964). *The testing and inspection of engineering materials* (3rd ed.) (p. 7). McGraw-Hill.

Dehmelt, H. (1988). A Single Atomic Particle Forever Floating at Rest in Free Space: New Value for Electron Radius. *Phys. Scr. T22*, 102-110.

Discover (2005, August). Fiber optics: Venus's flower-basket (p. 47). Discover Magazine.

Doyle, J., and Walker, J. C. F. (1985). Indentation hardness of wood. *Wood and Fiber Science 17*, 369-376.

Dmitriyev, V. P. (2002). Mechanical analogy for the wave-particle: helix on a vortex filament. *Journal of Applied Mathematics 2(5)*, 241-263.

Dmitriyev, V. P. (2005). Helical waves on a vortex filament. *American Journal of Physics 73(6)*, 563-565.

Dmitriyev, V. P. (2007). Mechanical realization of the medium imitating electromagnetic fields and particles. *Meccanica 42*, 283-291.

Elices, M. (Eds.). (2000). *Structural biological materials: Design and structure—property relationships* (pp. xii, xiii). Elsevier Science.

Ennos, A. R. (2005). Chapter 2: Compliance in plants. In C. H. M. Jenkins (Ed.), *Compliant structures in nature and engineering* (p. 25, 28). WIT Press.

European Commission (2004). Nanotechnology: Innovation for tomorrow's world. Available from ftp.cordis.europa.eu/pub/nanotechnology/docs/nano_brochure_en.pdf

Faraday, M. (1857, February 27). Addendum. *Proceedings of the Royal Institution*. Available from http://www.tyler.net/hermital/book/holoprt4-5.htm

Fisher, C. A. J. (2001). Theory, simulation and design of advanced ceramics and composites. In European white book on fundamental research in materials science (section 4.3). Munich: Max Planck Society for the Advancement of Science.

Forest Products Laboratory. (1999). Wood handbook: wood as an engineering material. *Gen. Tech. Rep. FPL-GTR-113* (p 4.31-32). Madison, WI: US Department of Agriculture, Forest Service.

Gaffrey, D., and Kniemeyer, O. (2002). The elasto-mechanical behavior of Douglas fir, its sensitivity to tree-specific properties, wind and snow loads, and implications for stability: a simulation study. *Journal of Forest Science 48*(2), 49-69.

Gao, H. (2001). Modelling strategies for nano- and biomaterials. In European white book on fundamental research in materials science (section 4.4, p. 148). Munich: Max Planck Society for the Advancement of Science.

Gauthier, R. (2008). Superluminal quantum models of the electron and the photon. Available from www.superluminalquantum.org

Gindl, W., and Gupta, H.S. (2002). Cell-wall hardness and Young's modulus of melamine-modified spruce wood by nano-indentation. *Composites Part A: Applied Science and Manufacturing 33*, 1141-1145.

Ginzburg, V. B. (2006). *Prime elements of ordinary matter: Dark mater and dark energy* (p. 270). Helicola Press.

Gooding, D. (1980). Metaphysics versus measurement: The conversion and conservation of force in Faraday's physics. *Annals of Scicence 37*, 1-29.

Groom, L., Mott, L., and Shaler, S. (2002a). Mechanical properties of individual southern pine fibers: part I, determination and variability of stress-strain curves with respect to tree height and juvenility. *Wood and Fiber Science 34*, 14-27.

Groom, L., Mott, L., and Shaler, S. (2002b). Mechanical properties of individual southern pine fibers: part II, comparison of earlywood and latewood fibers with respect to tree height and juvenility. *Wood and Fiber Science 34*, 221-237.

Groom, L., Mott, L., and Shaler, S. (2002c). Mechanical properties of individual southern pine fibers: part III, global relationships between fiber properties and fiber location within an individual tree. *Wood and Fiber Science 35*, 238-250.

Guitard, D. G., and Castera, P. (1995). Experimental analysis and mechanical modeling of wind-induced tree sways. In M. P. Couts and J. Grace (Eds.), *Wind and Trees* (pp.182-194). Cambridge.

Haddad, Y. M. (2000). Static and quasi-static loading. *Mechanical behaviour of engineering materials, vol. 1*. Kluwer Academic Publishers.

Haggag, F. M., and Murty, K. L. (1996). A novel stress-strain microprobe for nondestructive evaluation of mechanical properties of materials. In P. K. Liaw, O. Buck, R. J. Arsenault and R. E. Green Jr. (Eds.), *Nondestructive evaluation and material properties III* (pp. 101-106). Minerals, Metals, and Materials Society.

Haggag, F. M., Nanstad, R. K., Hutton, J. T., Thomas, D. L., and Swain, R. L. (1990). Use of automated ball indentation to measure flow properties and estimate fracture Toughness in metallic materials. In A. A. Braun, N. E. Ashbaugh and F. M. Smith (Eds.), *Applications of automation technology to fatigue and fracture testing, ASTM1092* (pp. 188-208). Philadelphia: American Society for Testing and Materials.

Hepworth D. G., Gathercole, L. J., Knight, D. P., Feng, D., and Vincent, J. F. V. (1994). Correlation of ultrastructure and tensile properties of a collagenous composite-material, The egg capsule of the dogfish, Scyliorhinus Spp, A sophisticated collagenous material. *Journal of Structural Biology 112(3)*, 231-240.

Hepworth, D. G., and Vincent J. F. V. (1999). The growth response of the stems of genetically modified tobacco plants (Nicotianatabacum `Samsun') to flexural stimulation. *Annals of Botany 83*, 39-43.

Hestenes, D. (1990). The zitterbewegung intepretation of quantum mechanics. *Foundations of Physics, 20(10)*, 1213–1232.

Ingber, D. E. (1998). The architecture of life: basic rules of tensegrity guide molecular self-assembly, noting application to cytoskeleton tissue formation, etc., with reference to geodesic domes. *Scientific American 278*, 56.

Jeronimidis, G. (2000). Biomimetics: lessons from nature for engineering. *35th John Player memorial lecture*. London: The Institution of Mechanical Engineers.

Jirasek, C. (2000). A biomechanical model of branch shape in plants expressed using L-systems (thesis, University of Calgary, 2000).

Kastelic, J., Galeski, A., and Baer, E. (1978). The multicomposite structure of tendon. *Connective Tissue Research 6(1)*, 11-23.

Kelly, D. W. and Tosh, M. W. (2000). Interpreting load paths and stress trajectories in elasticity. *Engineering Computations, 17(2)*, 117-135.

King, R. B. (1987). Elastic analysis of some punch problems for a layered medium. *Int J Solids Struct 23*,1657-64.

King, Jr., T. R. (2001). The electron as orbiting quantum. Available from www.memetaworks.com/e_as_Quantum

Kobayashi, A. S. (Ed.) (1987). *Handbook on experimental mechanics*. Prentice Hall.

Kremer, K. (2001). From basic principles to computer aided design. In European white book on fundamental research in materials science (section 4.2, pp. 134-137). Munich: Max Planck Society for the Advancement of Science.

Kretschmann, D. E., Schmidt, T. W., Lakes, R. S., and Cramer, S. M. (2002). Micromechanical measurement of wood substructure properties. *Proceedings of society of experimental mechanics annual conference, Jun 10-11, 2002*. Milwaukee, WI.

Lakes, R. S. (1993). Materials with structural hierarchy. *Nature 361*, 511-515.

Lakes, R. S. (1995). Experimental methods for study of Cosserat elastic solids and other generalized elastic continua. In H. Mühlhaus (Ed.), *Continuum models for materials with micro-structure* (pp. 1-22). New York: Wiley.

Lakes, R. S., and Benedict, R. L. (1982). Noncentrosymmetry in micropolar elasticity. *International Journal of Engineering Science 29(10)*, 1161-1167.

Lakes, R. S., and Wang, Y. C. (2004, October 10-13). Freedom and stability in elastic solids. 41st Meeting, Society of Engineering Science, Lincoln, NE.

Lang, M. (2007). Lighting up the mechanome. *The Bridge 37(4)*. Available from web.mit.edu/~langlab/Publications/Lang-Mechanome.pdf

Lawson, E. R. (1990). Pinus echinata Mill: shortleaf pine. In R. M. Burns and B. H. Honkala (Eds.), *Silvics of North America, vol. 1, conifers* (pp. 316-326). Washington DC: USDA Forest Service Agricultural Handbook, 654.

Levesque, L. C. (2001). *Breakthrough creativity: achieving top performance using the eight creative talents*. Davies-Black.

Little, C. H. A., Lavigne, M. B. (2002). Gravimorphism in current-year shoots of Abies balsamea: Involvement of compensatory growth, indole-3-acetic acid transport and compression wood formation. *Tree Physiology 22*, 311–320.

Liu, J. Y., and Ross, R. J. (1998). Wood mechanical property variation with grain slope. In H. Murakami and J. E. Luco (Eds.), *Engineering mechanics: A force for the 21st century* (pp. 1351-1354). Reston, VA: American Society Chemical Engineers.

Liu, J. Y. (2000). Effects of shear coupling on shear properties of wood. *Wood Fiber Sci. 32(4)*, 458-465.

Liu, J. Y. (2002). Analysis of off-axis tension test of wood specimens. *Wood Fiber Sci. 34(2)*, 205-211.

Marieb, E. N., and Mallatt, J. (1997). *Human anatomy* (2nd ed.) (pp. 130, 131, 134). Addison Wesley.

Mattheck, C. (1991). *Trees: The mechanical design* (pp. 116-117). Heidelberg: Springer-Verlag.

Mickovski, S. B., and Ennos, A. R. (2003). Anchorage and asymmetry in the root system of Pinus peuce. *Silva Fennica 37(2)*, 161-173.

Millon, T. (1991). Classification in psychopathology: rationale, alternatives, and standards. *Journal of Abnormal Psychology 100(3)*, 245-261.

Mosbrugger, V. (1990). The Tree Habit in Land Plants. In S. Bhattacharji, G. M. Friedman, H. J. Neugebauer and A. Seilacher (Eds.), *Lecture notes in earth sciences, vol. 28* (p. 35). Berlin: Springer-Verlag.

Moser, W. K., Treiman, T., Moltzan, B., Lawrence, R., and Brand, G. J. (2003). Missouri's forest resources in 2001. *USDA Forest Service, North Central Research Station, NC-226*.

MTS (2004, August). Continuous stiffness measurement. Available from www.mts.com/nano/CSM.htm

Mueller, T. (2008). Biomimetics: Design by nature. National Geographics. Available from ngm.nationalgeographic.com/2008/04/biomimetics/tom-mueller-text

Nahin, P. J. (1992). Maxwell's grand unification. *Spectrum, IEEE 29(3)*, 45.

National Physical Laboratory (2004, August). Instrumented indentation for hardness and material properties. Available from www.npl.co.uk/force/guidance/hardness/instrumented.html

Niklas, K. L. (1992). *Plant biomechanics, An engineering approach to plant form and function* (pp. 50-51). University of Chicago Press.

Otto, K., and Wood, K. (2001). *Product design, techniques in reverse engineering and new product development* (p. 44). Prentice Hall.

Pavsic, M., Recami, E., Rodrigues, Jr., W. A., Maccarrone, G. D., Raciti, F., and Salesi, G. (1993). Spin and electron structure. *Physics Letters B, 318(3)*, 481-488.

Pink, R. (2007). Subatomic particles: An overview. Available from cr4.globalspec.com/blogentry/2566/Subatomic-Particles-An-Overview

Plant Information Center. (2004a, August). Shortleaf pine. Available from www.ibiblio.org/pic/NCTrees/shortleafpine.htm

Plant Information Center. (2004b, August). Loblolly pine. Available from: www.ibiblio.org/pic/NCTrees/loblollypine.htm

Pruyn, M. L., Ewers, B., and Telewski, F. W. (2000). Thigmomorphogenesis: changes in the morphology and mechanical properties of two Populus hybrids in response to mechanical perturbation. *Tree Physiology 20*, 535-540.

Raju, P. K., and Gibson, R. F. (Eds.) (1993). *Dynamic characterization of advanced materials*. ASME.

Rapoff, A. J., Götzen, N., Cross, A. R., and Ifju, P. G. (2001). Understanding stress concentration around a nutrient foramen. Proceedings of the ASME Summer 2001 Bioengineering Conference (p. 55). ASME.

Reinold, C. (2007). Potholes in graphene make electrons go slow. *Materials Today 10(9)*, 9.

Rodrigues, Jr., W. A., Vaz, Jr., J., Recami, E. and Salesi, G. (1993). About zitterbewegung and electron structure. *Physics Letters B, 318(4)*, 623-628.

Rudnitsky, V. A., Kren, A. P., and Tsarik, S. V. (2004, August). Method of identification of viscoelastic materials with a stress relaxation function. Available from www.ndt.net/article/wcndt00/papers/idn227/idn227.htm

Sakaguchi, T., and Ohya, J. (1999). Modeling and animation of botanical trees for interactive virtual environments. In Proceedings of the ACM VRST symposium (pp. 139-146). ACM.

Salesia, G. and Recami, E. (1994). Field theory of the spinning electron and internal motions. *Physics Letters A, 190(2)*, 137-143.

Salesi, G. and Recami, E. (2000). Effects of spin on the cyclotron frequency for a Dirac electron. *Physics Letters A, 267(4)*, 219-224.

Saunders, F. (2007). Ice entwined: Frozen water takes on intricate multi-helix shapes when confined in tiny spaces at high pressures. *American Scientist 95(2)*, 121.

Scholberg, K. (2005). Tiny particles, big questions. *American Scientist 93*, 80-81.

Scientific Consulting Services International (2008). The Alexander arrangement of the elements. Available from www.scs-intl.com/alexander.htm

Settergren, C., and McDermott, R. E. (2000). Trees of Missouri. *University Extension, University of Missouri-Columbia, SB-767*. University of Missouri.

Sharma, M., and Oderwald, R. G. (2001). Dimensionally compatible volume and taper equations. *Can J For Res/Rev Can Rech For 31(5)*, 797-803.

Shaddix, C. R., and Williams, T. C. (2007). Soot: Giver and taker of light, The complex structure of soot greatly influences the optical effects seen in fires. *American Scientist 95(3)*, 238.

Shadwick, R. E. (1998). Elasticity in arteries, A similar combination of rubbery and stiff materials creates common mechanical properties in blood vessels of vertebrates and some invertebrates. *American Scientist 86(6)*, 535.

Shu, F. H, (1982). *The physical universe, An introduction to astronomy* (pp. 107-108). University Science Books.

Silk, W. K. (1997). Mechanics of the twining habit of plant stems. In G. Jeronimidis and J. F. V. Vincent (Eds.), *Plant biomechanics 1997, Conference proceedings I* (pp. 89-95). The University of Reading.

Silver, D. S. (2006). Knot theory's odd origins. *American Scientist 94*, 158-165.

Spicer, R., and Gartner, B. L. (2002). Compression wood has little impact on the water relations of Douglas-fir (Pseudotsuga menziesii) seedlings despite a large effect on shoot hydraulic properties. *New Phytologist 154*, 633-640.

Stanford Linear Accelerator Center (2008a). Forces and interactions. Available from www2.slac.stanford.edu/VVC/theory/interactions.html

Stanford Linear Accelerator Center (2008b). Spin. Available from http://www2.slac.stanford.edu/VVC/theory/spin.html#Fermions

Stathers, R. J., Rollerson, T. P., and Mitchell, S. J. (1994). Windthrow handbook for British Columbia forests. In BC Ministry of Forests, *Research branch working paper 9401*. Victoria, BC: BC Ministry of Forests.

Steenhuysen, J. (2008, October 10). Sticky glue out-geckos the geckos: 1-inch square of the stuff could anchor real-life Spider-Man, scientists say. Reuters. Available from www.msnbc.msn.com/id/27108642/from/ET/

Tabil, Jr., L. G., Sokhansanj, S., Crerar, W. J., Patil, R. T., Khoshtaghaza, M. H., and Opokul, A. (2002). Physical characterization of alfalfa cubes: I. hardness. *Canadian Biosystems Engineering 44(3)*, 55-63.

Telewski, F. W., and Pruyn, M. L. (1998). Thigmomorphogenesis: a dose response to flexing in Ulmus americana seedlings. *Tree Physiology 18*, 65-68.

Timoshenko, S. P., and Goodier, J. N. (1951). *Theory of elasticity* (p. 372). New York: McGraw-Hill.

Timoshenko, S. P. (1983), *History of strength of materials* (pp. 1, 23, 47, 50, 67-70, 97, 104-112, 116, 118, 156). McGraw-Hill.

Tomos, D. (1997). Cell turgor pressure in tissues. In G. Jeronimidis and J. F. V. Vincent (Eds.), *Plant biomechanics 1997, Conference proceedings I* (p. 81). The University of Reading.

USDA Forest Service (2004, August). US forest facts and historical trends. Available from fia.fs.fed.us/library/ForestFactsMetric.pdf

Venkataraman, S., Haftka, R., and Rapoff, A. (2001, June). Strength optimization of a plate with hole using biologically inspired design variables. *Proceedings of 4th World Congress of Structural and Multidisciplinary Optimization*.

Weinberg, S. (1994). *Dreams of a final theory*. Vintage Books.

Weisstein, E. W. (2008). Phyllotaxis. Available from mathworld.wolfram.com/Phyllotaxis.html

Weinstock, M. (2006, February). Magnetism (p. 12). Discover Magazine.

Wikipedia (2008a). Force. Available from en.wikipedia.org/wiki/Force

Wikipedia (2008b). Heliospheric current sheet. Available from en.wikipedia.org/wiki/Heliospheric_current_sheet

Wikipedia (2008c). Isaac Newton. Available from en.wikipedia.org/wiki/Isaac_Newton

Wolf, B. (2000). Inference of mechanical properties from instrumented depth sensing indentation at tiny loads and indentation depths. *Crystal Research and Technology 35(4)*, 377-400.

Young, J. F., Mindess, S., Gray, R., and Bentur, A. (1998). *The Science and Technology of Civil Engineering Materials* (p. 324). New Jersey: Prentice Hall.

VITA

Jeffery Scott Thomas was born on November 4, 1971 to James L. and L. Kaye Thomas in Springfield, Missouri. He received B.S. and M.S. degrees in Mechanical Engineering from the University of Missouri-Rolla (UMR) in 1995 and 1996, respectively. He received a Ph.D. in Engineering Mechanics from the Missouri University of Science and Technology (Missouri S&T) in 2009.

Dr. Thomas was employed as a lecturer in the Basic Engineering department at UMR in 1996. The department name changed to Interdisciplinary Engineering in 2007, and his position transitioned into an assistant teaching professor the same year. The university name changed to Missouri S&T in 2008, where he continues to work to the present. He has published over 5000 pages of teaching manuscripts and received teaching commendations each year since 1999.

He is a registered professional engineer in the state of Missouri and has managed one of the university's mechanical testing facilities since 1996. He feels that hands-on, laboratory investigations are essential to a quality engineering education. He has provided testing services to 16 campus departments and over 30 companies. He has also provided laboratory demonstrations to approximately 340 middle-school students and 3000 high-school students.

Dr. Thomas enjoys creative hobbies. He has played percussion for several years, authored poems, paintings and carvings, and won a handful of awards in these areas.